TECHNO-ECONOMIC FEASIBILITY STUDY ON LIGHTNING PROTECTION OF OVERHEAD TRANSMISSION LINE HAVING MULTI-CHAMBER INSULATOR ARRESTERS (MCIA). (CASE STUDY: MATHUGAMA-KUKULE, 132KV TRANSMISSION LINE)

Kanduboda Panditha Ralalage Dhammika Saman Kumarasiri Dharmadasa

(119122G)

Dissertation submitted in partial fulfillment of the requirement for the degree Master of Science

Department of Electrical Engineering

University of Moratuwa

Sri Lanka

May 2016

DECLARATION OF THE CANDIDATE AND SUPERVISORS

I declare that this is my own work and this dissertation does not incorporate without acknowledgement any material previously submitted for a Degree or Diploma in any other University or institute of higher learning and to the best of my knowledge and belief it does not contain any material previously published or written by another person except where the acknowledgement is made in the text.

Also, I hereby grant to University of Moratuwa the non-exclusive right to reproduce and distribute my dissertation, in whole or in part in print, electronic or other medium. I retain the right to use this content in whole or part in future works (such as articles or books).

…….

(K.P.R.D.S.K. Dharmadasa)

May 17, 2016

The above candidate has carried out research for the Masters dissertation under our supervision.

……..

(Dr. K.M.T.U. Hemapala)

May 17, 2016

ABSTRACT

Transmission lines are a key factor of the transmission network of a country which connects Grid Substations and the Power stations. Performance of transmission lines has a great impact on reliability aspects of a particular power supply system of a country. Unreliable transmission lines can lead to partial or even total power failures resulting with great financial losses. Radially connected power stations can be isolated from the transmission network by tripping the connected lines to the transmission system. The lightning back flashover effects are recognized as one of the major causes of transmission line outages.

Several types of solutions are presently available to address the issue of lightning back flashovers. Installing of Transmission Line Arresters (TLA) is of great popularity due to its good performance, with low cost compared to the other traditional solutions. However, latest technology called "Multi Chamber System (MCS)" are now being widely used worldwide to protect transmission lines as well as distribution lines from lightning surges including direct and indirect lightning surges. A novel technology, extension of MCS, Multi Chamber Insulator Arresters (MCIA) are the latest arrester technology which has great advantages over all the traditional surge mitigation techniques including installation of TLAs.

This report describes a case study which was carried out on one of a critical 132kV transmission line of the Sri Lankan transmission network, having several past records of lightning back flashover related outages resulting with partial system failures.

The study described in this report is mainly focuses on the way of analyzing the back flashover events by transient modeling and subsequent simulation of the selected transmission line in an electromagnetic transient computer program. The study uses the Power System CAD (PSCAD) software program as the software tool for the purpose of modeling and simulation of selected 132kV, Mathugama-Kukle transmission line.

Simulation of the created transmission line model is carried out with and without MCIA model to evaluate the improvements in lightning back flashover performance after installation of MCIAs in the selected transmission line.

The result of the simulations shows that the installation of 06 Nos. of MCIAs on all phases of a selected tower improves the back flashover mitigation performance on the same tower as well as the towers on the either sides of the selected tower. Thus, lightning performance of the selected transmission line is improved.

DEDICATION

To my loving Parents, Wife and Son

ACKNOWLEDGEMENT

I sincerely thank my supervisor, Dr. K.T.M.U. Hemapala for his great supervision and guidance offered for the successful completion of this study. I extent my sincere thanks to lecturers of Electrical Engineering Department, University of Moratuwa, who gave me the theoretical knowledge and the support during the study period to make the study practical and meaningful.

My special thanks go to Dr. U.N. Gnanarathna, University of Manitoba, Canada, who spent his valuable time to guide me and providing valuable information required for this study.

Further, my great gratitude goes to Mr. Matthieu ZINCK, Asia-Pacific Manager, Mr. Potcharamon KALAPONG, Regional Office Manager for their valuable support and the MCIA samples given free of charge to the University of Moratuwa. Also, my special thanks to the Supplies Unit of the University of Moratuwa, Sri Lanka for the support given for obtaining free samples from the Streamer Company.

I would like to express my sincere gratitude to Eng. W.W.R.Pitawala, Eng. W.N. Jayalath, Eng. K.S.S.Kumara, Eng. C.D. Wijeweera, Eng. M.Chanaka, Eng. D.L.P. Munasinghe, Eng. S.C.D. Kumarasinghe, Eng. R.C.P. Rajapakshe, Eng. A.D.G. Chandrasena Eng. L.A.A.N. Perera, Eng. W.M.O.M. Withanage working at Ceylon Electricity Board for their excellent support and the encouragement towards the success of this academic work.

Further, I would like to thank many individuals, friends and colleagues who have not been mentioned here personally in making this educational process a success.

Finally, I admire with great pleasure that I remember the encouragement and support extended by my parents and my wife. May be I could not have completed this research without their valuable support.

K.P.R.D.S.K. Dharmadasa
May 17, 2016

TABLE OF CONTENTS

LIST OF FIGURES

LIST OF TABLES

LIST OF ABBREVIATIONS

BFR	Back Flashover Rate
CEB	Ceylon Electricity Board
CFO	Critical Flashover
CIGRE	Conseil International des Grands Réseaux Électriques
CPDL	Constant Parameter Distributed Line
EMTDC	Electromagnetic Transients including DC
EMTP	Electromagnetic Transients Program
GFD	Ground Flash Density
GSW	Galvanized Steel Wire
GUI	Graphical User Interface
GW	Ground Wire
IEEE	Institute of Electrical and Electronics Engineers
IKL	Isokaraunic Level
KMDL	Kukule Mathugama Double Circuit Line
MCIA	Multi Chamber Insulator Arrester
MCS	Multi Chamber System
OPGW	Optical Fiber Ground Wire
PSCAD	Power System Computer Aided Design
TLA	Transmission Line Arrester

LIST OF APPENDICES

CHAPTER - 01

INTRODUCTION

1.1 Back Flash-Over Effect of Transmission Lines

A lightning stroke, terminating on the shield wires, produces waves of currents and voltages travelling on the shield wires called travelling waves and reflections occurs at every points where impedance discontinuities. Accordingly surge voltages can be developed across line insulators exceeding the Critical Flashover Voltage (CFO) where flashovers occur from tower to line called Back Flash or Back Flashover and the number of flashovers per 100km per year is defined as the Back Flashover Rate or BFR.

Towers which have high tower footing resistance in lightning prone areas have higher probability for occurrence of back flashover and the cases are getting worst in hill terrains.

Most of the transmission lines of Sri Lanka are traversed through hilly terrain areas (mountains) of heavy lightning prone zones and therefore, so many lines have back flashover problems and hence reduce the transmission system reliability. Among these transmission lines, Kukule-Mathugama, 132kV transmission line has a huge problem of back flashover and therefore, most of the time Kukule Power Station (35MW X 2) is separated from the Transmission network causing the low system reliability.

Therefore, study for back flashover of Kukule-Mathugama, 132kV transmission line is important to improve the system reliability of the Sri Lankan Transmission network.

Following sections described the lightning phenomenon related to the back flashover effect for the transmission lines.

1.2 Historical Overview of Lightning

It is likely that lightning was present on Earth long before life evolved on our planet about three billion years ago. Further, it is possible that lightning played a role in producing the organic molecules necessary for the formation of every life form

(Oparin 1938)[1]. Encounters of early humans with lightning undoubtedly were frightening and fascinating. All ancient civilizations incorporated lightning and thunder in their religious beliefs.

There exists a long record of lightning damage to tall structures, particularly churches, covering the period from the Middle Ages to the modern era. For example, the Campanile of St. Mark in Venice, which is about 100 m high, was damaged or destroyed by lightning in 1388, 1417, 1489, 1548, 1565, 1653, 1745, 1761, and 1762.

In 1766, a lightning protective system, invented in 1752 by Benjamin Franklin and often referred to as a Franklin rod system, was installed and no further lightning damage has occurred since [1].

Not only the tall structures in the lands got damaged, but also in the sea by the lightning strikes. Many ships with wooden masts have been severely damaged or totally destroyed by lightning. Harris (1834, 1838, 1839, 1843) reported that from 1799 to 1815 there were 150 cases of lightning damage to British naval vessels. One ship in eight was set on fire, nearly 100 lower masts were destroyed, about 70 sailors were killed, and more than 130 people were wounded. In 1798, the 44-gun ship Resistance exploded as a result of a lightning discharge [1].

Systematic studies of thunderstorm electricity can be traced back to 10 May 1752 in the village of Marly-la-Ville, near Paris. On that day, in the presence of a nearby storm, a retired French dragoon, acting on instructions from Thomas-Fran¸cois Dalibard, drew sparks from a tall iron rod that was insulated from ground by wine bottles. The results of this experiment, proposed by Benjamin Franklin, provided the first direct proof that thunderclouds contain electricity, although several scientists had previously noted the similarity between laboratory sparks and lightning (Prinz 1977; Tomilin 1986).

Franklin also showed that lightning flashes originate in clouds that are “most commonly in a negative state of electricity, but sometimes in a positive state” (Franklin 1774).

Experiments on lightning continued without discontinuing and in the late nineteen century, photography and spectroscopy became available as diagnostic tools for

lightning research. Time-resolved photographs showing that lightning flashes often contain two or more strokes, similar to that shown in Figure 1.1, were obtained [1].

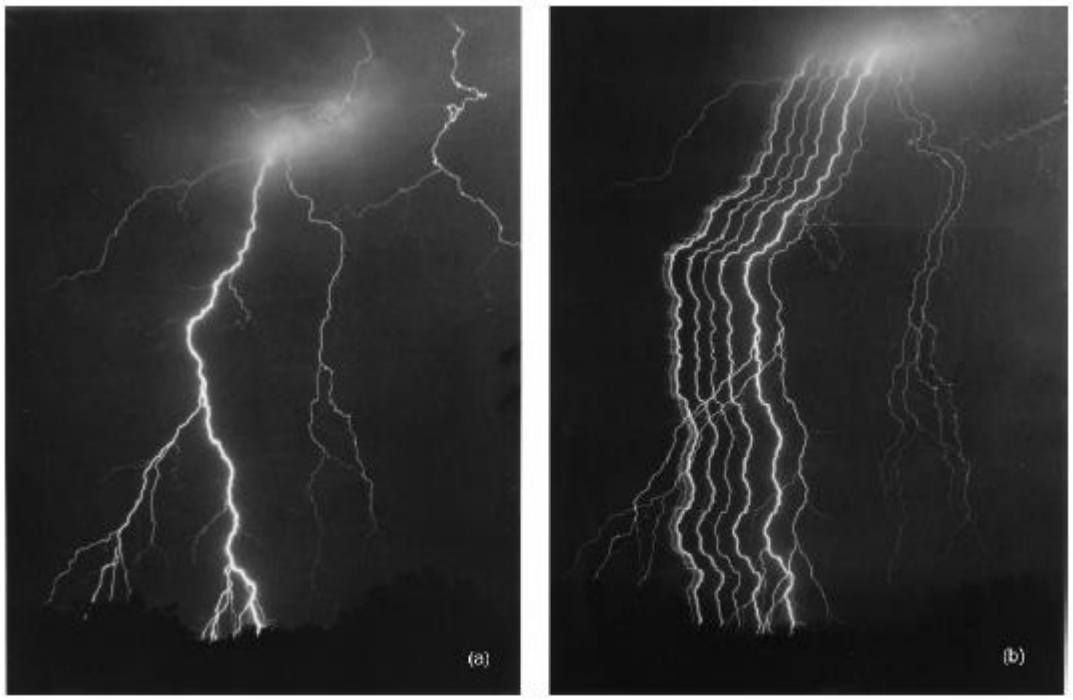

Figure 1.1 - Time-resolved photograph of a lightning flash

As researches on lightning continues, first estimation of peak currents were made by made by Pockels (1900). The first oscillographic recordings of lightning current waveforms were obtained using tethered balloons in Russia (Stekolnikov and Valeev 1937) and in England (Davis and Standring 1947) [1].

The most comprehensive data on lightning current waveforms to date were acquired by K. Berger and his associates on two instrumented towers on Monte San Salvatore in Switzerland.

Even though the Benjamin Franklin had showed that the lightning is a discharge of static electricity; the development of theoretical understanding was rises as the field of power engineering came in to practice, where the power transmission and distribution lines were severely affected by lightning. As a result there were lot of experiments on lightning and in 1900, Nikola Tesla generated artificial lightning by using a large Tesla coil, enabling the generation of enormously high voltages sufficient to create lightning.

1.3 Mechanism of Lightning

As described in [3], lightning is an electric discharge in the form of a spark or flash originating in a charged cloud. It has now been known for a long time that thunder clouds are charged, and that the negative charge centre is located in the lower part of the cloud where the temperature is about - 5^0C, and that the main positive charge centre is located several kilometres higher up, where the temperature is usually below - 20^0C. In the majority of storm clouds, there is also a localised positively charged region near the base of the cloud where the temperature is 0^0C. Figure 1.2 shows such a cloud located above an overhead transmission line.

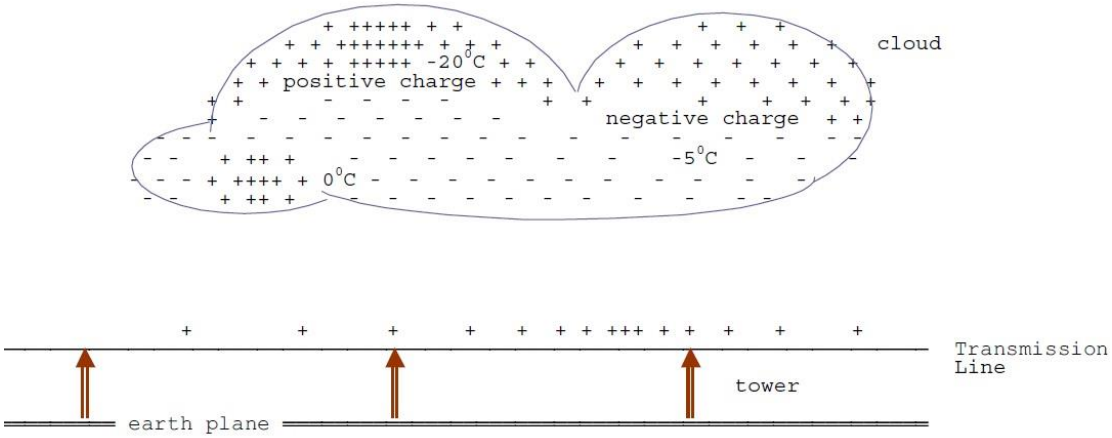

Figure 1.2 - Induced charges on transmission lines

Fields of about 1000 V/m exist near the centre of a single bipolar cloud in which charges of about 20 C are separated by distances of about 3 km, and indicate the total potential difference between the main charge centres to be between 100 and 1,000 MV. The energy dissipated in a lightning flash is therefore of the order of 1,000 to 10,000 MJ, much of which is spent in heating up a narrow air column surrounding the discharge, the temperature rising to about 15,000 ^{0}C in a few tens of microseconds. Vertical separation of the positive and negative charge centres is about 2 - 5 km, and the charges involved are 10 - 30 C. The average current dissipated by lightning is of the order of kilo-amperes. During an average lightning storm, a total of the order of kilo-coulombs of charge would be generated, between the 0^0C and the -40 ^{0}C levels, in a volume of about 50 km^3 [3].

1.4 Charge separation of thunder clouds

The very first process of generating lightning is considered as the charge separation in a thunder cloud. There are two hypotheses describing the process of charge separation in a thunder cloud called “Polarization mechanism” and “Electrostatic induction” [9].

The Polarization mechanism has two sub components as mentioned below.

a) Falling droplets of ice and rain become electrically polarized as they fall through the atmosphere's natural electric field
b) Colliding ice particles become charged by electrostatic induction

Ice and super-cooled water are the keys to the process. Turbulent winds move violently these super-cooled water droplets, causing them to collide. When the super-cooled water droplets hit ice crystals, some negative ions transfer from one particle to another. The smaller, lighter particles lose negative ions and become positive; the larger, more massive particles gain negative ions and become negatively charged.

According to the electrostatic induction hypothesis charge separation appears to require strong updrafts which carry water droplets upward, super-cooling them to between -10 and -20^0C. These collide with ice crystals to form a soft ice-water mixture called Graupel. The collisions result in a slight positive charge being transferred to ice crystals and a slight negative charge to the Graupel. Updrafts drive lighter ice crystals upwards, causing the cloud top to accumulate increasing positive charge. The heavier negatively charged Graupel falls towards the middle and lower portions of the cloud, building up an increasing negative charge. Charge separation and accumulation continue until the electrical potential becomes sufficient to initiate lightning discharges, which occurs when the gathering of positive and negative charges forms a sufficiently strong electric field.

Therefore due to charge separation process, in most of the thunder clouds there is a Negative Charge Centre at the bottom of the cloud where the temperature is about -5^0C, whereas Positive Charge Centre appears at the top of the cloud at temperature about -20^0C. In addition to these there are localized positively charged region formed near the base of the cloud where the temperature is about 0^0C.

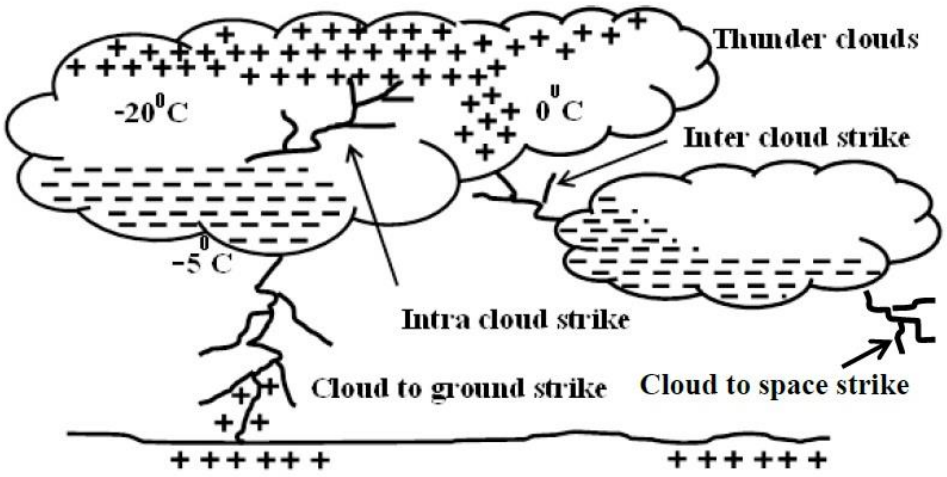

Figure 1.3 - Charge distribution of thunder clouds and types of lightning

1.5 Breakdown Process and leader formation

Under the influence of sufficiently strong fields, large water drops become elongated in the direction of the field and become unstable, and streamers develop at their ends with the onset of corona discharges. Drops of radius 2 mm develop streamers in fields exceeding a 9 kV/cm - much less than the 30 kV/cm required to initiate the breakdown of dry air. The high field need only be very localized, because a streamer starting from one drop may propagate itself from drop to drop under a much weaker field.

When the electric field in the vicinity of one of the negative charge centres builds up to the critical value (about 10 kV/cm), an ionized channel (or streamer) is formed, which propagates from the cloud to earth with a velocity that might be as high as one-tenth the speed of light. Usually this streamer is extinguished when only a short distance from the cloud.

Forty micro-seconds or so after the first streamer, a second streamer occurs, closely following the path of the first, and propagating the ionized channel a little further before it is also spent. This process continues a number of times, each step increasing the channel length by 10 to 200 meters. Because of the step like sequence in which this streamer travels to earth, this process is termed the stepped leader stroke. This process is shown diagrammatically in Figure 1.4.

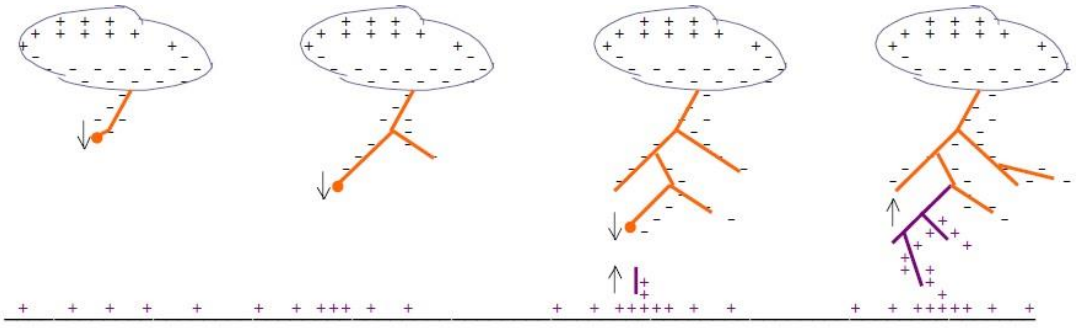

Figure 1.4 - Propagation of lightning channel

When eventually the stepped leader has approached to within 15 to 50 meters of the earth, the field intensity at earth is sufficient for an upward streamer to develop and bridge the remaining gap. A large neutralizing current flows along the ionized path, produced by the stepped leader, to neutralize the charge. This current flow is termed the return stroke and may carry currents as high as 200 kA, although the average current is about 20 kA.

The luminescence of the stepped leader decreases towards the cloud and in one instances it appears to vanish some distance below the cloud. This would suggest that the current is confined to the stepped leader itself. Following the first, or main stroke and after about 40 ms, a second leader stroke propagates to earth in a continuous and rapid manner and again a return stroke follows. This second and subsequent leader strokes which travel along the already energized channel are termed dart leaders.

What appears as a single flash of lightning usually consist of a number of successive strokes, following the same track in space, at intervals of a few hundredths of a second. The average number of strokes in a multiple stroke is four, but as many as 40 have been reported. The time interval between strokes ranges from 20 to 700 ms, but is most frequently 40-50 ms. The average duration of a complete flash being about 250 ms.

The approximate time durations of the various components of a lightning stroke are summarized as follows.

Stepped leader	= 10 ms
Return stroke	= 40 μs
Period between strokes	= 40 ms
Duration of dart leader	= 1 ms

For the purpose of surge calculations, it is only the heavy current flow during the return stroke that is of importance. During this period it has been found that the waveform can be represented by a double exponential of the form,

$$i = I\,(e^{-\propto t} - e^{-\beta t})$$

With wave front times of 0.5 – 10 μs, and wave tail time of 30 – 200 μs (An average lightning current waveform would have the wave front of the 6μs and a wave tail of the order of 25μs). The values of the exponential coefficients are described in the Chapter-3.

1.6 Types of lightning

Currently there are few number of major lightning types have been recognized based on particular characteristics exhibits by each types of lightning strokes [9].

1. Cloud to Ground
2. Inter Clouds
3. Intra Clouds
4. Cloud to Space

are few major types of them (See Figure 1.3). In addition, there are few minor types were also recognized called Dry lightning, Rocket lightning, Positive lightning, Ball lightning and Upper-atmospheric lightning.

1.7 Frequency of occurrence of lightning flashes

A knowledge of the frequency of occurrence of lightning strokes is of utmost importance in the design of protection against lightning. The frequency of occurrence is defined as the flashes occurring per unit area per year.

However, this cannot be measured very easily, and without very sophisticated equipment. This information is difficult to obtain. However, the keraunic level at any location can be quite easily determined. The keraunic level is defined as the number of days in the year on which thunder is heard. It does not even distinguish between whether lightning was heard only once during the day or whether there was a long thunderstorm. Fortunately, it has been found by experience that the keraunic level is

linearly related to the number of flashes per unit area per year. In fact it happens to be about twice the number of flashes/square mile/year. By assuming this relationship to hold good throughout the world, it is now possible to obtain the frequency of occurrence of lightning in any given region quite easily

1.8 Lightning data of Sri Lanka

The isokeraunic level map, which shows contours of equal keraunic level, for Sri Lanka is shown in Figure 1.5.

The map is based on the findings of the study “Lighning conditions in Ceylon and measures to reduce damage to electrical equipment” by Dr Gi-ichi Ikeda in 1968 (Asian Productivity organization report, May 1969 – AP) Project TES/68).

Department of Meteorology of Sri Lanka records the Number of thunder days at 24 locations all over the country and can be obtained with the written request to the Department of Meteorology of Sri Lanka.

Figure 1.5 - Isokeraunic level map of Sri Lanka

1.9 Lightning Problem for Transmission Lines

The negative charges at the bottom of the cloud induces charges of opposite polarity on the transmission line. These are held in place in the capacitances between the cloud and the line and the line and earth, until the cloud discharges due to a lightning stroke. The Figure 1.6 shows the problems facing the transmission engineer caused by lightning. There are three possible discharge paths that can cause surges on the line.

a) In the first discharge path (1), which is from the leader core of the lightning stroke to the earth, the capacitance between the leader and earth is discharged promptly, and the capacitances from the leader head to the earth wire and the phase conductor are discharged ultimately by travelling wave action, so that a voltage is developed across the insulator string. This is known as the induced voltage due to a lightning stroke to nearby ground. It is not a significant factor in the lightning performance of systems above about 66 kV, but causes considerable trouble on lower voltage systems.

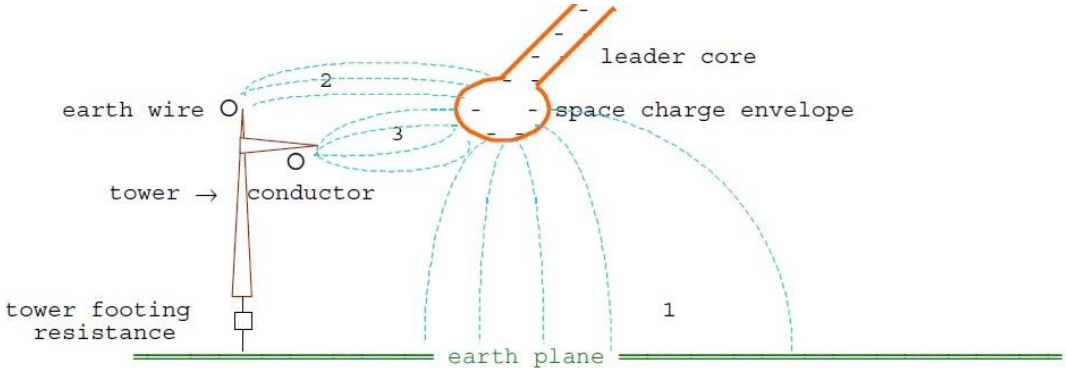

Figure 1.6 - Geometry of lightning leader stroke and transmission line

b) The second discharge path (2) is between the lightning head and the earth conductor. It discharges the capacitance between these two. The resulting travelling wave comes down the tower and, acting through its effective impedance, raises the potential of the tower top to a point where the difference in voltage across the insulation is sufficient to cause flashover from the tower back to the conductor. This is the so-called back-flashover mode.

c) The third mode of discharge (3) is between the leader core and the phase conductor. This discharges the capacitance between these two and injects the main discharge current into the phase conductor, so developing a surge impedance voltage across the insulator string. At relatively low current, the insulation strength is exceeded and the discharge path is completed to earth via the tower. This is the shielding failure or direct stroke to the phase conductor.

The protection of structures and equipment from the last mode of discharge by the application of lightning conductors and/or earth wires is one of the oldest aspects of lightning investigations, and continue to do so.

1.10 Lightning Parameters

There are several lightning parameters (See Table 1.1) of primary interest to the electric power utility engineer are defined and used to address the lightning issues as described in the previous section. Some of them are described in the following sections**.**

Table 1.1: Range of values for lightning parameters

Parameter	Minimum	Typical	Maximum
Number of return strokes per flash	1	2 to 4	26
Duration of flash (s)	0.03	0.2	2
Time between strokes (ms)	3	40 to 60	100
Peak current per return stroke (kA)	1	10 to 20	250
Charge per flash (C)	1	15 to 20	400
Time to peak current (μs)	<0.5	1.5 to 2	30
Rate of rise (kA/μs)	<1	20	210
Time to half value (μs)	10	40 to 50	250
Duration of continuing current (ms)	50	150	500
Peak continuing current (A)	30	150	1600
Charge in continuing current (C)	3	25	330

1.10.1 The quantity of lightning activity in a given area

The quantity of lightning activity is ideally measured in terms of the number of lightning flashes per unit area per year, called the Ground Flash Density (GFD). This value, denoted as N_g, is in units of flashes per km^2 per year. Today, the GFD is usually measured by use of lightning location systems, either by gated wideband magnetic direction-finding systems or time-of-arrival systems. Before using these advanced systems the GFD is calculated with the aid of local IKL data. The IEEE and CIGRE recommend a rough relationship of GFD and local IKL as shown in the equation 1-1 below [6].

$$GFD = 0.04\ T_d^{1.25} = 0.054\ T_h^{1.1} \qquad (1\text{-}1)$$

Where,

GFD = average flashes to earth/km^2/year

T_d = average thunder days per year (keraunic level)

T_h = average thunder hours per year (keraunic level)

1.10.2 The distribution of the crest current of a lightning flash

A primary database for lightning parameters was initially developed by Professor Karl Berger in Switzerland based on the number of strokes recorded on 70m and 80m high masts, located on top of the 650m high Mount San Salvatore. There were 1196 flashes in 11 years. Out of these, 75% were negative-upward, 11% were negative-downward, and the remainder was positive-upward [6]. These data was used in combination with some other recorded data at different countries to form the well know CIGRE crest current distribution curve. In addition to the CIGRE distribution cure there was a another equation formulated to obtain the crest current distribution curve by Anderson [6] and adopted by the IEEE/PES Working Group on Estimating the Lightning Performance of Transmission Lines. Both these curves give almost the same distribution with deviations at very low and very high currents where the available lighting data is minimum (See Figure 1.7).

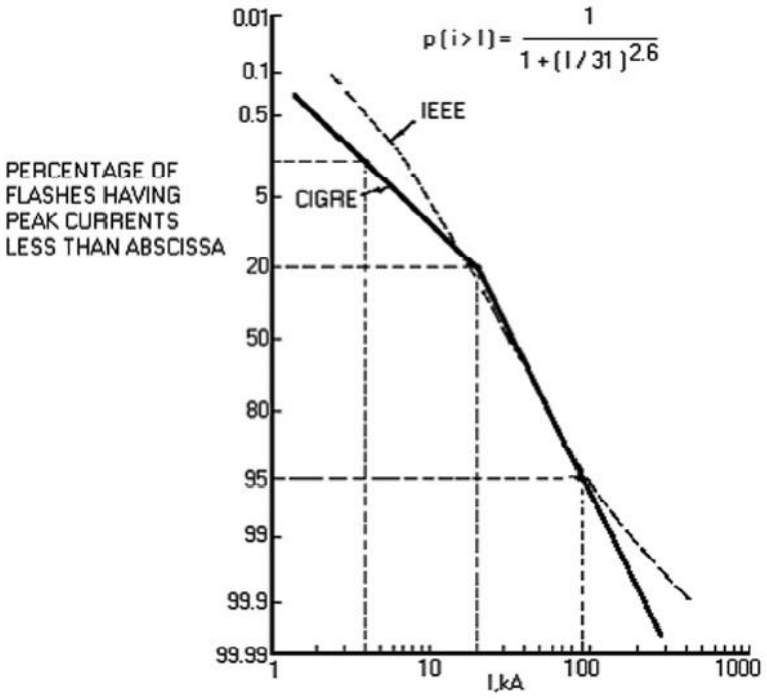

Figure 1.7 - Lightning Stroke Current Probability Distribution [6]

1.10.3 The wave shape of a lightning flash

Almost all lightning strokes are different from each other and therefore no two stroke current wave shapes are exactly alike, and the variations in wave shape are substantial. Most computer programs that calculate line lightning performance assume a straight rising front, a double exponential wave shape, or a CIGRÉ wave shape.

There is no exact rule for the use of a wave shape for EMTP simulations and the selection is depending on the type of EMTP analysis or the application. The front time, tail time, peak current magnitude and the total charge delivered by the stroke current are the basic parameters govern by the wave shape.

1.10.4 Total charge delivered by a lightning stroke

An approximated estimate of total charge delivered by a lightning stroke can be obtained by integrating its current waveform. By this integration results, it clearly shows that higher potion of the total charge delivered is associated with the tail side of the waveform rather at the front of it after the crest current is reached. Therefore the tail time of a lightning current stroke is the governing fact which determines the total charge delivery. Also the total charge in a lightning flash that determines the energy fed into surge arresters, and it is also the charge that causes pitting and burning of shield wires at contact points. It has been noted that, between some stroke current peaks and at the current decay at the end of lightning flashes, a low, almost direct current, can flow for many milliseconds; more charge can be delivered by this low current than by the high current peaks in a flash. These low currents, because of their longer duration, act somewhat like an arc welder. Continuing currents of hundreds of amperes lasting hundreds of milliseconds have been measured on instrumented towers. These continuing currents can transfer many coulombs of charge in addition to the main portion of the lightning wave shape [29].

Berger [29] integrated the current records of downward flashes to Monte San Salvatore in Switzerland to determine the charges delivered and reported that in one case a positive charge reached 300 coulombs. The positive flashes tend to deliver

almost 10 times as much charge as negative flashes, but positive flashes are much less frequent [29].

1.11 Selected transmission line for the study

The case study described in this report is based on the 132kV, transmission line which connects Kukule Generation Station to Mathugama Grid Substation as shown in the Figure 1.8.

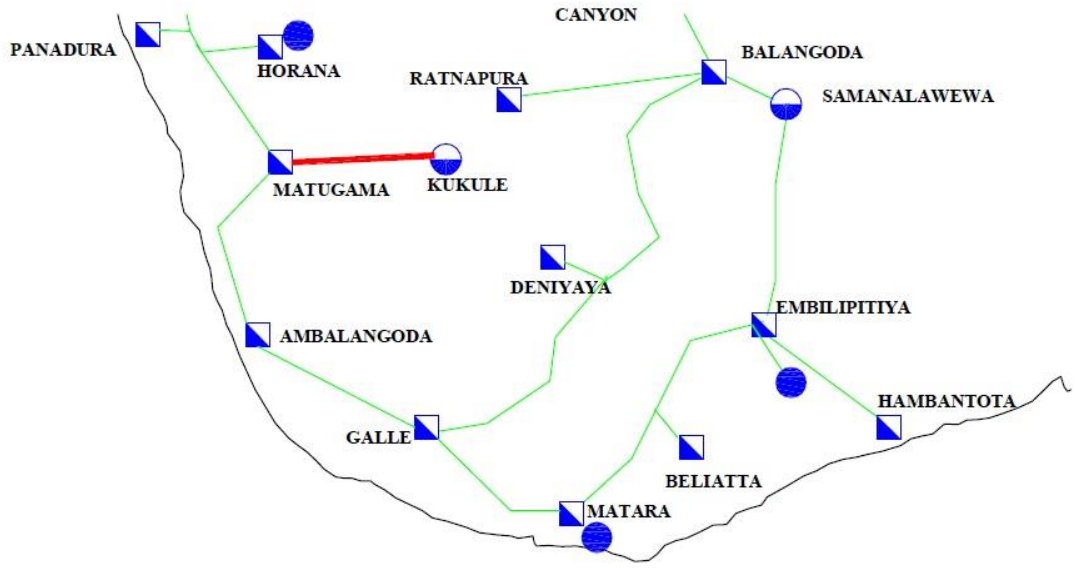

Figure 1.8 - Mathugama-Kukule, 132kV Transmission Line

The transmission line selected in this study is about 30km in length and having 79 Nos. of double circuit steel lattice towers with 02 nos. of Earth Wires of Galvanized Steel and OPGW providing protection against lightning. The phase conductors are Lynx and the complete set of line data is attached as Annex 3.

Even though, this line segment is short, the effect of tripping of both circuits of this lines severely affect the stability of the transmission network of the southern region of the country which shown in Figure 1.9.

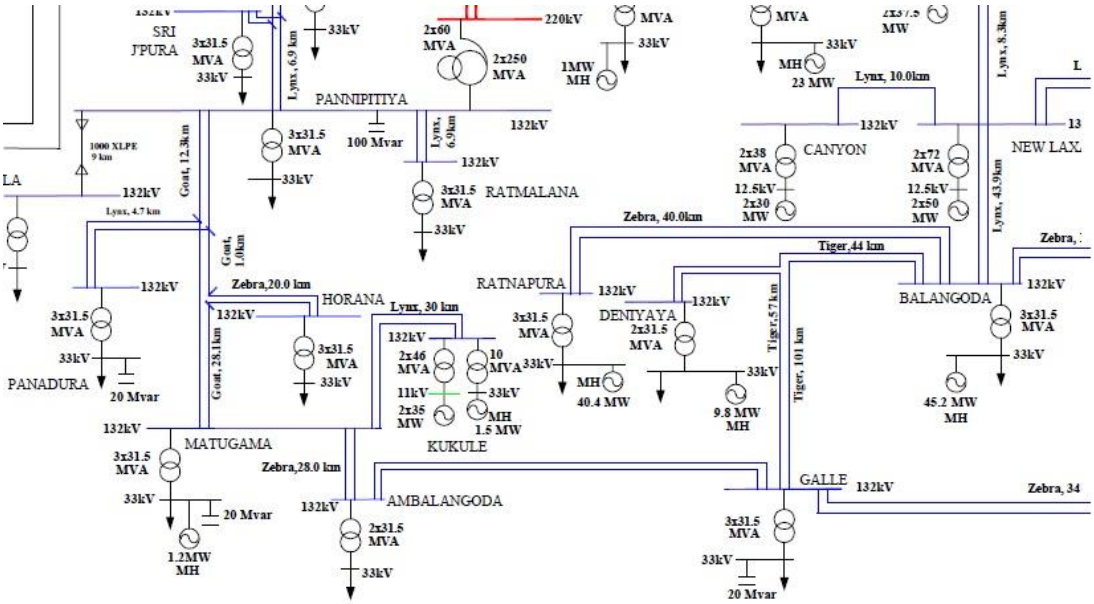

Figure 1.9 - Single Line Diagram of Transmission Lines in Southern Part

1.12 Kukule Power Station

Kukule Power Station is a run-of-river type hydroelectric power plant (35 MW × 2 units) equipped with a regulation pond (Figure 1.10) in the Kukule Ganga (River) – a tributary of the Kalu Ganga (River) – which is a large rainfall zone (average precipitation of 3,750 mm per year) in Sri Lanka; thereby contributing to the alleviation of the tight supply-demand situation for electricity and to the socio-economic development of Sri Lanka. Figure 1.11 shows the Vicinity of the Kukule Ganga Hydroelectric Power Plant

Figure 1.10 - Regulation Pond of the Kukule Ganga Hydro Power Plant

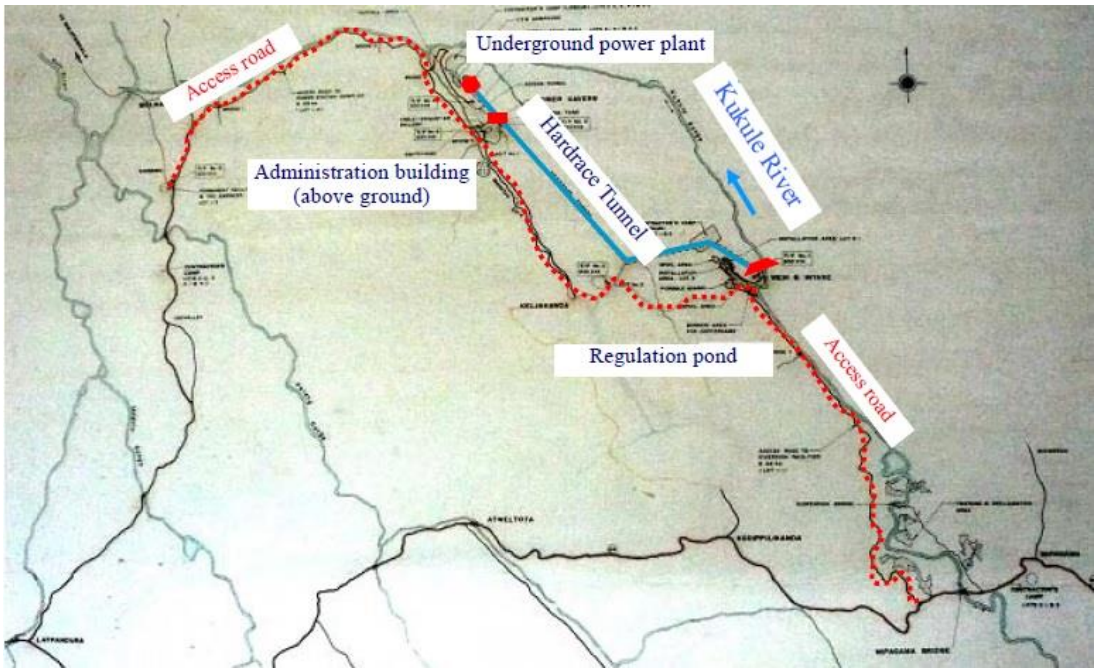

Figure 1.11 - Vicinity of the Kukule Ganga Hydroelectric Power Plant

The rated output of the power plant is 70 MW, but the power plant is capable of producing a maximum of 80 MW of electricity. Until 2005, the power plant had been generating 80 MW of electricity per year not to waste the river flow as much as possible, but for the sake of safety, since the outbreak of the fire near Generator No. 2 in 2005, the power plant has been operating at 75 MW capacity or lower.

Electricity produced by the Kukule Ganga Hydroelectric Power Plant is being supplied to all parts of Sri Lanka through a national power grid. In 2006, the power plant supplied about 4.0% of the total amount of electricity supplied in Sri Lanka at peak hours, and about 3.4% of the amount of electricity supplied per annum. Thus, the project is contributing to the provision of the stable supply of electricity mainly at peak hours [30]. Table1.2 shows the Maximum output and the Annual Power Generation since year 2003.

Table 1.2: Maximum power and the Annual power generation

	2003 Oct–Dec	2004	2005	2006	2007
Maximum output (MW)	80	80	80	75	75
Annual power generation (GWh)	79	318	317	319	270
Annual operating hours (2 units total: hours)	2,098	8,865	8,797	9,003	7,665

1.12.1 Transmission Towers and configuration

As described in the previous section the selected transmission line consists of 79 Nos. double circuit, self-standing, steel lattice towers with standard 3m, 6m, 9m and 12m body extensions at some certain locations to maintain the minimum ground clearance value of 6.7m. Therefore, the typical tower height will vary between 25 to 40m. Conductor arrangement at towers is in vertical formation where each cross arm holds a Lynx conductors for each phase. A typical tower drawing is attached as Annex 4.

1.12.2 Insulators and arc horn gaps

Toughen glass and porcelain Cap & Pin type insulator discs along with galvanized insulator hardware are used to form both suspension and tension insulator strings. Each line insulator string of this transmission line is consists of an arc horn gap where the gap is adjustable at line termination ends only. The gap of arcing horn for a 132kV line is set to be 1.5m whereas the gap at termination ends will be adjusted as per the insulation coordination requirements of the substation equipment. CEB specification for a single insulator disc is given in Table 1.3.

Table 1.3: CEB specification for a single insulator disc

Dimensions	**Units**	**Suspension string**	**Tension string**
Nominal diameter of disc	mm	254	280
Nominal spacing of disc	mm	146	146
Nominal creepage distance	mm	280	300
Withstand voltages			
Power frequency, Dry	kV	70	70
Power frequency, Wet	kV	40	40
Impulse 1.2x50uS	kV	110	110
Puncture voltage	kV	110	110
Electro mechanical failure load	kN	120	160

1.12.3 Phase conductors

Single Lynx conductors having overall area of 226.2 mm^2 are used for the phase conductors of the selected transmission line having maximum operating temperature at 75^0C.

1.12.4 Earthing of towers

Earthing of towers is of great importance due to its direct impact on line performance at lightning events. Most of the tower earthing has been done through the tower foundation where a strip of metal bonded to the tower leg is taken out and earth separately. Very low earth resistances in the order of 2Ω to 3Ω are obtained where insitu or precast pile foundations used in marshy soil conditions.

Achieving of CEB specified 10Ω earthing resistance is of great difficulty in the areas where the towers are located in rocky lands or gravel soil conditions. In such cases counterpoise wires were used with specified lengths. Figure 1.12 shows the variation of earthing resistances of selected line starting from Mathugama end. Figure 1.13 and the Figure 1.14 illustrate the condition of a specific tower footing and the elevation profile along the line extracted from the Google Earth software.

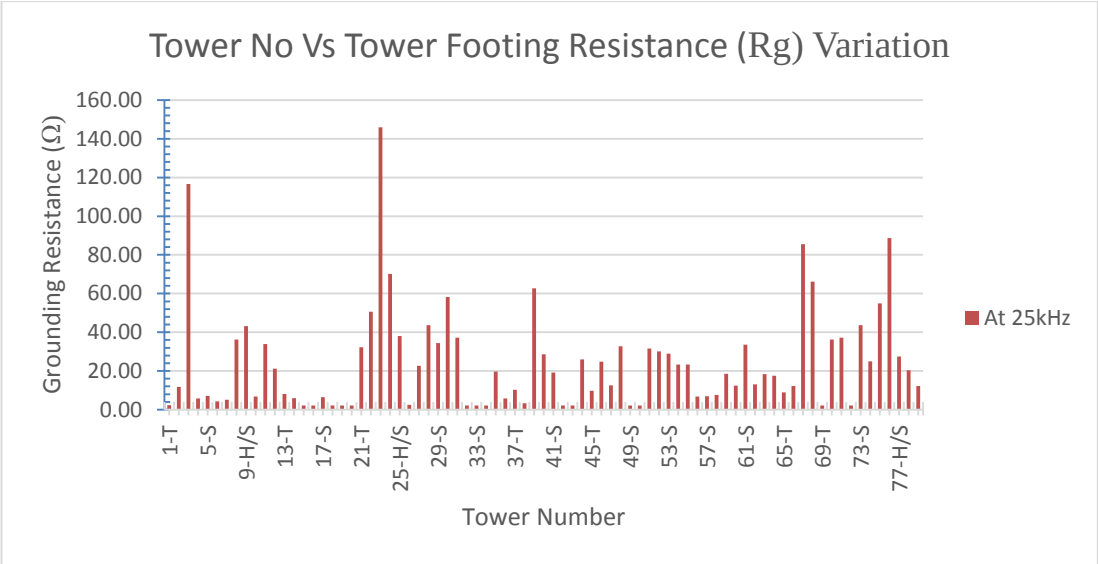

Figure 1.12 - Tower Footing Resistance Variation

Figure 1.13 - Tower footing condition of the Tower-09

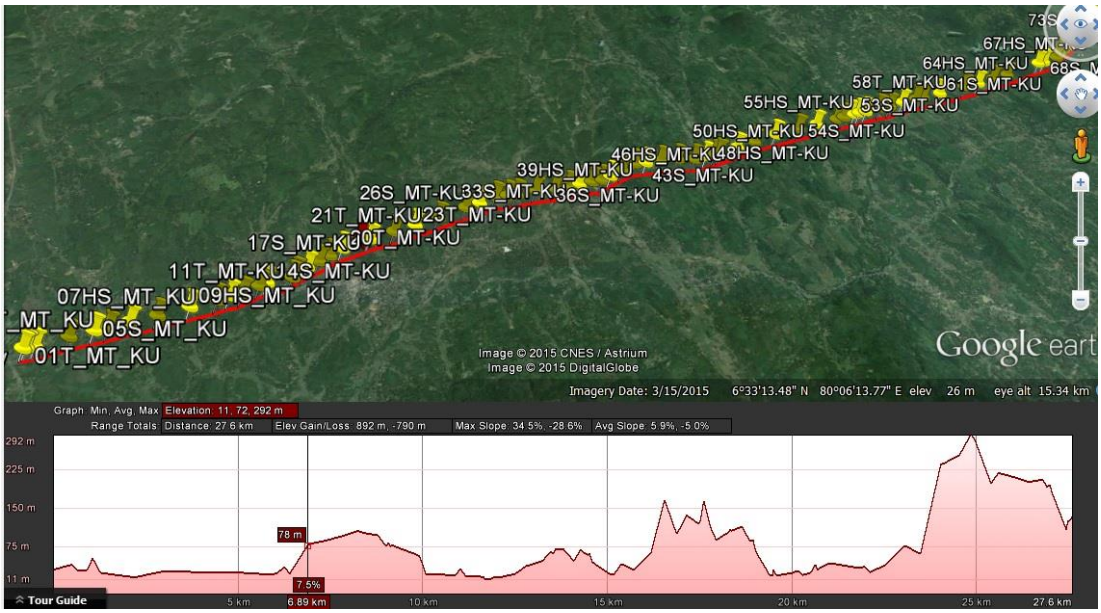

Figure 1.14 - Elevation profile of the line

CHAPTER - 02

PROBLEM IDENTIFICATION

2.1 Introduction

The performance of a power system is mainly depending on the performance of transmission lines. Therefore continues operation of transmission lines without sudden outages is utmost important for the performance in the view point of power delivery as well as system stability. Lightning effects on transmission lines are one of the major reasons which lead to sudden line outages. As described in the Chapter-01, the back flashover events are the dominant reason of line outages.

The selected 132kV, Mathugama-Kukule transmission line is a double circuit line which delivers the generated power of the Kukule Power Station to the transmission network and then mainly delivers to the southern part of the country.

A single Circuit of Lynx conductor can carry approximately 80MW of generated power and hence, tripping of single circuit may carry total generated power of the Kukule Power Station. Therefore, for this study, only the both circuit tripped occasions were considered. Kukule Power Station is meant to supply for the peak time and sudden outage of this power station creates system frequency to go down and need to recover the loss of generation from the spinning reserve hydro machines or from the thermal generation. The loss of Kukule generation tends to create low voltage of the southern part of the transmission network and sometimes under frequency load shedding schemes may also activated.

Therefore it is utmost important to avoid any double circuit failures by improving the lightning performance of the selected Mathugama-Kukule transmission line to avoid partial failures and associated severe financial losses.

2.2 Preliminary studies

According to the past performance records of this transmission line, it has been noticed that the failure of this transmission line has great influence towards a partial failures of the system. Out of those, most of the line outages were due to the effect of

lightning, since most of them were recorded in the months, April to June and October to November where the lightning is frequent.

2.2.1 The relationship between monthly Isokeraunic level and line failures

According to the studies [4], [9] it has been found that there is a clear relationship between the monthly Isokeraunic level (IKL) variations with the monthly average failures of this line. Tables and graphs showing the "monthly failures" and "IKL variation with monthly failure variation" respectively are reproduced here including few more recently available data. Table 2.1 shows the monthly line failures from 2011 to 2015 whereas the Figure 2.1 illustrates the relationship of IKL level with the monthly transmission line failures.

Table 2.1: Monthly Line Failures and IKL

Month/ Year	Number of Thunder Days										Total Trippings of the Line
	Rathnapura Recording Station					Colombo Recording Station					
	2011	2012	2013	2014	2015	2011	2012	2013	2014	2015	
January	4	4	5	11	5	8	5	1	4	4	**1**
February	6	11	9	7	15	4	11	8	3	11	**6**
March	19	12	26	10	18	12	11	11	9	18	**10**
April	24	24	25	28	27	22	21	7	23	19	**25**
May	14	9	19	17	22	10	4	11	10	12	**3**
June	5	10	9	10	13	9	4	8	9	14	**5**
July	7	4	9	5	7	5	3	7	6	1	**0**
August	7	9	5	11	12	3	9	3	4	6	**2**
September	7	13	8	20	17	4	10	4	10	10	**0**
October	10	21	14	22	22	17	17	7	22	17	**7**
November	19	17	21	14	17	12	9	18	13	16	**11**
December	9	7	4	17	15	6	11	0	15	14	**1**

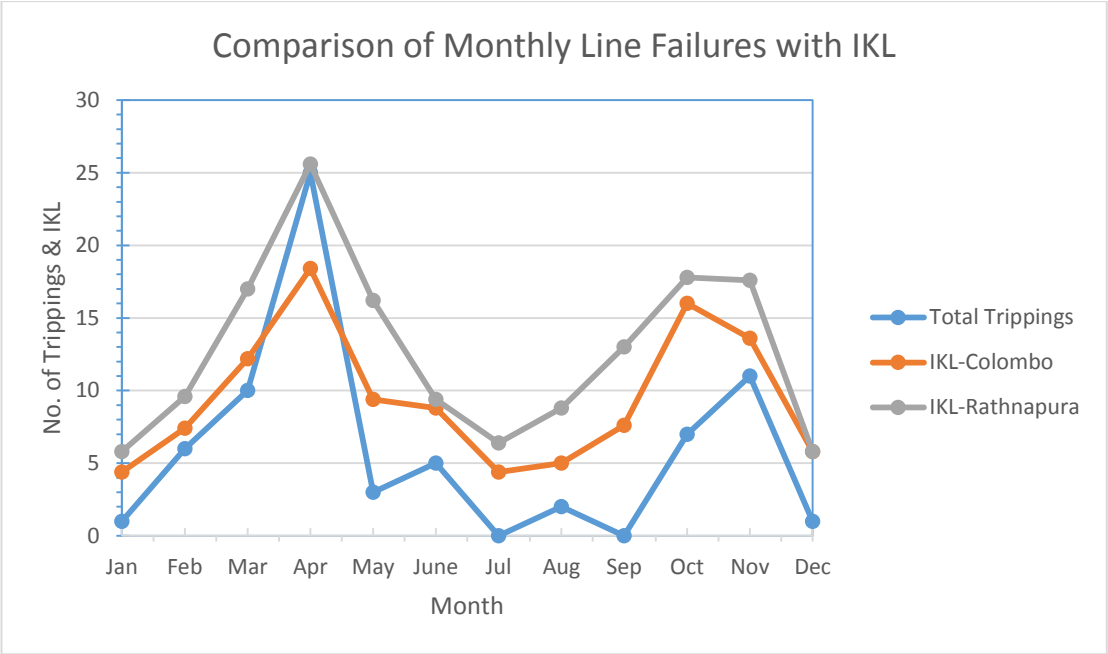

Figure 2.1 - Comparison of Monthly Line Failures with IKL

2.2.2 Line sections/towers having higher probability of insulator failures

Maintenance records of the Hot Line Maintenance Unit of the Transmission Operation and Maintenance Branch of CEB have shown that Tower – 09 and the Tower -23 were the places where frequent insulator damages or flashovers marks were recorded.

Therefore, Tower – 09 has been selected for the study and the simulation criteria covers the characteristics of the Tower-23 and hence, automatically both cases were analyzed.

2.3 Back flashover effects on transmission lines

According to [9], as described in Chapter-01, back flashover events occur when the lightning strikes on either tower or shield wires. These strikes produce waves of currents and voltages travelling on the shield wires called travelling waves and reflections occurs at every points where impedance discontinuities. Accordingly surge voltages can be developed across line insulators exceeding the Critical Flashover Voltage (CFO) where flashovers occur from tower to line called back

flashovers. The following list shows the parameters those affect the line Back Flashover Rate (BFR).

a) Ground flash density (See equation 1-1)

b) Surge impedances of the shield wires and towers

c) Coupling factors between conductors

d) Power frequency voltage

e) Tower and line height

f) Span length

g) Insulation strength

h) Footing resistance and soil composition

2.3.1 Earth faults at power frequency voltage due to back flashover events

An ionization path forms between the Arc horn gaps, when the air insulation between the gaps is breakdown due to a back flashover event. This ionization path acts as a conductive path to form an earth fault condition even at the power frequency voltages. When a transmission line protection system is provided with auto-reclosing facility, the circuit breaker will be reclosed automatically with a set time delay (500ms) after a back flashover trip event to avoid permanent line outage. An earth fault can be developed at power frequency voltage if the ionization path is persists at the moment of first reclosing operation. Therefore the reclosing operation will be blocked and the circuit breaker will be at opened position (breaker lockout) leaving the transmission line at dead condition. This type of line outages can develop severe system instabilities and even total failures. Such events have been reported in the selected Mathugama-Kukule transmission line in the past history of operation.

This issue has been addressed in [9] by proving a software based analysis approach to provide solutions through a Transmission Line Arrester (TLA) and this study addressed new concept of providing protection called Multi Chamber Insulator Arresters (MCIA) which embeds the Arrester function in to the Insulator String.

2.4 Prevention of Back flashover events

Improving tower earthing resistance is the key way of avoiding back flashovers. However, it is not practicable as well as not economical when the towers are located at hilly areas where the soil conditions are very bad (See Figure 1.13). Unbalanced or improved line insulation is another way of preventing back flashovers. However, this is also not an economical way due to the requirement of additional insulator discs as well as this may need modifications in the towers. In the study [9], it is found that the most economical and effective way of preventing back flashovers is to install Transmission Line Arresters at selected tower locations. However, installing TLAs also need special preparations of cross arms or special means of installing on the conductor.

By using MCIA, these issues are not arose and by replacing conventional Insulator String with MCIA String for the selected tower will protects the same and the either side towers from the back flashover effect. In the TLA method, it does not protect the either sides towers from the back flashover effect.

2.5 Project objectives

The objectives of this study are:

1. Modeling of Multi Chamber Insulator Arrester (MCIA) for EMTP simulations and validation of the model.
2. Check the performance for back flashover effect of the transmission line of the MCIA installed system for pre-identified locations.
3. Calculate the simple payback period for installation of MCIAs for pre-identified locations.

To achieve above objectives, following process will be followed,

1. Modeling and simulation of 132kV Mathugama-Kukule transmission line in EMTP software (PSCAD) for lightning back flashover analysis.
2. Modeling of Multi Chamber Insulator Arrester (MCIA) for EMTP simulations and validation of the model.
3. Modeling and simulation of MCIA installed system (for pre-identified locations) in EMTP software (PSCAD) for lightning back flashover analysis.

4. Conducting sensitivity analysis of MCIA line model for back flashover effects.
5. Performance comparison between existing transmission line with MCIA installed system.

CHAPTER - 03

METHODOLOGY

3.1 EMTP/PSCAD Modelling and Simulation

Electro Magnetic Transient Programs can be used for analysing the effects of lightning including back flashovers of power transmission lines consisting fast front transients. The power transmission line and the back flashover event was modelled by the frequency dependant fast front transient models due to nature of higher frequency dependency of lightning strokes typically ranging from 1kHz to 30MHz [1] [9].

3.2 Proposed Electromagnetic transient model for Kukule-Mathugama Transmission Line

The basic hypothetical fast front transient transmission line model which developed in the PSCAD Software is shown in the Figure 3.1. The complete line model consists of several sub-models representing the following transmission line elements [9],

i. "Transmission line section models" including towers up to the line end terminations (Ex: line section with towers from tower no.01 to L1 as shown in the Figure 3.1)
ii. "Transmission line span models" between consecutive towers under study (Ex: span between tower no. L1 to M as shown in the Figure 3.1)
iii. Transmission tower model
iv. Tower grounding resistance model
v. Line insulator string with back flashover model
vi. Line end termination model
vii. Surge Arrester model
viii. Lightning surge generator model
ix. Power frequency phase voltage generator model

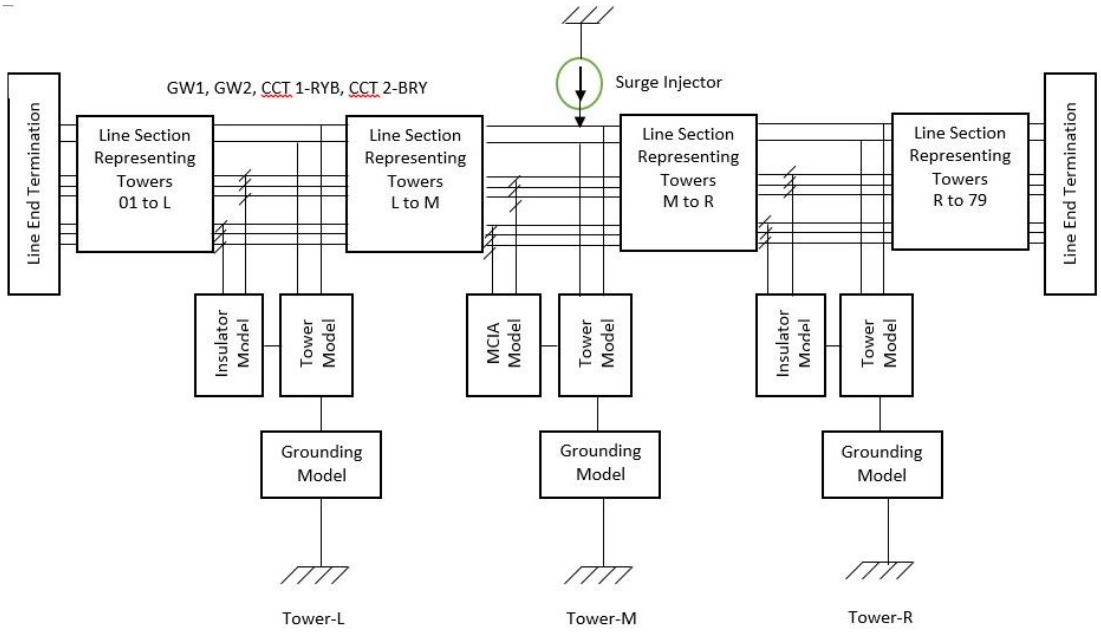

Figure 3.1 – Complete Transmission Line Model for Analysis

As shown in Figure 3.1, the complete line model consists of three towers named by tower number M, L1 and R1 represent a typical tower and two adjacent towers at the left and right sides of it respectively. The two line spans between these three towers were represented by the "line span models" whereas the rest of the line sections at each side up to the end terminations were represented by "line section models". Six number of inter connecting lines were used to connect each modules while representing the ground and phase conductors from top to bottom sequence as shown in the Figure 3.1. The corresponding phase conductor configuration at towers is shown in the Annex 4. All three tower models are connected to the Ground Wire-1(GW-1) and Ground Wire-2 (GW-2) whereas the connections to the phase conductors are made through the insulator models. The surge generator (Current source) is always connected to the top of the middle tower under study.

3.3 Electromagnetic fast front transient sub models for transmission line elements

The sub models used for the implementation of complete EMTP line model is describes in the following sections.

3.3.1 Frequency dependent (Phase) model representing Transmission line sections and spans

The transmission line sections as well as line spans were modelled by using a standard fast front transient module available in the PSCAD library called "Frequency Dependent (Phase) Model" component with different parameter settings to suit both these line elements.

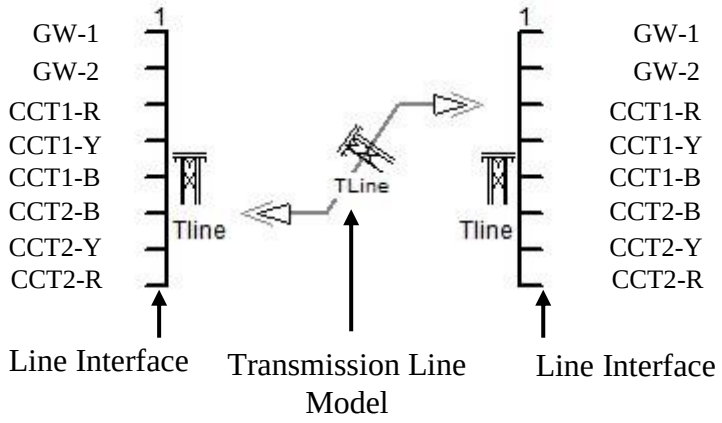

Figure 3.2 - Frequency Dependent (Phase) Model in PSCAD and its connections

Basically the Frequency Dependent (Phase) Model is developed based on the distributed RLC travelling wave model while incorporating the frequency dependency of all line parameters by its internal transformation matrices.

The basic parameters those were fed in to the model are attached as Annex 3.

The Figure 3.2 shows a typical Frequency Dependent (Phase) Model component available in PSCAD with its connection arrangement. Two standard line interface modules available in the PSCAD were also used to build up the interconnection between the Phase modules to the rest of the system at both sides.

3.3.2 Loss-Less Constant Parameter Distributed Line (CPDL) model representing the transmission towers.

The transmission towers were represented by a transient model used in [5], called "Loss-Less, Constant Parameter Distributed Line Model (CPDL)" for lightning Surge Analysis of transmission towers. The model was also used in [6].

A transmission tower is represented by a set of series surge impedances, each individually represents the tower section between the cross arms as shown in the Figure 3.3. The transmission tower is assumed as a loss less vertical transmission line in this study. The surge impedance of a tower is calculated by the formula given in [5,6,7,8,9,10,13] for waist tower shape as shown in Figure 3.3. The formula is given in the equation 3-1 below. The surge impedances representing each tower sections between cross arms as well as bottom cross arm to ground are assumed to be equivalent to form the CPDL tower model in this study. The cross arms are not represented in the tower model.

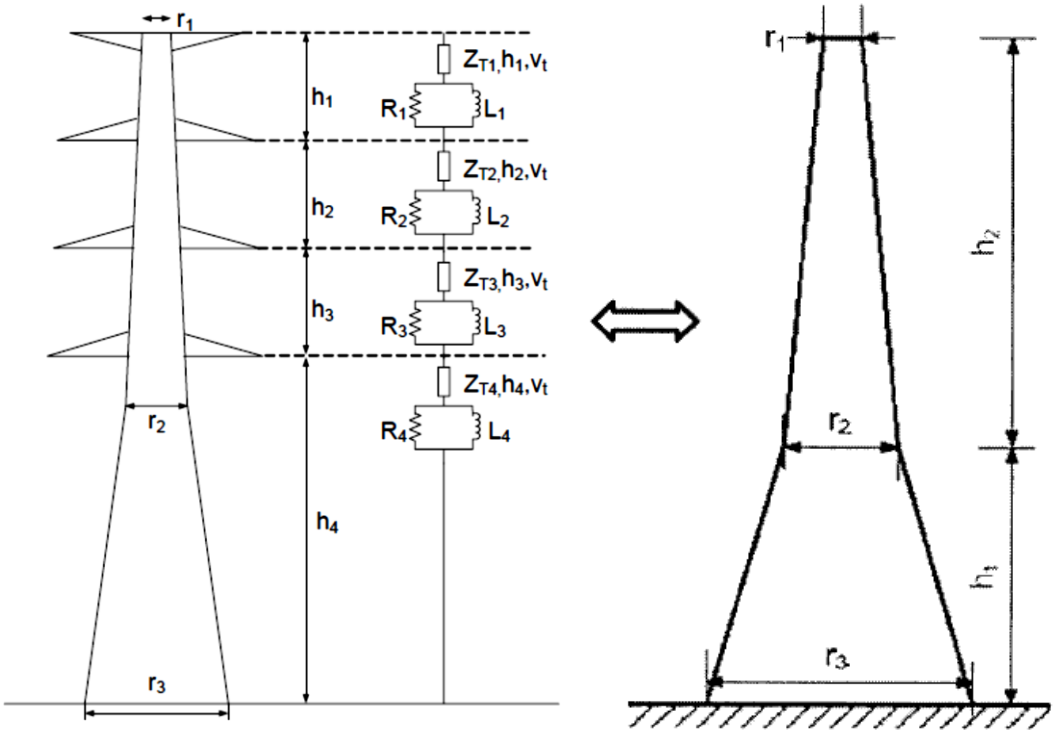

Figure 3.3 - Constant Parameter Distributed Line (CPDL) Model for Towers

$$Z_{T-waist} = 60.\ln\left[\cot\left\{\frac{\tan^{-1}\left(R/h\right)}{2}\right\}\right] \quad (3\text{-}1)$$

Where,

$$R = \frac{(r_1h_2 + r_2h + r_3h_1)}{h} \text{ and } h = h_1 + h_2$$

The frequency dependent effects have to be considered when the surge waves travelling along the towers. Therefore, parallel R-L circuits were introduced for each body sections to represent travelling wave attenuation and distortion as shown in the Figure 3.3. The propagation wave speed in the tower is assumed to be equal to the Speed of light. The tower travelling time (τ_t) is given by the equation 3-2.

$$\tau_t = \frac{h}{c} \tag{3-2}$$

Where,

h = tower height and c = Speed of light (300m/μs)

The R and L values are determined as a function of surge impedance, travel time (τ_t), distance between cross arms (X_1, X_2, X_3, X_4) and attenuation factor (α = 0.89 [5]) as shown in equation (3-3) and (3-4) respectively.

$$R_i = \frac{x_i}{h} .2. Z_i . \ln\left[\frac{1}{\alpha}\right] \tag{3-3}$$

$$L_i = 2. \tau_t . R_i \tag{3-4}$$

Where, i=1,2,3,4

Calculated parameters for a tower models are shown in the Table 3.1.

Table 3.1- Calculated parameters for a KMDL Tower model

Parameter	Symbol	Unit	Value				
			KMDL+0	KMDL+3	KMDL+6	KMDL+9	KMDL+12
Tower Surge Impedance	ZT	Ω	184.58	184.31	183.94	183.53	183.11
Travelling Time	τt	μs	0.09	0.10	0.11	0.12	0.13
Damping Resistance	R1	Ω	3.16	2.85	2.59	2.38	2.19
	R2	Ω	6.54	5.89	5.36	4.92	4.54
	R3	Ω	6.61	5.96	5.43	4.97	4.59
	R4	Ω	26.71	28.25	29.49	30.51	31.36
Damping Inductance	L1	μH	0.59	0.59	0.59	0.58	0.58
	L2	μH	1.22	1.21	1.21	1.21	1.21
	L3	μH	1.23	1.23	1.23	1.22	1.22
	L4	μH	4.97	5.82	6.66	7.51	8.34
Tower Data							
Tower Height	h	m	27.90	30.90	33.90	36.90	39.90
Tower Radius	r1	m	0.70	0.70	0.70	0.70	0.70
	r2	m	0.70	0.70	0.70	0.70	0.70
	r3	m	2.60	2.93	3.27	3.60	3.94
Cross arm distances	x1	m	2.05	2.05	2.05	2.05	2.05
	x2	m	4.24	4.24	4.24	4.24	4.24
	x3	m	4.29	4.29	4.29	4.29	4.29
	x4	m	17.32	20.32	23.32	26.32	29.32

3.3.3 Tower Grounding Resistance Model

The tower grounding resistance is not a constant for a fast front surges and it varies as per the surge current magnitude. This is due to the soil ionization and breakdown characteristics of the soil surrounding the tower grounding electrodes. At certain surge current magnitudes create voltage gradients sufficient to breakdown the soil and forms conductive paths to flow the current, ultimately reduces the grounding resistance. Therefore the impulse grounding resistance is less than the grounding resistance values measured at low current and low frequency states. The relationship between impulse and non-impulse grounding resistances can be expressed as in Equation 3-5.

$$R_f = \frac{R_g}{\sqrt{\left(1+{}^{I}/_{I_g}\right)}} \quad (3\text{-}5)$$

Where,

R_f is the impulse tower grounding resistance (Ω)

R_g is the tower grounding resistance at low current and low frequency (Ω)

I is the surge current in to ground (kA)

I_g is the limiting current initiating soil ionization (kA) as given in the Equation 3-6

$$I_g = \frac{1}{2\pi} . \frac{E_0 \rho_0}{R_g^2} \quad (3\text{-}6)$$

Where,

ρ_o is the soil resistivity (Ωm)

E_o is the soil ionization gradient (about 300kV/m)

The variation of impulse grounding resistance (R_f) of towers 1 to 79 for surge currents from 30kA to 200kA with 10kA step was calculated and graphed as shown in the Annex 6. It was observed that the variation is raging from maximum 37.75Ω to minimum 2.18Ω for the surge currents from 30kA to 200kA.

Therefore the grounding resistance values can exist higher than the CEB specified value (which is the 10Ω) even with the soil ionization effect.

Therefore the grounding resistance of a tower is represented as a variable resistance in the EMTP (PSCAD) model.

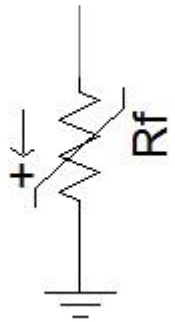

Figure 3.4 - Tower Grounding Resistance Model

3.3.4 Line Insulators and Back Flashover Model

3.3.4.1 Conventional Cap and Pin Insulator String

The line insulator strings between tower and phase conductors are represented as a capacitor in the EMTP (PSCAD) model. Each high voltage glass insulator disc has a capacitance of (approximate) 10pF[8]. An equivalent capacitance of 0.91 pF is used for an insulator string having 11 nos. of insulator discs.

The transient-voltage withstand capability of an insulator string with an arc horn gap is vary with the time of which it is under voltage stress [5,8,9]. An insulator string can withstand very high transient-voltages for shorter time duration whereas it may breakdown by a comparatively low transient-voltage if applied for a longer duration. This characteristic of an insulator string is known as the volt-time characteristic or in another term called flashover characteristics. This characteristic variation of flashover voltage of an insulator string can be modelled by a simplified expression given in the Equation 3-7.

$$V_{f0} = K_1 + \frac{K_2}{t^{0.75}} \qquad (3\text{-}7)$$

Where,

V_{fO} is the flashover voltage (kV)

$K_1 = 400 \times A_g$

$K_2 = 710 \times A_g$

A_g is the Arc-horn gap length (m)

t is the elapsed time after lightning stroke (μs)

Flashover voltage-time characteristic of 132kV line insulator string having 1.5m Arc-horn gap is shown in the Figure 3.5.

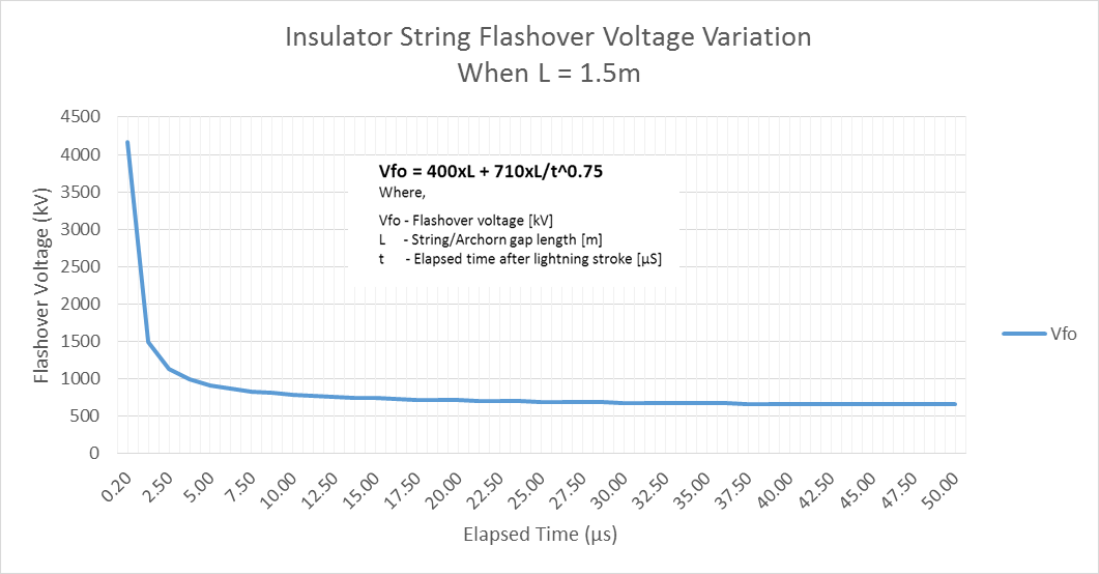

Figure 3.5 - Flashover voltage-time characteristic of 132kV line insulation with 1.5m Arc-horn gap

The back flashover event occurs when the transient voltage developed across the insulator string is greater than its withstanding voltage (Flashover voltage - Vfo).

Once the back flashover mechanism is triggered the voltage across the insulator string will be collapsed to zero by creating conductive path through the air insulation. Therefore back flash over event is modelled by a Circuit Breaker used as a switch, placed in parallel to the equivalent capacitance of insulator string. The close-operation of the Circuit Breaker (in this case closing the switch) is controlled by an external control module as shown in the Figure 3.6 [8,9].

The external control module compares the voltages developed across the insulator string with its volt-time characteristics [9]. If the developed voltage profile crosses the flashover volt-time characteristics of insulators, the control module closes the circuit breaker to create a back flashover event. The back flashover control module is developed by using the standard control components available in the PSCAD. The line insulator string voltage and line voltage are used as the basic input parameters to generate the elapsed time as shown in the Figure 3.7. Generated elapsed time and Arc-horn gap length are taken as inputs to Flashover V-t curve generator module to produce the flashover voltage. Finally the voltage comparator module compares the

insulator string voltage with generated flashover voltage and issues the Circuit Breaker close signal if a back flashover voltage is present [9].

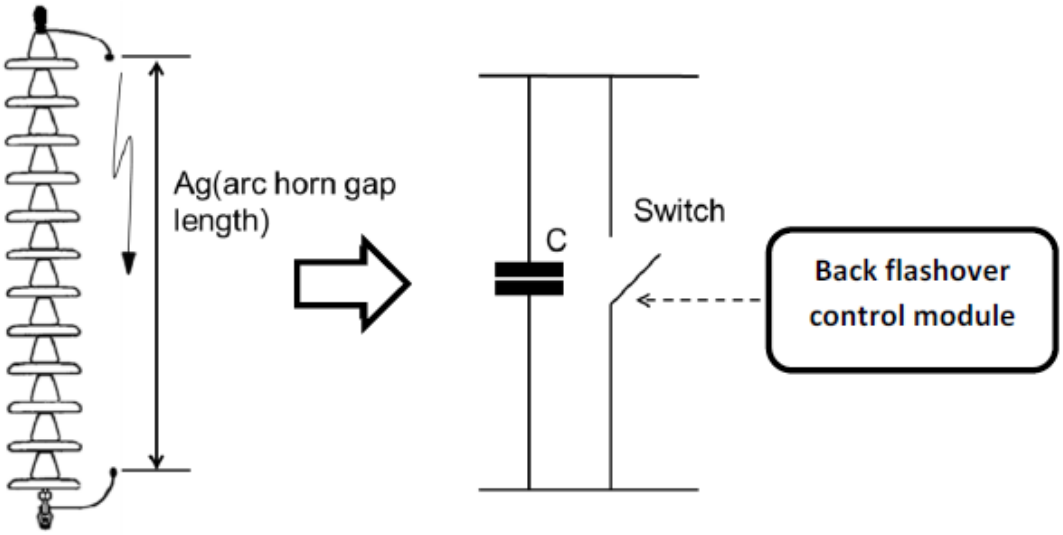

Figure 3.6 - Insulator string and back flashover model

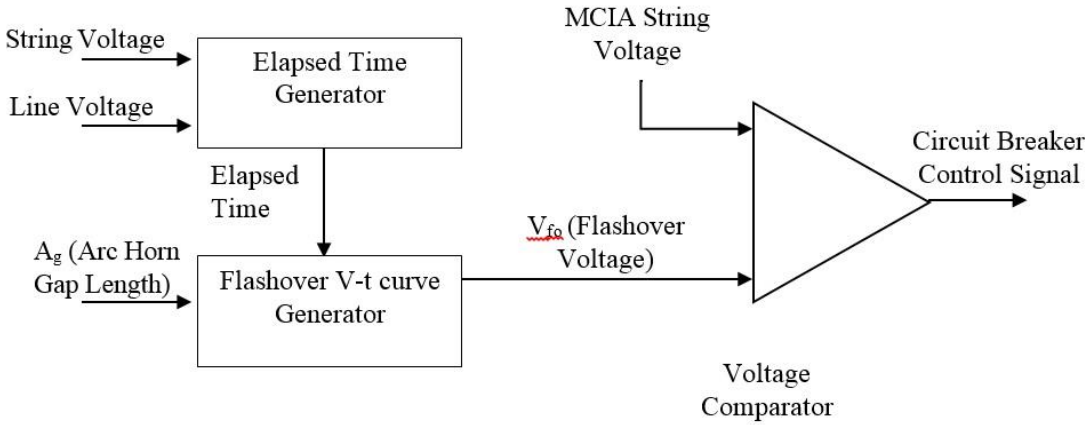

Figure 3.7 - Basic logic diagram for back flashover control module for conventional insulator string

3.3.4.2 Multi Chamber Insulator Arrester (MCIA) String

The flashover voltage characteristics of MCIA is predicted from the data available in the [17-23] and [25 – 28] and illustrated in Figure 3.8.

The line insulator strings between tower and phase conductors are represented as a capacitor in the EMTP (PSCAD) model. It is assumed that each MCIA disc has a

capacitance of (approximate) 10pF. An equivalent capacitance of 1 pF is used for an insulator string having 10 nos. of MCIA discs.

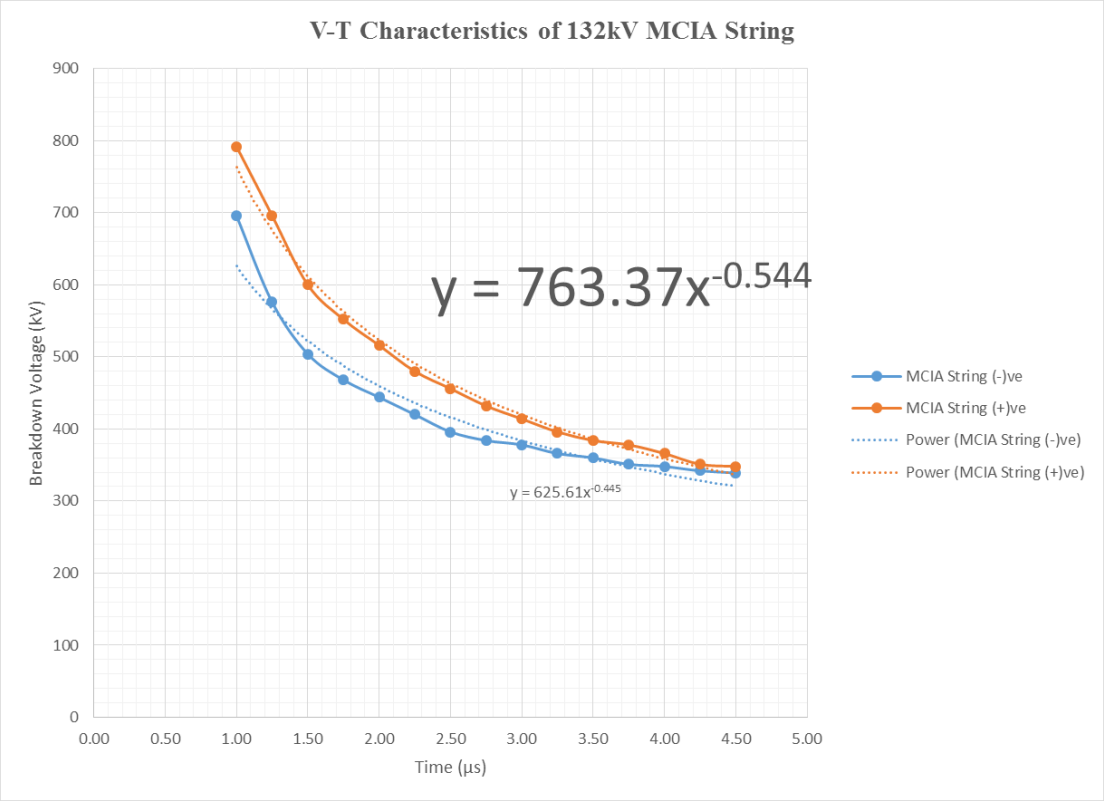

Figure 3.8 - Voltage-time curves of a 10 U120AD unit string and a MCIAS

The transient-voltage withstand capability of an MCIA string is vary with the time of which it is under voltage stress [20, 28]. MCIA string can withstand very high transient-voltages for shorter time duration whereas it may breakdown by a comparatively low transient-voltage if applied for a longer duration, but relatively low compared with normal insulator string. This characteristic of a string is known as the volt-time characteristic or in another term called flashover characteristics. This characteristic variation of flashover voltage of an MCIA string can be modelled by a simplified expression given in the Equation 3-8.

$$V_{f0,MCIA} = 763.67 \text{ x } t^{-0.544} \quad (3\text{-}8)$$

Where,

$V_{fO.MCIA}$ is the flashover voltage of MCIA string (kV)

t is the elapsed time after lightning stroke (µs)

Once the back flashover mechanism is triggered the voltage across the MCIA string will be collapsed by creating conductive path through the MCS. Therefore, back flash over event is modelled by a Circuit Breaker used as a switch, placed in parallel to the equivalent capacitance of MCIA string. The close-operation of the Circuit Breaker (in this case closing the switch) is controlled by an external control module as shown in the Figure 3.6 [8,9]

The external voltage control module describes in [9] is modified to suit the characteristics of MCIA string. The external control module compares the voltages developed across the insulator string with its volt-time characteristics. If the developed voltage profile crosses the flashover volt-time characteristics of MCIA string, the control module closes the circuit breaker to create a back flashover event. The back flashover control module is developed by using the standard control components available in the PSCAD. The line insulator string voltage and line voltage are used as the basic input parameters to generate the elapsed time as shown in the Figure 3.9. Generated elapsed time is taken as input to Flashover V-t curve generator module to produce the flashover voltage. Finally the voltage comparator module compares the MCIA string voltage with generated flashover voltage and issues the Circuit Breaker close signal if a back flashover voltage is present.

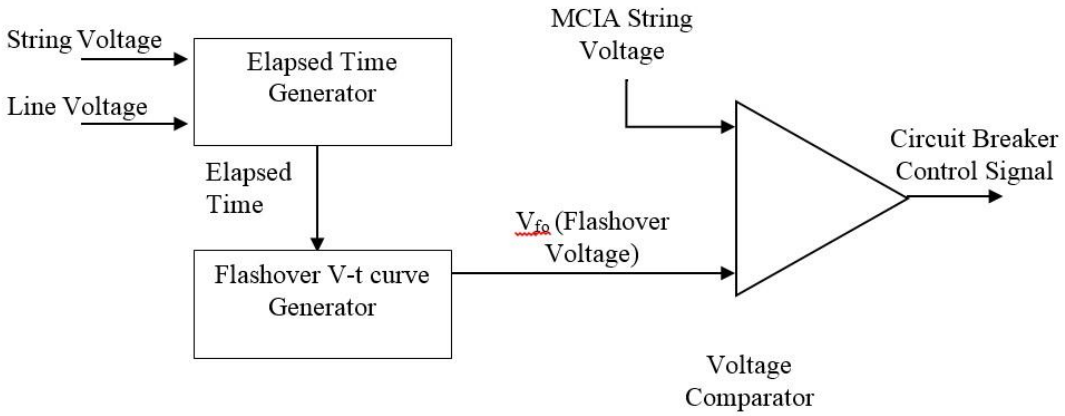

Figure 3.9 - Basic logic diagram for back flashover control module for MCIA string

3.3.5 Line Termination Model

The two ends of transmission line model were grounded through equivalent surge impedances of the line and ground conductors to avoid end reflections. An equivalent impedance of 417.7Ω for phase conductors and 422.2Ω for ground conductors were used at both ends and the calculations are illustrated in Annex-6 [4]. The grounding arrangement of a typical end termination model is shown in the Figure 3.10.

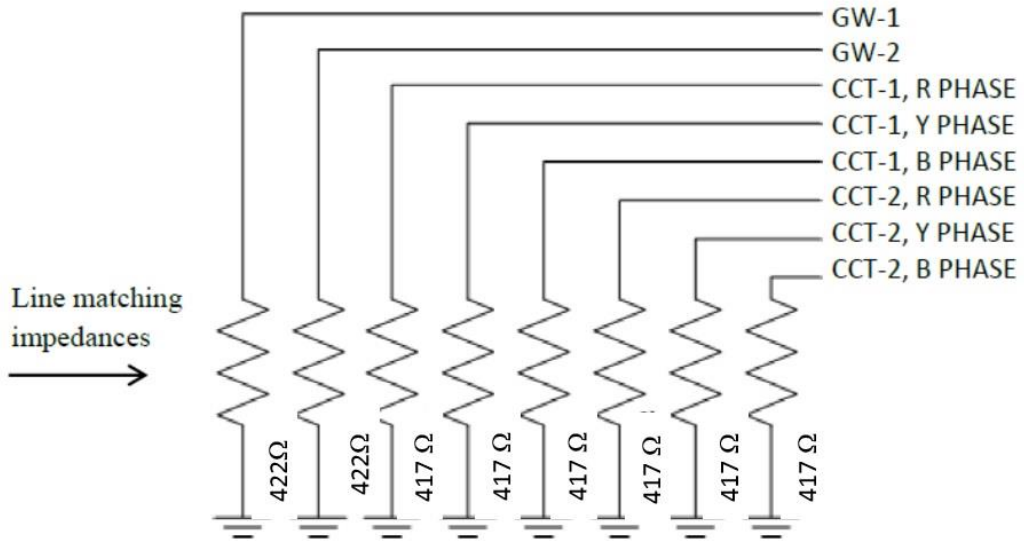

Figure 3.10 - Grounding Arrangement of a typical end termination model.

3.3.6 Multi-Chamber Insulator Arrester (MCIA) Model

3.3.6.1 Multi Chamber System (MCS)

MCS is the base design of the MCIA and it has invented since 19th century and this technology is widely used in the distribution level. In the 20th century, the MCIA manufacturer, the Streamer Company extended their MCS, a novel design called MCIA.

The base of multi chamber arresters (MCA), including MCIA, is the MCS shown in Figure 3.11. It comprises a large number of electrodes mounted in a length of silicon rubber. Holes drilled between the electrodes and going through the length act as miniature gas discharge chambers.

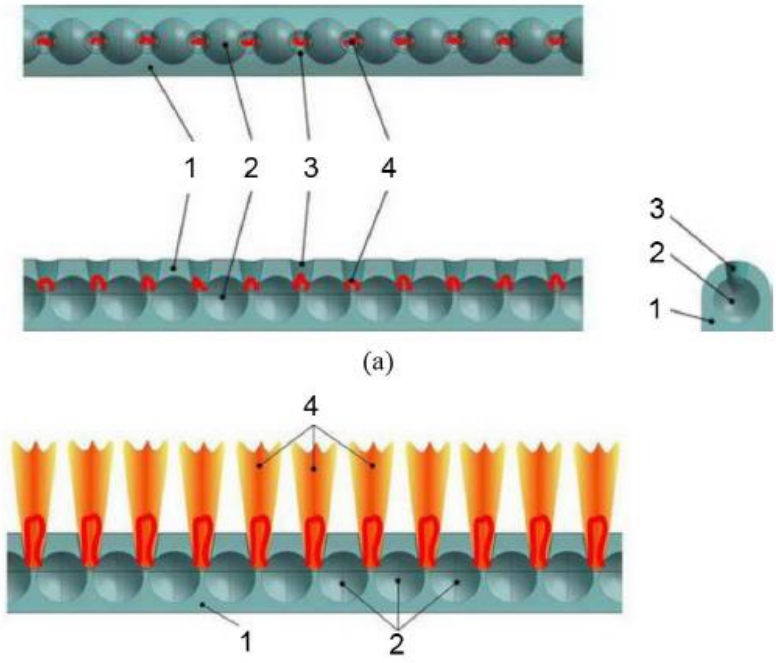

1 – silicon rubber length; 2 – electrodes;
3 – arc quenching chamber; 4 – discharge channel.

Figure 3.11- Multi Chamber System (MCS)

3.3.6.2 Operating Principle of MCS

When a lightning overvoltage impulse is applied to the arrester, it breaks down gaps between electrodes. Discharges between electrodes occur inside chambers of a very small volume; the resulting high pressure drives spark discharge channels between electrodes to the surface of the insulating body and, hence, outside into the air around the arrester. A blow-out action and an elongation of inter electrode channels lead to an increase of the total resistance of all channels (i.e., that of the arrester), which limits the lightning overvoltage impulse current [23].

In advanced MCS, to increase the follow current quenching efficiency of an MCS, it is offered to have a four-to twenty-fold longer elementary gap of a discharge chamber. A low discharge voltage can be attained through use of creeping discharge and cascading operation of MCS circuit chambers as shown in Figure 3.12.

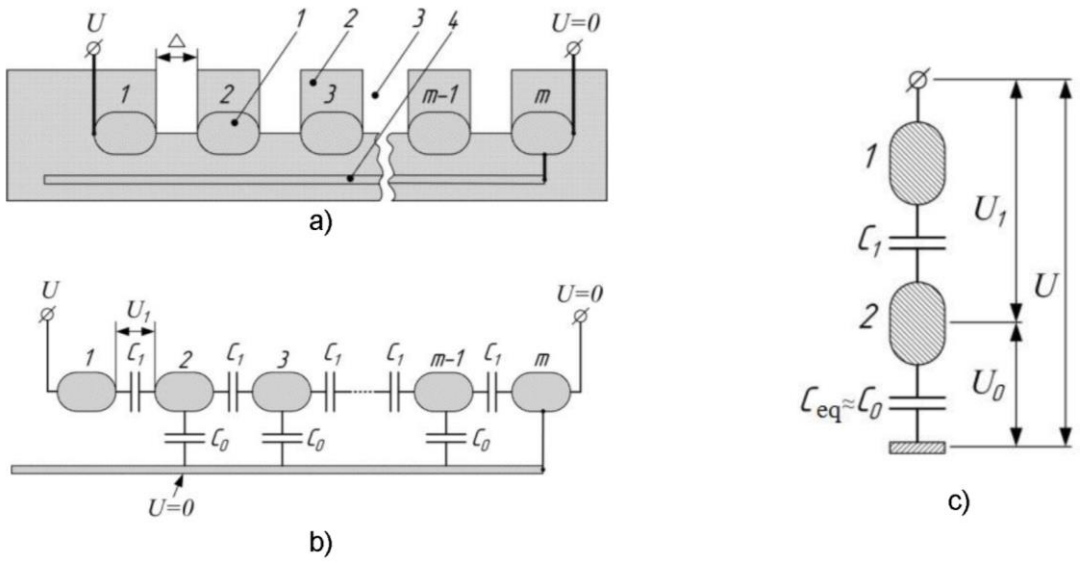

Figure 3.12 – Cascading operation of MCS [21]

(a-sketch of MCS, b-circuit diagram of MCS, c-circuit diagram of a chamber)

Creeping discharge flashover voltage is known to depend little on the electrode spacing. i.e. a fairly large gap can be flashed over even at a relatively low voltage [26]. Cascading is caused by effect of an additional electrode set up along the entire MCS. It is connected to the last electrode of the last chamber and isolated from all the other electrodes.

The additional electrode is connected to the ground and thus has a zero potential. As the MCS gets actuated the high potential U is applied to the first electrode. The voltage gets distributed among chambers' spark gaps most unevenly, as follows from the circuit diagram (Figure 3.12-b).

Let's estimate voltage that is applied between the electrodes in the first chamber. The entire capacitance circuit in Figure 3.12-b can be visualized as a string of two capacitances (see Figure 3.12-c) between the first and second electrode C_1 and the equivalent ground capacitance C_{eq} of the remaining capacitance string excepting C_1. It is to be noted that C_{eq} is determined basically by the chamber electrode-additional electrode capacitance C_0, i.e. $C_{eq} \approx C_0$. Capacitances C_1 and C_0 are series connected (see Figure 3.12-c). Their voltages are distributed in inverse proportion to their values, thus the voltage across electrodes of the first chamber is $U_1 \approx U/(1 + C_1/C_0)$.

Due to the relatively large area of the chamber electrode's surface that faces the additional electrode, as well as because permittivity of a solid dielectric, ε is much higher than of air, ε_0 (Generally $\varepsilon/\ \varepsilon_0 \approx 2\sim3$), capacitance of the intermediate electrode to the additional electrode (i.e. capacitance of this intermediate electrode to ground) is substantially larger than its capacitance to the adjacent intermediate electrode, i.e. $C_0 > C_1$and respectively $C_1/\ C_0 <1$. With the ratio $C_1/\ C_0$ ranging from 0.1 to 0.9, voltage U_1 remains within $U_1 = (0.53 \sim 0.91)U$. therefore, as the MCS gets exposed to voltage U, a larger part of the voltage drop (at least more than half) occurs in the first spark gap between the first and second electrodes. Under effect of this voltage, the first gap gets sparked over, the potential of the second electrode rises to that of the first high voltage electrode, while the potential of the next intermediate electrode becomes U_0. With the spark over pattern repeating again and again, gaps between electrodes get sparked over in series. The cascade operation of discharge gaps assures needed low flashover voltages for actuation of an MCS as whole [21].

As the lightning overvoltage impulse ends, only power frequency voltage remains applied to the arrester. Studies have shown that spark discharge quenching can take place in two instances;

1) When 50 Hz follow current crosses zero (this type of discharge quenching is referred to as *Zero Quenching*)
2) When the instantaneous value of lightning overvoltage impulse drops to a level equal to or larger than the instantaneous value of power frequency voltage, i. e. lightning overvoltage current gets extinguished with no follow current in the grid (this type of discharge quenching is referred to as *Impulse Quenching*).

3.3.6.3 Construction of MCIA

Figure 3.13 features photos of an MCIA based on a porcelain rod insulator which is widely used in 3 kV DC railway overhead contact systems [18]. The MCS is mounted over three quarters of the circumference of an insulator shed. The left and right ends of the MCS are approached by the upper and lower feed electrodes, respectively, which are installed on the upper and lower terminals; there are spark air gaps between the feed electrodes and the ends of the MCS.

Figure 3.13 MCIA based on a porcelain rod insulator used in 3 kV DC railway overhead contact systems

When the MCIA is stressed by an overvoltage the air gaps get sparked over first, the MCS coming next. The lightning overvoltage current flows from the lower terminal and its feed electrode via the spark channel of the lower spark gap to the MCS and on to the upper terminal via the discharge channel of the upper spark gap and the upper feed electrode. Note that there are no intervening electrodes between the upper and lower feed electrodes on the MCS-bearing silicon rubber shed; thus the discharge develops over the MCS taking some three quarters of the sheds circumference, rather than between the feed electrodes.

Over recent years so called arc-quenching multi-chamber systems (MCS) have been developed, succeeding in production of new 10 to 35 kV multi-chamber arresters (MCA), as well as a novel device termed “Multi Chamber Insulator Arrester (MCIA)” which combines the properties and functions of bit insulator and arrester [20]. Figure-3.14 illustrate a typical U120D glass MCIA [22] and the Figure-3.15 shows a string of MCIA for 220kV transmission lines.

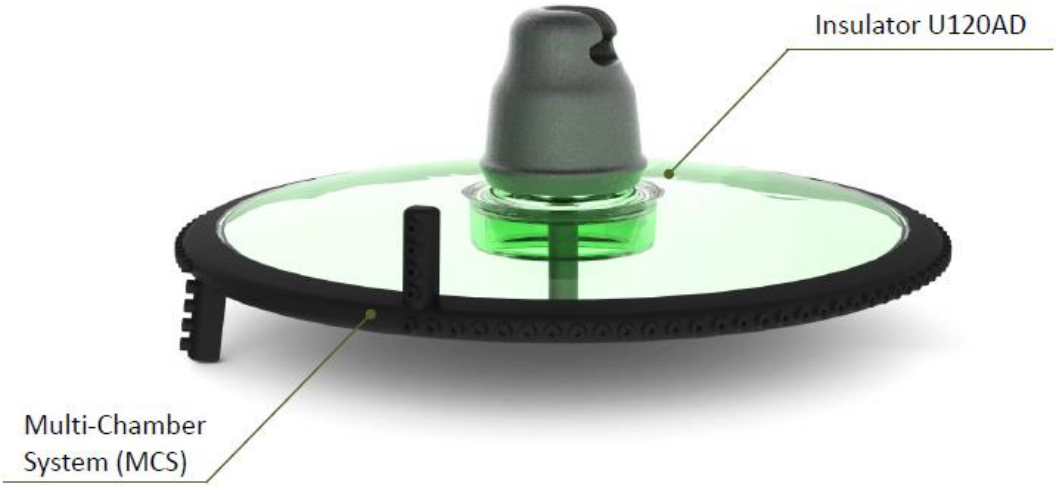

Figure 3.14 - U120D Glass MCIA

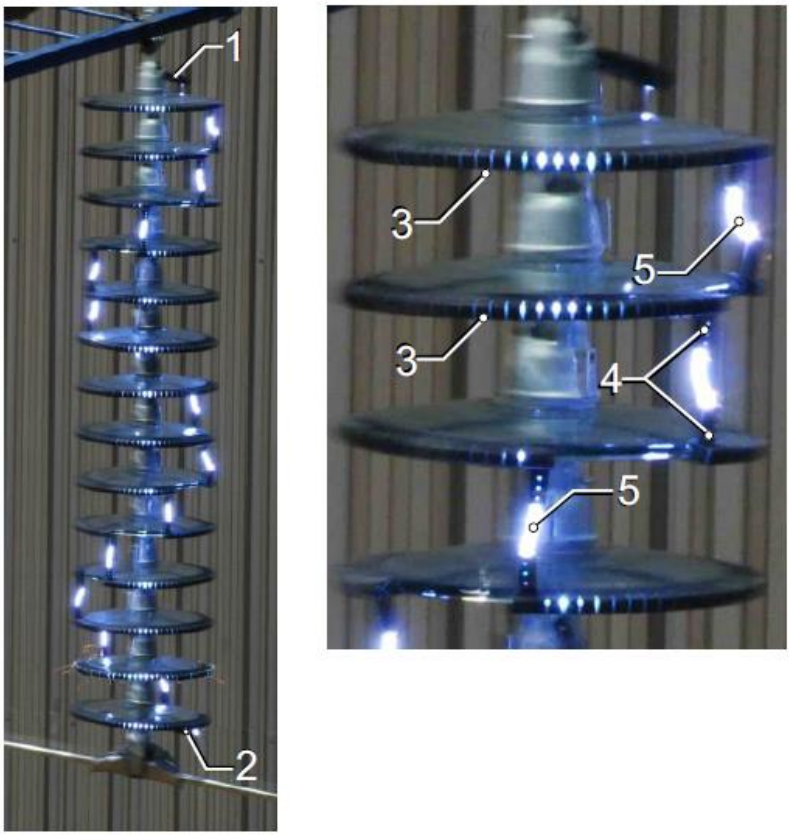

1 – upper supply electrode; 2 – lower supply electrode; 3 - multi-chamber system (MCS), 4 - MCS taps, 5 – air spark gaps.

Figure 3.15 - U120D Glass MCIA String

At a lower overall cost and with a better lightning performance, a line thus protected features a noticeably lower number of lightning failures, cuts damage from undersupply of energy, and lowers maintenance costs. Installation of an MCS confers arrester properties to insulators without any deterioration of their insulating capacity. For this reason, application of MCIA on overhead lines makes shield wires redundant, while the height, weight, and cost of poles or towers goes down. Application of MCIAs makes it possible to ensure lightning protection of overhead lines of any voltage ratings: the higher the line voltage, the larger is the number of units in a string and thus the higher are the rated voltage and the arc quenching capacity of a string of insulator-arresters.

3.3.6.4 Modelling of MCIA

Since the MCIA system is a latest technology, a developed model for fast front transient analysis is still un-available as for Metal oxide Surge Arrester. Therefore, this proposed model is developed considering the operation principle and the available few data from the manufacturer and the published papers

MCIA system can be considered as a series combination of small air gaps (short gap arcing horns) to form a larger air gap. Such short gap arcing horns can be modelled by a nonlinear inductor with series to a nonlinear resister [11, 12] as shown in the Figure 3.16

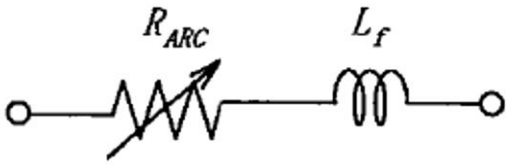

Figure 3.16 – Electrical representation of Short-Gap Arcing Horn

L_f represents the inductance of MCIA at its actuation and typically has a value of 1μH/m [12]. When consider the U120D, MCIA string having 10 numbers of MCIAs has 682mm (approximate) air gap. To calculate this air gap, it is considered that 5/6 of the perimeter of the MCIA is having the arrester with spacing between two consecutive insulators is 40mm. The air gap between upper electrode and the first

MCIA is 20mm while the spacing between bottom electrode and the lowest MCIA is 35mm [25]. According to the facts given in [17 – 25], it is assumed that 20% of the MCS has small air gaps and altogether 682mm approximate total air gap for 10 numbers of MCIAs is available. Hence, the nonlinear inductance is calculated as 0.682µH. To represent the nonlinear inductance in the PSCAD software, a variable inductor is used.

R_{ARC} represents the Ohmic Resistance of the MCIA at its actuation and [21] describes the variation of the ohmic resistance of two MCIAs at its actuation as illustrated in Figure 3.17

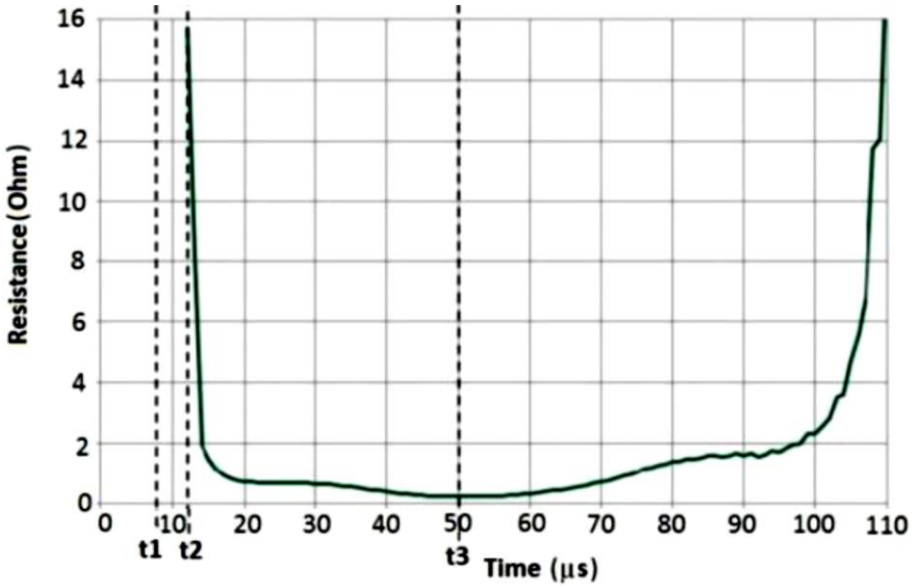

Figure 3.17 - Variation of the Ohmic Resistance of two MCIAs at its actuation

The characteristics of the curve (Time Vs Resistance) were extracted and variable resister with external control by the X-Y Transfer function of PSCAD is used to model the ohmic resistance of the two MCIAs at its actuation. The scaling factor of the X-Y Transfer function is set to 5 to represent the ohmic resistance of MCIA string having 10 numbers of insulators (during the final simulation in the transmission line) and used an external file having 120 data points which extracted from the Figure 3.17 to link the data points to the X-Y Transfer function.

To activate the MCIA string at 50% impulse flashover voltage, a Spark Gap model in the PSCAD library is connected in series to the nonlinear inductor and the resister and its value is set to 625kV, 50% impulse flashover voltage [27]. The final assembly of the MCIA model in PSCAD software is illustrated in Figure 3.18.

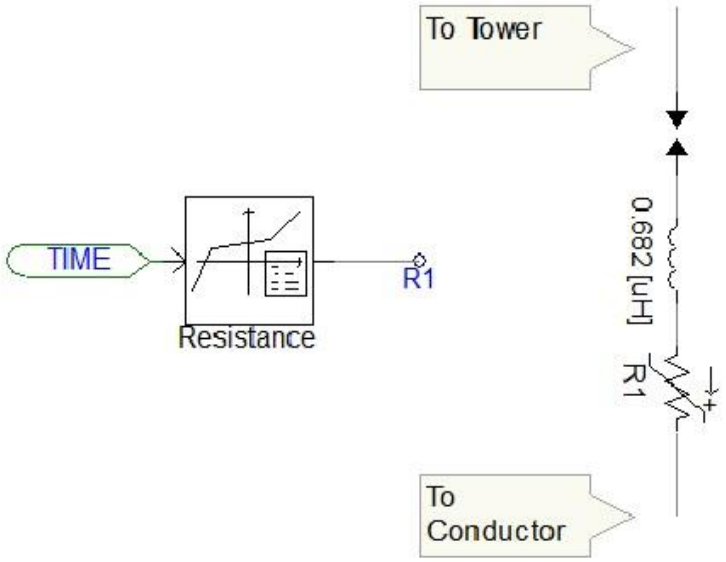

Figure 3.18 - MCIA model in PSCAD software

3.3.7 Lightning Stroke Current Generator

A lightning strike generally consists of several return strokes, where the average number of strokes in a lightning strike is roughly about three [9]. According to the statistics of return strokes peak current distribution, one can assume that the first return stroke in a lighting strike is at least severe as subsequent strokes. Therefore the latter can be ignored. Therefore in lightning transient studies, it is considered only the first return stroke [9].

The characteristics of real lightning current wave shapes are determine by its polarity, maximum instantaneous value, steepness and equivalent front/tail times. The maximum instantaneous value (peak current) is statistically related to the steepness or time to crest of the current waveform. The steepness increases as the peak current increases.

The lightning stroke is modelled by a current source which produces the standard double exponential (Equation 3-9) current waveform 8x20μs of positive polarity with variable peak current as shown in the Figure 3.19.

In addition to the 8x20μs current waveform; standard 1.2x50μs voltage waveform was also used separately for the simulations (Figure 3.19).

The same double exponential waveform was used with relevant α and β values to generate the 1.2x50μs lightning surge waveform.

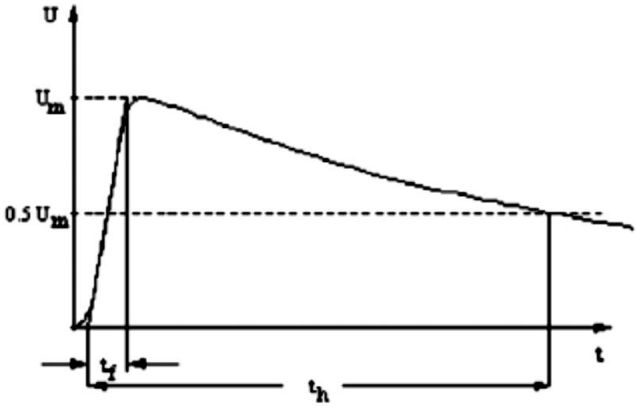

Standard 1.2x50μs voltage waveform

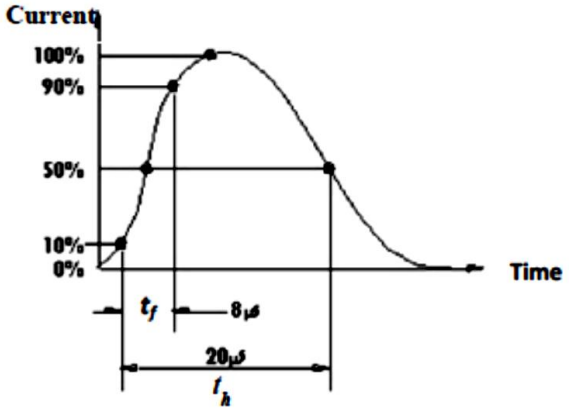

Standard 8x20μs current waveform

U_m = Peak magnitude

t_f = Wave front time (Time to reach current magnitude from $10\%U_m$ to $90\%U_m$)

t_h = Wave tail time (time to drop magnitude from peak to $50\%U_m$)

Figure 3.19 - Standard waveforms for lightning surge voltage and current

$$I(t) = I_0(e^{-\alpha t} - e^{-\beta t}) \quad (3\text{-}9)$$

Where,

I(t) = lightning current

I_0 = Peak current magnitude

$\alpha = 8.66 \times 10^4 s^{-1}$ for 8x20μs waveform [8]

$\beta = 1.732 \times 10^5 s^{-1}$ for 8x20μs waveform [8]

$\alpha = 1.426 \times 10^4 s^{-1}$ for 1.2x50μs waveform [3]

$\beta = 4.877 \times 10^6 s^{-1}$ for 1.2x50μs waveform [3]

t = time(s)

3.3.8 Power Frequency Phase Voltage Generator

Instantaneous power frequency voltages of each phase were generated by using the following equations [9].

$$Va = Vp \sin(\theta) \quad (3\text{-}10)$$

$$Vb = Vp \sin(\theta - 120) \quad (3\text{-}11)$$

$$Vc = Vp \sin(\theta + 120) \quad (3\text{-}12)$$

Where,

Va, Vb and Vc are the instantaneous phase voltages in kV

θ = the phase angle in radians

$$Vp = 132 \times \sqrt{(2/3)} = 107.7kV \quad (3\text{-}13)$$

Where,

Vp = peak value of phase voltage in kV

Generated power frequency phase voltages are taken as input data to calculate the actual insulator string voltage given to the voltage comparator as shown in the Figure 3.7 and Figure 3.9.

CHAPTER - 04

APPLICATION OF THE METHODOLOGY

4.1 Introduction

This chapter describes the way of implementation of transient modeling concepts which were described in the previous chapter. The implementation of the transient model concepts were carried out in the PSCAD software as a digital model. Further this chapter describes the way of simulation of implemented transient model with the aid of inbuilt "Multiple Run" component which provides effective means of simulation.

4.2 Power Systems Computer Aided Design (PSCAD) modeling tool

PSCAD (Power Systems CAD) is a well-developed software program which act as a Graphical User Interphase (GUI) to the world renowned electromagnetic transient solution engine called EMTDC (EMTDC stands for Electromagnetic Transients including DC). PSCAD facilitates the users to create models or circuits, simulate them and to analyze the results in a completely integrated graphical environment. Drag and drop type sophisticated Input-Output modules such as meters, controllers, plotters and graphs are available which can even control while the circuits are at simulation run mode. Therefore online control of circuit or model parameters and monitoring of results can be done easily.

PSCAD comes complete with a library of pre-programmed and tested models, ranging from simple passive elements and control functions, to more complex models, such as electric machines, FACTS devices, transmission lines and cables. If a particular model does not exist, PSCAD provides the flexibility of building custom models, either by assembling those graphically using existing models, or by utilizing an intuitively designed Design Editor.

4.2.1 PSCAD Graphical User Interface (GUI) window

PSCAD software comes with a user friendly GUI (Graphical User Interface) which provides an active environment for users to develop solutions by graphical means. The Figure 4.1 shows a typical GUI window of PSCAD software. The GUI can be

divided in to four basic working areas called Workspace Window, Output Window, Design Editor and the rest of the area consists of tool bars, menus and palettes.

The Workspace Window is the central project database for PSCAD which gives an overview of currently loaded projects (i.e. project tree), master library, data files, signals, controls, transmission lines, cable objects, display devices and etc. Further it provides the facility to organize them within the workspace window by drag and drop feature.

The Output Window section provides an easily accessible interface for viewing feedback and troubleshooting of simulations. All the error and warning messages either given by a component, PSCAD or EMTDC can be viewed from the output window section and also provides the facility to locate the errors by double clicking on the error messages.

The Design Editor window is probably the most important part of the PSCAD environment, and is where most (if not all) project design work is performed. The Design Editor is used mostly for the graphical construction of circuits (Circuit view), and also includes an embedded component definition editor.

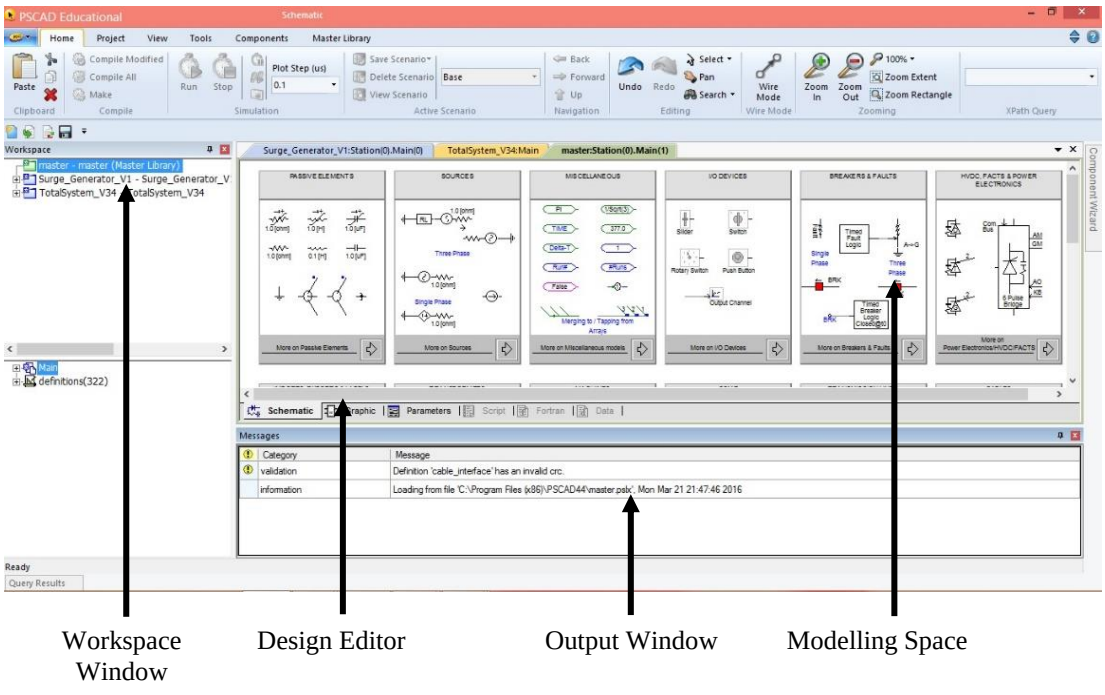

Figure 4.1 Working Space of PSCAD Software

4.3 Creation of sub models in PSCAD

Following sections describe the sub models which were developed in PSCAD based on the transient model concepts provided in the previous chapter.

4.3.1 Transmission line model

As described in the previous chapter, the transmission line sections and line spans were modelled by using the standard frequency dependent phase model available in the Master Library of the PSCAD. There are two basic ways of constructing a transmission line in PSACD by using the above standard model and in this study the remote end method was used (See the Figure 4.2).

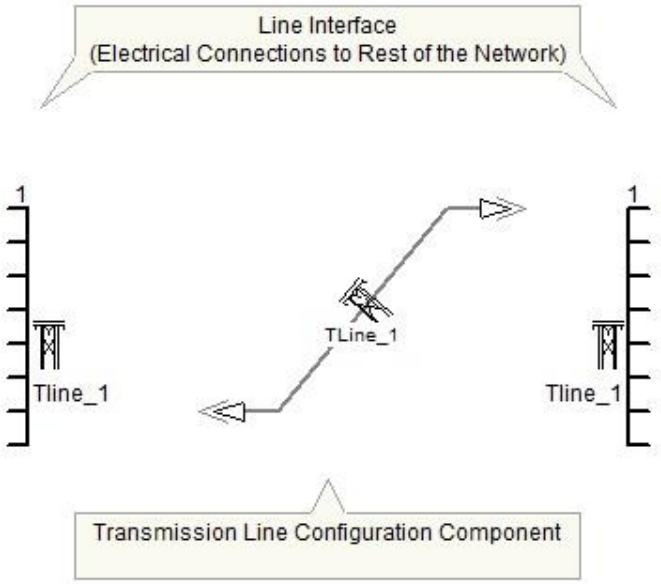

Figure 4.2 – Transmission Line Model (Remote End)

Creating the transmission line with two line interfacing end components having the same line name is called remote end method and conductor configuration of interfacing components is shown in the Figure 3.2.

Transmission line component's parameters were entered in the pop-up window as shown in the Figure 4.3. Selection of "Edit" button in front of the "Segment Cross-Section" as shown in the Figure 4.3 enables the user to enter the parameter values (geometrical and electrical properties as attached in Annex 3) of the towers, conductors and ground. A typical geometrical input data set which was fed in to the PSCAD is shown in the Figure 4.4.

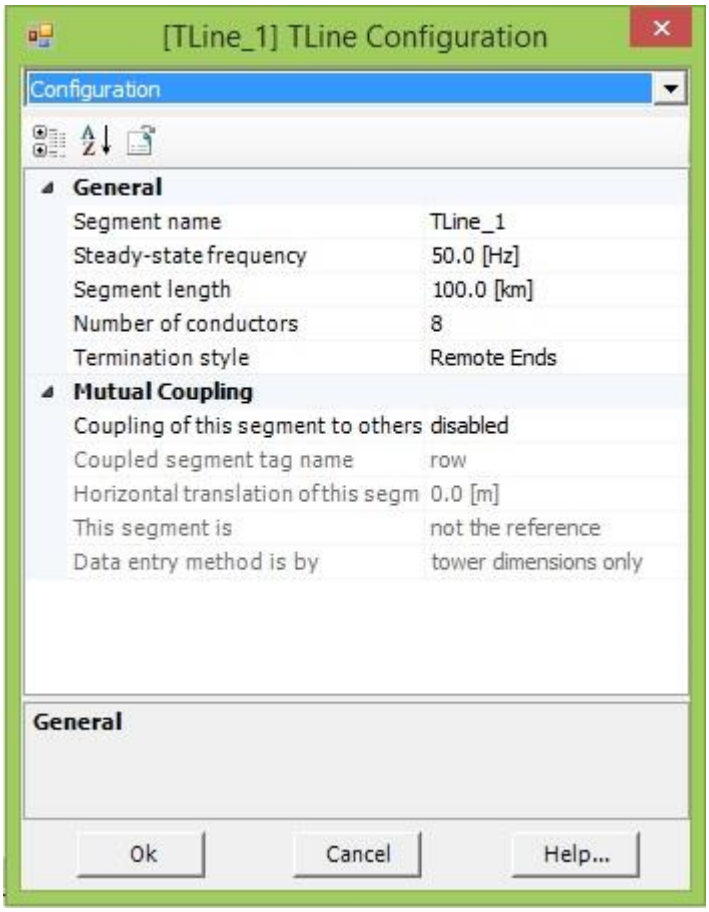

Figure 4.3 – Transmission Line Component Parameter Configuration

4.3.2 Transmission tower model

As per the proposed model in the previous chapter, the transmission towers were model by the Constant Parameter Distributed Line (CPDL) model which consists of four (04) numbers of impedances series with four numbers of parallel Resistance-Inductance branches as shown in the Figure 4.5.

The tower model is created completely by using two basic passive components named resistor and inductor available in the Master Library of the PSCAD. Parameter values of each resistors and inductors were set as shown in the Table 3.1.

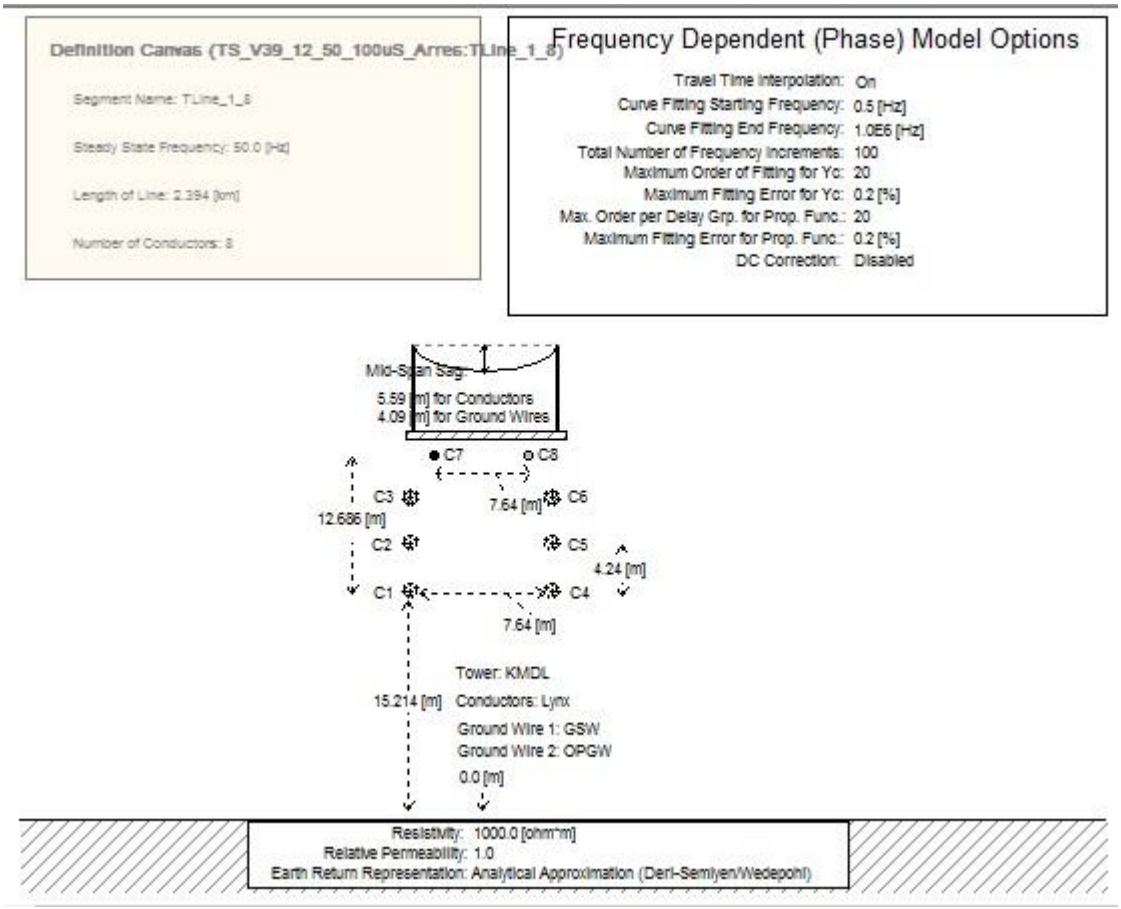

Figure 4.4 – General Line Geometry Data Input

4.3.3 Tower grounding resistance model

A variable resistance component available in the PSCAD Master Library is used to represent the Impulse grounding resistance of a transmission tower. The value of the variable resistance was varied externally by the "Multiple Run" simulation component as described in the section 4.5. Figure 4.6 shows a typical impulse grounding resistance model of a tower which was created by the aid of a variable resistor component in PSCAD.

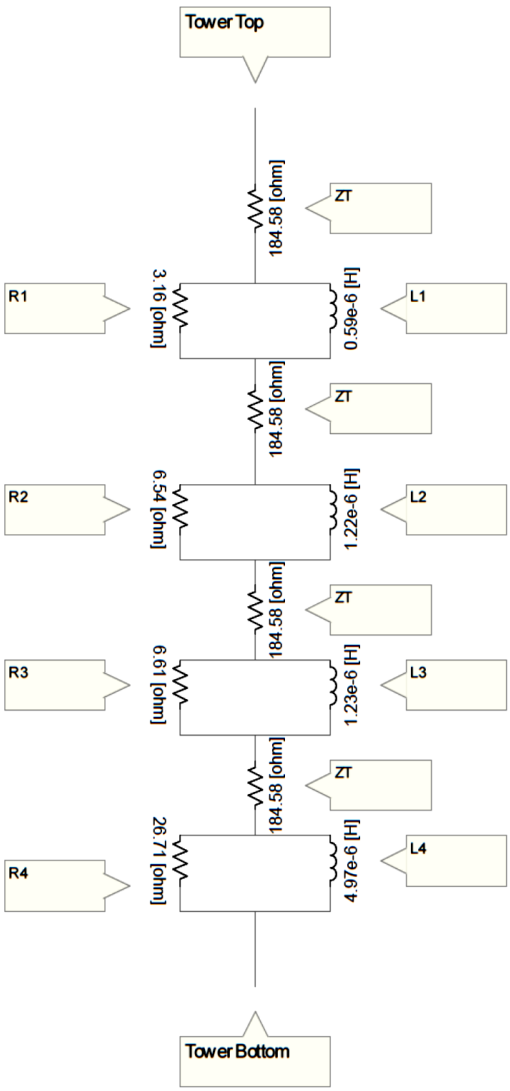

Figure 4.5 – Typical Tower Model creates in PSCAD

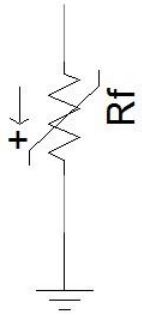

Figure 4.6 – Tower Grounding Resistance Model

4.3.4 Line insulator string with back flashover model

The insulator string and the back flashover event were modelled by an equivalent capacitor parallel with an externally controlled circuit breaker as shown in the Figure 4.7. As described in the section 3.3.4 in the previous chapter, the operation of circuit breaker is controlled by a back flashover control module shown in the Figure 3.7. The basic logic diagram shown in the Figure 3.7 was implemented in PSCAD (See Figure 4.8) by using basic Control Blocks available in the Master Library.

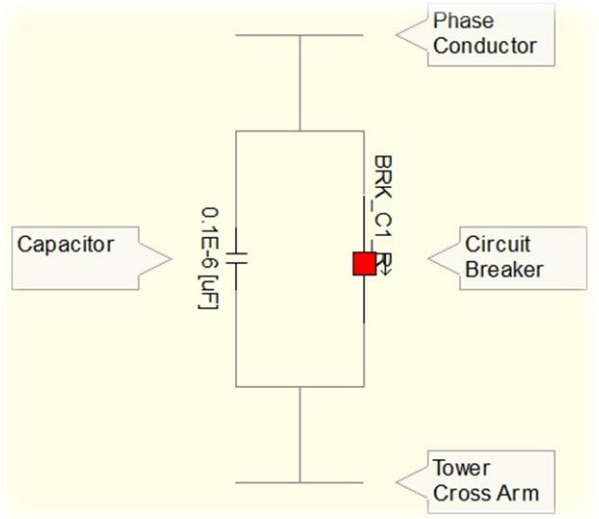

Figure 4.7 – Insulator String Capacitor and Back Flashover Breaker Model

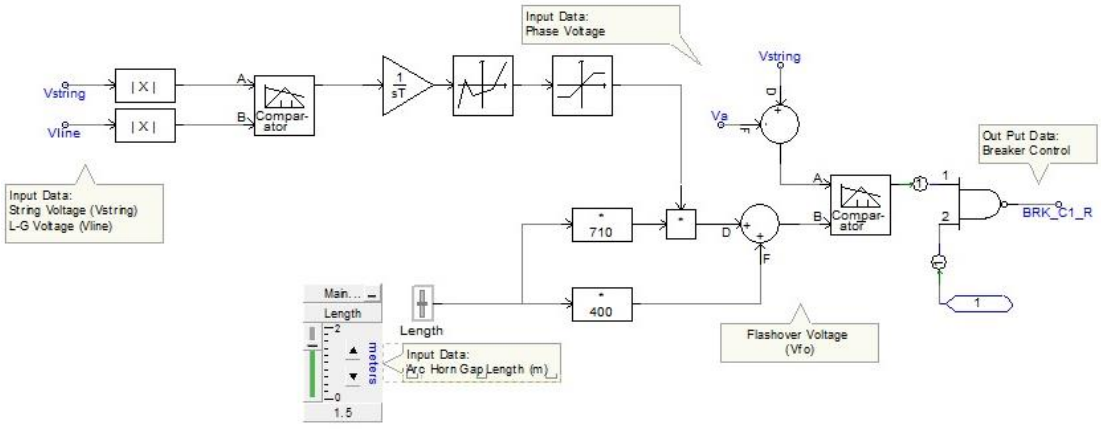

Figure 4.8 – Back Flashover Control Module for conventional insulator string implemented in PSCAD

Insulator String Voltage (Vstring), Line to Ground Voltage (Vline), Arc Horn Gap length (=1.5m) and Instantaneous Phase Voltage (Va) are taken as the input data for the above module. Inbuilt Voltmeter components and their output signals are used to

read the Insulator String Voltage (Vstring) and Line to Ground Voltage (Vline), whereas the Instantaneous Phase Voltages are given by the Power Frequency Phase Voltage Generator model described in the section 3.3.8.

Control components forming the left most branch of the module as shown in the Figure 4.8, is calculating the value $\frac{1}{t^{0.75}}$ (t=elapsed time) based on the input data Vstring and Vline. The control components forming the loop, generates the flashover voltage value (Vfo) taking the arc horn gap length (Ag=1.5m) and the $\frac{1}{t^{0.75}}$ value as the input parameters. The actual insulator string voltage is generated by the upper most Differencing Junction component taking the relevant power frequency phase voltage value and the measured string voltage as input data. Finally the comparator component compares the generated Vfo and actual string voltage values and gives the output signal as a positive pulse whenever the voltage profiles are crosses each other which formulate a back flashover event. Mono-stable component at the right most side of the model generates a digital output value "1" based on positive pulse generated by the comparator component. Invertor component at the end of the model generate the opposite digital value "0" required as an input data to the relevant Circuit Breaker to close the circuit. Close operation of the circuit breaker creates an external conductive path across the insulator string which simulates the back flashover arc generated across the arc horn gaps.

4.3.5 Power frequency phase voltage generator model

As described in the section 3.3.8, instantaneous power frequency phase voltages were generated by using the circuit created in PSCAD (See the Figure 4.9). The circuit is created by modelling the equations 3-15, 3-16 and 3-17 given for each phase voltage variation. Basic control components such as Summing/Differencing junctions, Real/Integer constants, Trigonometric Sin function and multipliers were used to create the circuit as shown in the Figure 4.9. The "phase angle" input data values are given by the "Multiple Run" simulation component as described in the section 4.5.

Output phase voltages, Va, Vb and Vc were directly used in the back flashover control modules to generate the actual insulator string voltages.

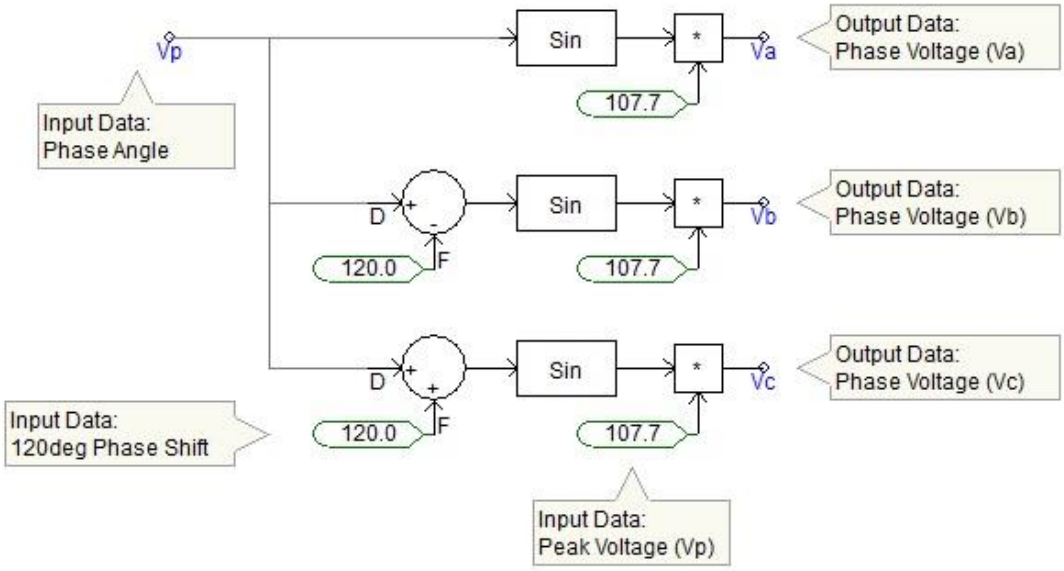

Figure 4.9 – Power Frequency Phase Voltage Generator Model

4.3.6 Line end termination model

Two ends of the transmission line were grounded through equivalent surge impedances of each ground and phase conductors as shown in the Figure 4.10. Each end of the grounded impedances was connected to the nearest interfacing component of the transmission line section as per the relevant connection arrangement. Top two terminals of the interfacing component stand for the two Ground Wires and the rest six terminals stand for the phase conductors of each circuit. Phase conductors of both circuits were grounded through 417.7Ω equivalent impedances and similarly the ground conductors were grounded through 422.2Ω equivalent impedances based on the calculation in Annex-7.

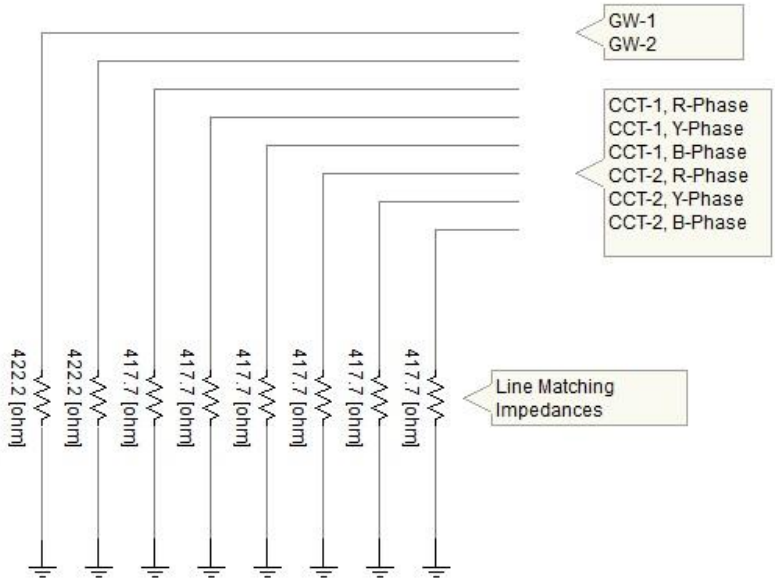

Figure 4.10 – Line Termination model created in PSCAD

4.3.7 Multi Chamber Insulator Arrester Model and the Back Flashover Control Module

4.3.7.1 Multi Chamber Insulator Arrester (MCIA) Model

MCIA string having 10 Nos. of insulators is modelled with an Arc Inductance series to the Ohmic Resistance of its actuation [11], [12] as described in the section 3.3.6 and illustrated below (Figure 4.11).

The calculated Arc Inductance is 0.682µH and the Ohmic Resistance at actuation [20], [21] is fed in to the Variable Resistor by using the X-Y Transfer Function in the PSCAD Master Library. 120 Nos. of data points were extracted from the Figure 3.17 and used the external file link option available in the X-Y Transfer Function to model the Ohmic Resistance of MCIA's actuation. Figure 4.12 illustrates the properties of the X-Y Transfer Function and X-Axis gain is set to "5" as the Figure 3.17 represents the resistance of actuation for two numbers of MCIAs.

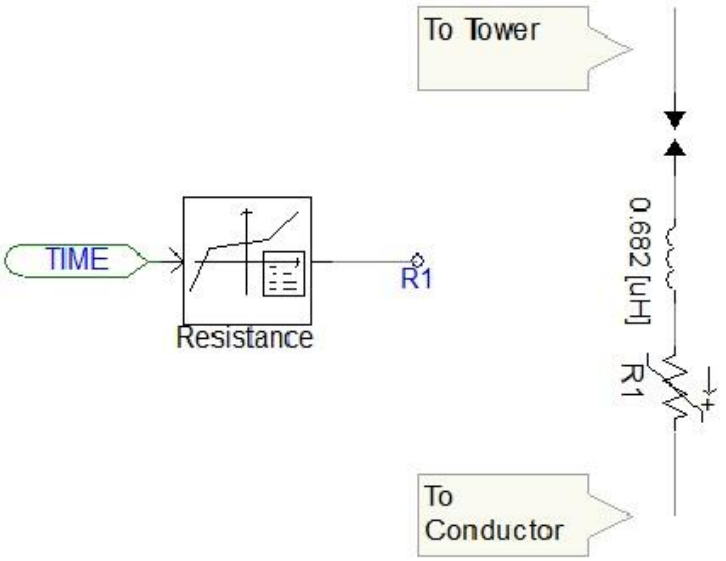

Figure 4.11 – MCIA model created in PSCAD

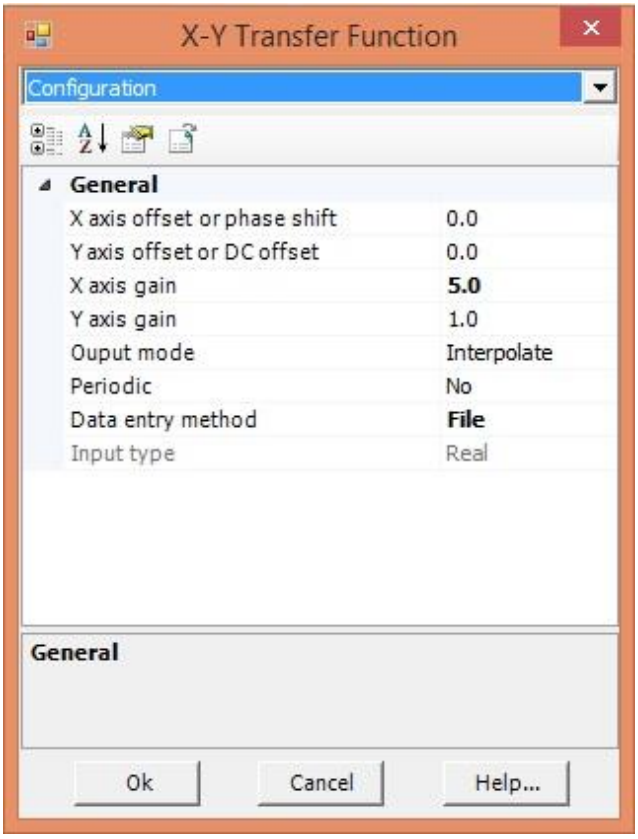

Figure 4.12 - Properties of the X-Y Transfer Function

Annex-8 shows the 50% Impulse Flashover Voltage for MCIA having 10 numbers of insulators is 625kV and to model this property for the MCIA model, External Spark Gap is used in series to the Arch Inductance and Ohmic Resistance and Figure 4.13 shows the properties window for the Spark Gap.

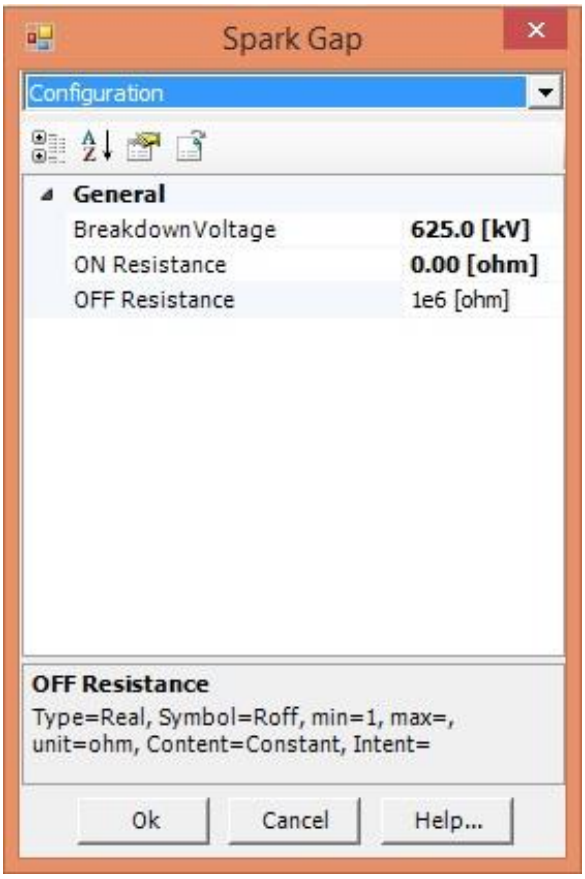

Figure 4.13 – Configuration of Spark Gap Properties

Then the voltage waveform mentioned in the [21] is used to validate the developed MCIA model in PSCAD. Obtained I-t graphs and the V-I graphs in PSCAD is illustrated in Figure 4.14 and Figure 4.15 respectively and these outputs resemble the MCIA behavior as mentioned in [21] and hence developed model is validated.

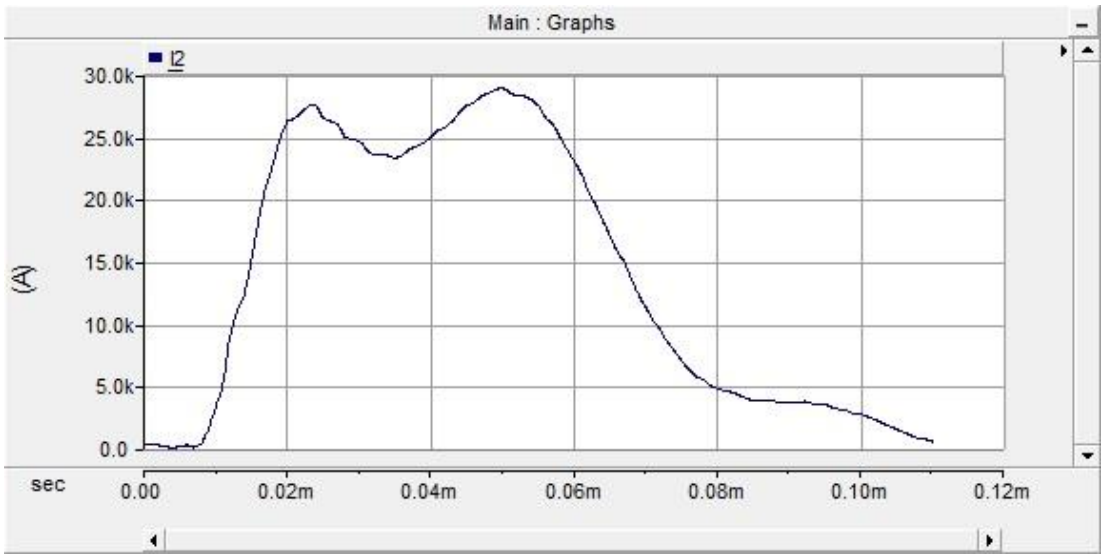

Figure 4.14 – MCIA model current variation with time

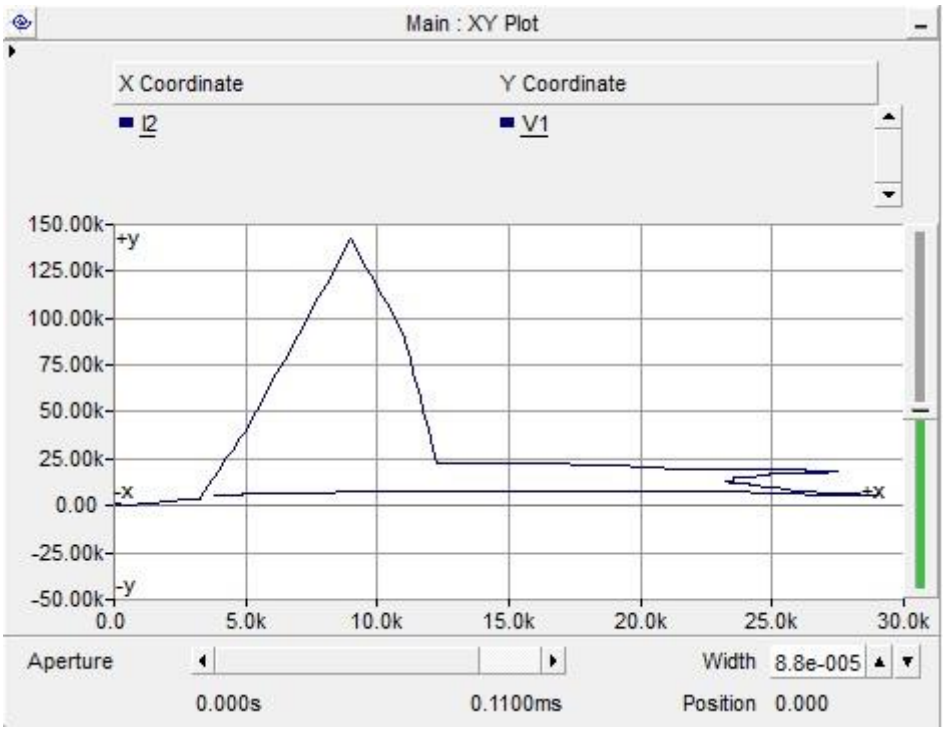

Figure 4.15 – MCIA model residual voltage variation with current

4.3.7.2 Back Flashover Control Module for MCIA

The basic logic diagram shown in the Figure 3.9 was implemented in PSCAD (See Figure 4.16) by using basic Control Blocks available in the Master Library.

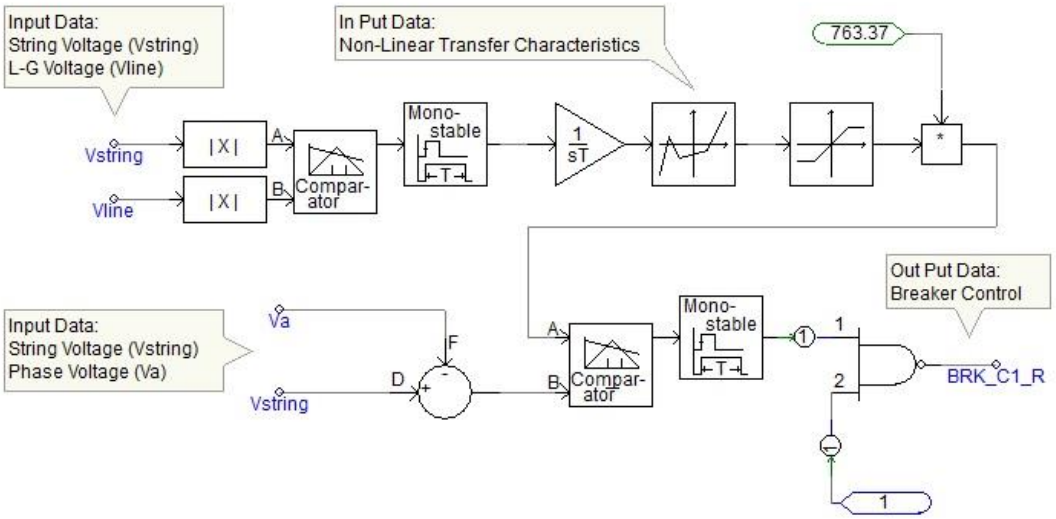

Figure 4.16 - Back Flashover Control Module for MCIA string implemented in PSCAD

Control components forming the left upper most branch of the module as shown in the Figure 4.16, is calculating the value $t^{-0.544}$ (t=elapsed time) based on the input data Vstring and Vline. The control components forming the loop, generates the flashover voltage value (Vfo) taking the magnitude component (763.37) and the $t^{-0.544}$ value as the input parameters. The actual MCIA string voltage is generated by the bottom left most Differencing Junction component taking the relevant power frequency phase voltage value and the measured string voltage as input data. Finally the comparator component compares the generated Vfo and actual string voltage values and gives the output signal as a positive pulse whenever the voltage profiles are crosses each other which formulate a back flashover event. Mono-stable component at the right most side of the model generates a digital output value "1" based on positive pulse generated by the comparator component. Invertor component at the end of the model generate the opposite digital value "0" required as an input data to the relevant Circuit Breaker to close the circuit. Close operation of the circuit breaker creates an external conductive path across the MCIA string which simulates the back flashover arc generated through the MCS.

MCIA string and the back flashover event were modelled by an equivalent capacitor parallel with an externally controlled circuit breaker as shown in the Figure 4.17.

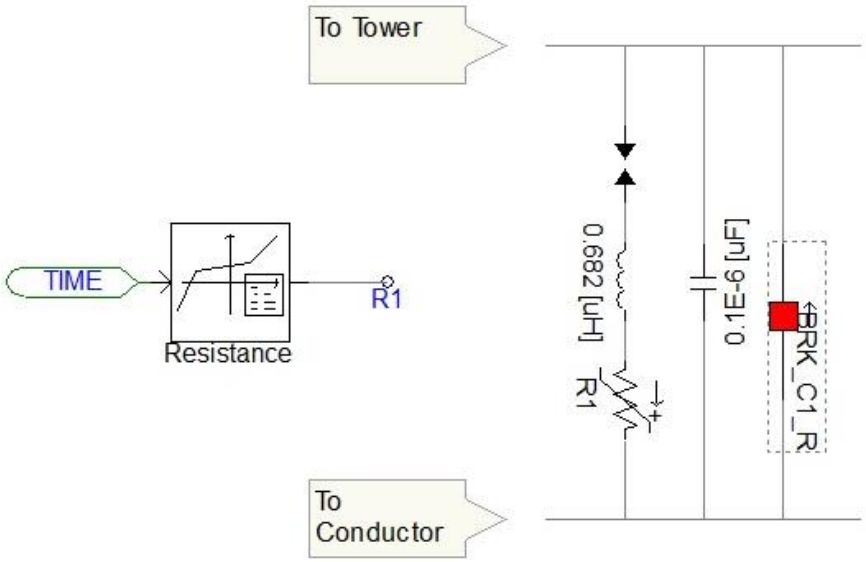

Figure 4.17 - MCIA String Capacitor and Back Flashover Breaker Model

4.3.8 Lightning surge generator model

As per the equation 3.9 given in the section 3.3.7, the standard 8/20μs double exponential waveform was generated by an inbuilt current source having its magnitude controlled by an external control circuit (see the Figure 4.18).

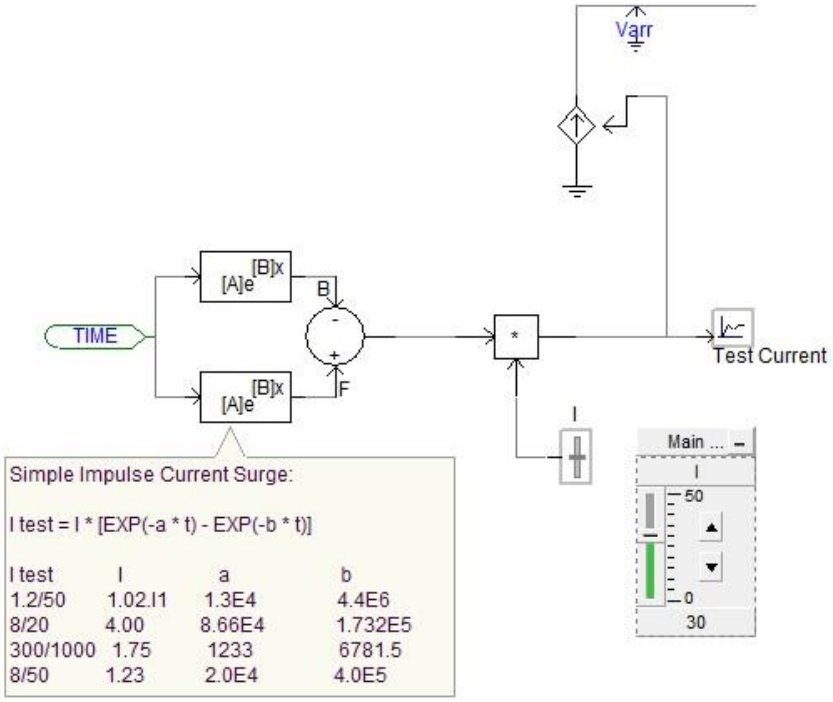

Figure 4.18 – Lightning Surge Generator Model created in PSCAD

The external control circuit consists of two similar parallel branches with a common input parameter component giving the simulation time of the system. Each branch consists of an exponential function component and a multiplier component in series. The multiplier component determines the magnitude of the current waveform which controlled externally by the “Multiple Run” simulation component as described in the section 4.5. As shown in the Figure 4.18, the Differencing junction component gives the instantaneous values of double exponential waveform to the current source. Current source generates the complete waveform based on the instantaneous values given by the control circuit. Figure 4.19 shows the module output for 8/20µs surge waveform.

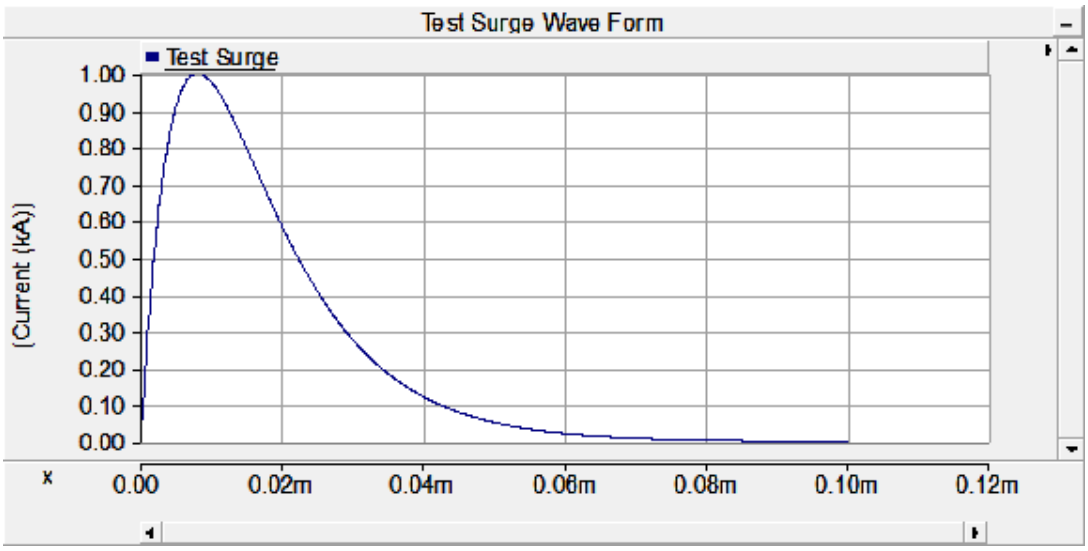

Figure 4.19 – 8/20µs surge from the Created model

Similarly, a voltage source is used instead of the current source to generate the standard 1.2/50µs voltage surge waveform and Figure 4.20 shows the module output for 1.2/50µs surge waveform.

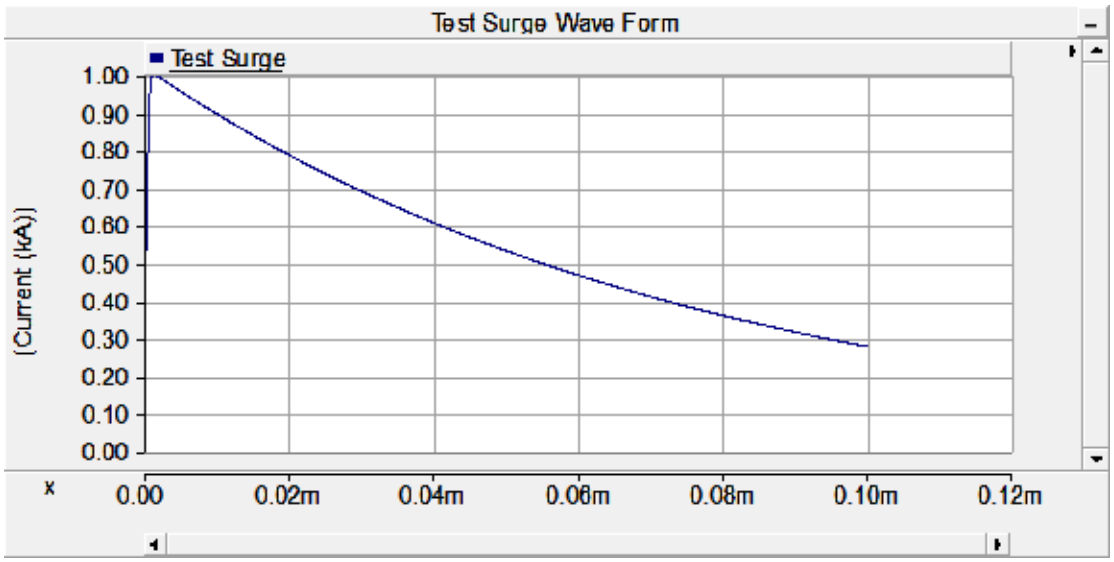

Figure 4.20 – 1.2/50μs surge from the Created model

Inter dependent sub models such as back flashover model and phase voltage generator model were virtually inter connected by giving an identical reference names for each common variables. For an example, the "Phase Voltage" variable is referred as Va in both phase voltage generator model as well as in the back flashover model. The phase voltage Va is an output variable produces by the phase voltage generator model whereas it is an input as well for the back flash model in the same time frame.

Similarly the data signals of common variables were managed by assigning them with identical data signal labels.

4.4 Method of simulation

4.4.1 Multiple Run component and variable settings

Simulation of the completed final transmission line model was carried out by using the "Multiple Run" simulation component (See Figure 4.21) available in the Master Library of PSCAD. This component can be used to control a multiple run, while manipulating variables from one run to the next. These variables are output from the component (up to six outputs) and can be connected to any other PSCAD components. The Multiple Run component can also record up to six channels each run.

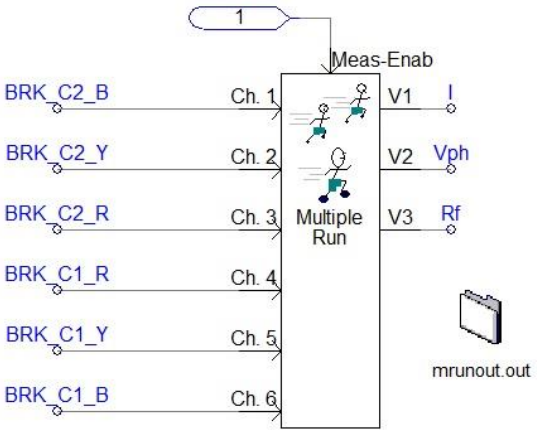

Figure 4.21 – Multiple-Run Simulation component of PSCAD

Three (03) numbers of variables those directly affecting the back flashovers were varied in each run of the simulation by using the Multiple Run component. The variables are,

1. Magnitude of the lightning surge current labelled as "I" in the model is set as V1 of Multiple Run component
2. Phase angle of the power frequency phase voltage labelled as "Ph" in the model is set as V2 of Multiple Run component
3. Grounding resistance of Tower-M labelled as "Rf" in the model is set as V3 of Multiple Run component

The range of values set for each variable in the Multiple Run component is shown in the Table 4.1.

Table 4.1 – Range of values used for variables in Multiple-Run component

Variable in Multiple Run component	**Data label used in the model**	**Range of values**
V1	I	20kA to 200kA with 10kA steps
V2	Ph	0^0 to 360^0 with 10^0 steps
V3	Rf	38Ω, 146Ω, 9Ω

According to [6], the shielding failure flashovers are more frequent at surge current values less than 20kA; whereas the back flashovers take place at higher surge current

ratings around 80kA. Therefore a range of values from 20kA to 200kA with 10kA step is selected for the variable "I" as shown in the Table 4.1.

Simulations were carried out from 0^0 to 360^0 full range of phase angles with a 10^0 phase angle step to examine the effect of phase angle on back flashovers.

Grounding resistance of the Tower-M (Middle tower which is subjected to the lightning surge as shown in the Figure 3.1 is set for one of the three values as shown in the Table 4.1 in each simulation.

As shown in Annex-6, the recorded maximum tower grounding resistance even with the soil ionization effect is around 38Ω when the surge current is about 30kA. Therefore the value 38Ω is the recorded worst case of tower grounding resistance with the soil ionization effect and is selected as one of the three values used in the simulations.

As shown in the Figure 1.12, the maximum recorded tower grounding resistance is about 146Ω when the soil ionization effect is not considered. Therefore the value 146Ω is the worst case of tower grounding resistance when the soil ionization effect is neglected. Therefore the value 146Ω is also selected as the second value to be used in the simulations as tower grounding resistance variable V3 as shown in the Table 4.1.

The standard value specified by the local utility for the tower grounding resistance of any transmission line is about 10Ω. Therefore a value less than 10Ω (i.e.9 Ω) is also used in the simulations to investigate the performance of towers against lightning back flashovers.

While changing the value of above variables in each run of the simulations, the control signal output of each back flashover control modules were recorded by the aid of six channel recorders available in the same Multiple Run component. The recorded control signal outputs are stored in an output file assigned to the Multiple Run component. These control signal output data are in binary form where the output "0" means a back flashover event.

4.4.2 Simulation criteria

Simulation of complete line model is carried out in two major steps. At first step, the model is simulated without MCIA for selected three (03) critical tower grounding resistance values 9Ω, 38 Ω and 146 Ω for both 8x20μs and 1.2x50μs surge waveforms.

In the second step the model is simulated with MCIA with three different arrester configurations for both 8x20μs and 1.2x50μs surge waveforms.

For all simulations the lightning surge current was injected on top of the Tower M (Middle tower as shown in the Figure 3.1).Detailed criteria of each simulation including the tower grounding resistance setting and expected control signal output data to be recorded are described in the Table 4.2 and Table 4.3.

Step 1: Simulation of the model without arrester protection

Table 4.2 – Simulation criteria for step-1

Simulation number	**Surge waveform**	**Tower grounding resistance (Ω)**	**Expected phases where the control signal output data to be recorded**
01	8x20μs	9	Tower-M, Circuit-1and Circuit-2 All six (06) phases
02	8x20μs	38	Tower-M, Circuit-1and Circuit-2 All six (06) phases
03	8x20μs	146	Tower-M, Circuit-1and Circuit-2 All six (06) phases
04	1.2x50μs	9	Tower-M, Circuit-1and Circuit-2 All six (06) phases
05	1.2x50μs	38	Tower-M, Circuit-1and Circuit-2 All six (06) phases
06	1.2x50μs	146	Tower-M, Circuit-1and Circuit-2 All six (06) phases

Step 2: Simulation of the model with arrester protection

Table 4.3 – Simulation criteria for step-2

Simulation number	Surge waveform	Tower grounding resistance (Ω)	Expected phases where the control signal output data to be recorded
With 02 arresters installed at TOP phase of Circuit-1and Circuit-2 of Tower-M			
07	8x20µs	9	Tower-M, Circuit-1and Circuit-2 All six (06) phases
08	8x20µs	38	Tower-M, Circuit-1and Circuit-2 All six (06) phases
09	8x20µs	146	Tower-M, Circuit-1and Circuit-2 All six (06) phases
10	1.2x50µs	9	Tower-M, Circuit-1and Circuit-2 All six (06) phases
11	1.2x50µs	38	Tower-M, Circuit-1and Circuit-2 All six (06) phases
12	1.2x50µs	146	Tower-M, Circuit-1and Circuit-2 All six (06) phases
With 04 arresters installed at TOP and MIDDLE phases of Circuit-1and Circuit-2 of Tower-M			
13	8x20µs	9	Tower-M, Circuit-1and Circuit-2 All six (06) phases
14	8x20µs	38	Tower-M, Circuit-1and Circuit-2 All six (06) phases
15	8x20µs	146	Tower-M, Circuit-1and Circuit-2 All six (06) phases
16	1.2x50µs	9	Tower-M, Circuit-1and Circuit-2 All six (06) phases
17	1.2x50µs	38	Tower-M, Circuit-1and Circuit-2 All six (06) phases
18	1.2x50µs	146	Tower-M, Circuit-1and Circuit-2 All six (06) phases
With 06 arresters installed on all the phases of Circuit-1and Circuit-2 of Tower-M			
19	8x20µs	9	Tower-M, Circuit-1and Circuit-2 All six (06) phases
20	8x20µs	38	Tower-M, Circuit-1and Circuit-2 All six (06) phases
21	8x20µs	146	Tower-M, Circuit-1and Circuit-2 All six (06) phases
22	1.2x50µs	9	Tower-M, Circuit-1and Circuit-2 All six (06) phases
23	1.2x50µs	38	Tower-M, Circuit-1and Circuit-2 All six (06) phases

24	1.2x50μs	146	Tower-M, Circuit-1and Circuit-2 All six (06) phases
25	8x20μs	9	Tower-L, Circuit-1and Circuit-2 All six (06) phases
26	8x20μs	38	Tower-L, Circuit-1and Circuit-2 All six (06) phases
27	8x20μs	146	Tower-L, Circuit-1and Circuit-2 All six (06) phases
28	1.2x50μs	9	Tower-L, Circuit-1and Circuit-2 All six (06) phases
29	1.2x50μs	38	Tower-L, Circuit-1and Circuit-2 All six (06) phases
30	1.2x50μs	146	Tower-L, Circuit-1and Circuit-2 All six (06) phases
31	8x20μs	9	Tower-R, Circuit-1and Circuit-2 All six (06) phases
32	8x20μs	38	Tower-R, Circuit-1and Circuit-2 All six (06) phases
33	8x20μs	146	Tower-R, Circuit-1and Circuit-2 All six (06) phases
34	1.2x50μs	9	Tower-R, Circuit-1and Circuit-2 All six (06) phases
35	1.2x50μs	38	Tower-R, Circuit-1and Circuit-2 All six (06) phases
36	1.2x50μs	146	Tower-R, Circuit-1and Circuit-2 All six (06) phases

4.4.3 Project simulation settings

For each simulation runs, following project simulation settings were assigned.

1. Duration of each run = 200μs
2. Solution time step = 0.1μs
3. Channel plot step = 0.1μs

CHAPTER - 05

RESULTS AND ANALYSIS

5.1 Introduction

This chapter provides the technical and economic analysis with results of each simulation carried out as per the detailed simulation criteria mentioned in the previous chapter. The results are provided in this chapter as the same sequence of simulations carried out as per the Table 4.2 and Table 4.3.

5.2 Technical Analysis

5.2.1 Introduction to Simulation Results

The results of each simulation are given by an output data file which contains a set of binary values giving the occurrence of back flashover events for each simulation run. The binary value “0” means an occurrence of a back flashover event whereas “1” gives the negation of that event. A typical view of an output data file is shown in the Figure 5.1. As shown in the Figure 5.1, the columns BRK_C2_B, BRK_C2_Y and BRK_C2_R gives the back flashover events occurred on TOP, MIDDLE and BOTTOM phases of Circuit-2 of Tower-M respectively. Similarly the columns BRK_C1_R, BRK_C1_Y and BRK_C1_B gives the back flashover events occurred on TOP, MIDDLE and BOTTOM phases of Circuit-1 of Tower-M respectively.

Based on the information provided by the output files of each simulation; the variation of minimum current required for back flashover event were plotted and are produced here as the final results.

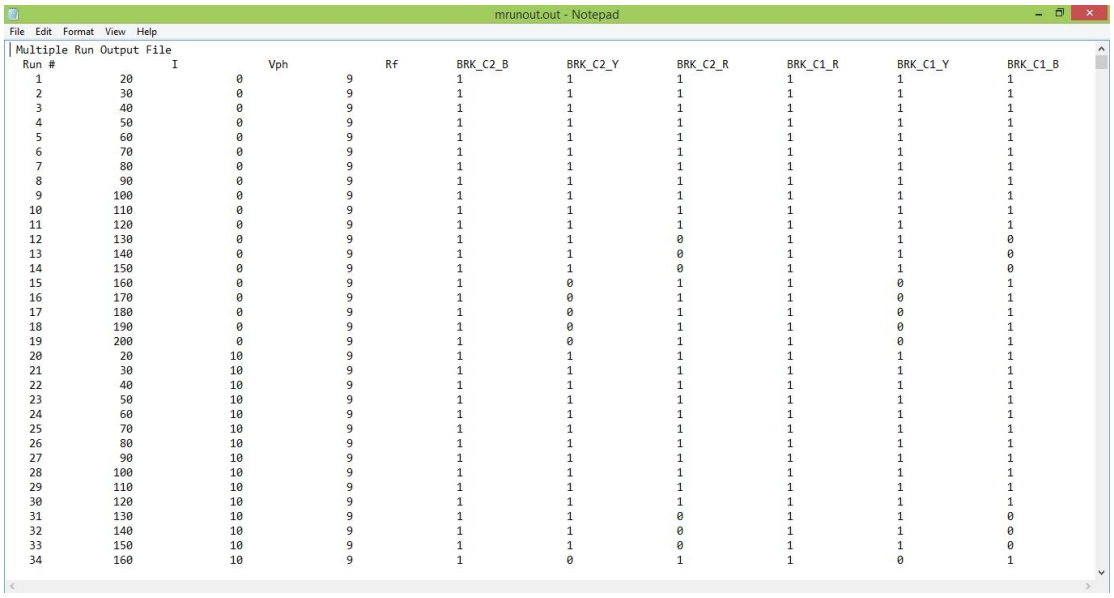

mrunout.out - Notepad

File Edit Format View Help

Multiple Run Output File

Run #	I	Vph	Rf	BRK_C2_B	BRK_C2_Y	BRK_C2_R	BRK_C1_R	BRK_C1_Y	BRK_C1_B
1	20	0	9	1	1	1	1	1	1
2	30	0	9	1	1	1	1	1	1
3	40	0	9	1	1	1	1	1	1
4	50	0	9	1	1	1	1	1	1
5	60	0	9	1	1	1	1	1	1
6	70	0	9	1	1	1	1	1	1
7	80	0	9	1	1	1	1	1	1
8	90	0	9	1	1	1	1	1	1
9	100	0	9	1	1	1	1	1	1
10	110	0	9	1	1	1	1	1	1
11	120	0	9	1	1	1	1	1	1
12	130	0	9	1	1	0	1	1	0
13	140	0	9	1	1	0	1	1	0
14	150	0	9	1	1	0	1	1	0
15	160	0	9	1	0	1	1	0	1
16	170	0	9	1	0	1	1	0	1
17	180	0	9	1	0	1	1	0	1
18	190	0	9	1	0	1	1	0	1
19	200	0	9	1	0	1	1	0	1
20	20	10	9	1	1	1	1	1	1
21	30	10	9	1	1	1	1	1	1
22	40	10	9	1	1	1	1	1	1
23	50	10	9	1	1	1	1	1	1
24	60	10	9	1	1	1	1	1	1
25	70	10	9	1	1	1	1	1	1
26	80	10	9	1	1	1	1	1	1
27	90	10	9	1	1	1	1	1	1
28	100	10	9	1	1	1	1	1	1
29	110	10	9	1	1	1	1	1	1
30	120	10	9	1	1	1	1	1	1
31	130	10	9	1	1	0	1	1	0
32	140	10	9	1	1	0	1	1	0
33	150	10	9	1	1	0	1	1	0
34	160	10	9	1	0	1	1	0	1

Figure 5.1 – Typical view of an output data file

5.2.2 Back flashover minimum current variation results and analysis

5.2.2.1 Results of simulations without MCIA protection (Step-1)

The step-1 consists of six numbers of simulations from simulation no-01 to 06. All these six numbers of simulations were carried out without MCIA module for both 8x20µs and 1.2x50µs surge waveforms respectively. Further, above simulations were also done by applying selected 9Ω, 38Ω and 146Ω tower grounding resistances values.

As per the results shown in Figure-5.2 (Step-1, Simulation No.01), it can be seen that for 8/20µS Surge, for 9Ω tower footing resistance, all the Six phases of both circuits get back flashover at different peak values of the surges. Among these peak values, TOP phases has the 40kA minimum peak current value while 70kA for MIDDLE phases and 180kA for TOP phases. This similar pattern, but with different peak values are followed for the ground resistance values of 38Ω and 146Ω (Figure-A9.1, Figure-A9.2, Figure-A9.3 and Figure-A9.4 on Annex-09).

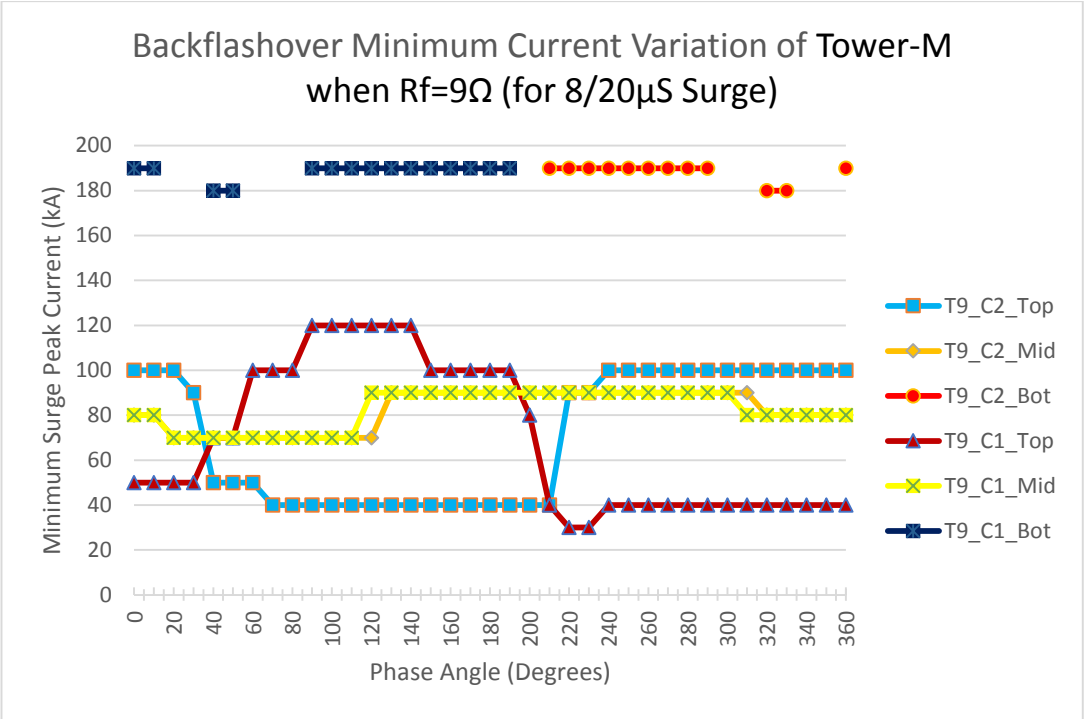

Figure 5.2 – Simulation results with no MCIA protection for 8/20µS Surge for the ground resistance of 9Ω

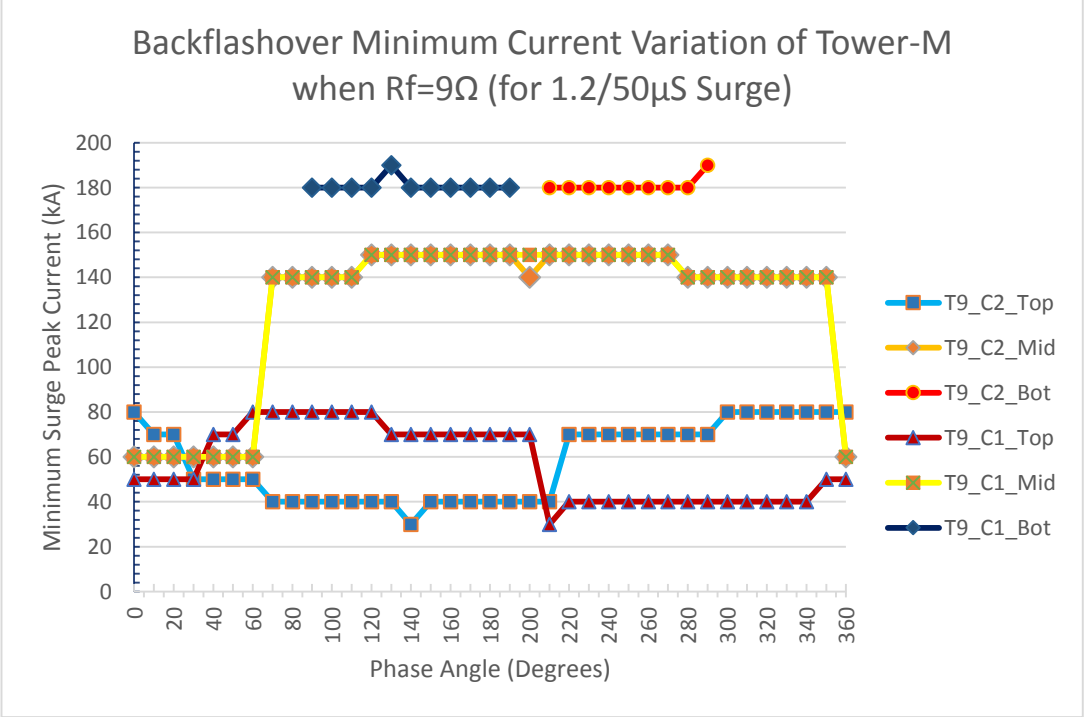

Figure 5.3 – Simulation results with no MCIA protection for 1.2/50µS Surge for the ground resistance of 9Ω

For 1.2/50µS Surge and for 9Ω tower footing resistance, as shown in Figure-5.3 (Step-1, Simulation No.04), all the Six phases of both circuits get back flashover at different peak values of the surges as for 8/20µS surge for 9Ω tower footing resistance. However, TOP phase flashover minimum peak surge current drops to 30kA and for MIDDLE phases it is reduced to 60kA when compared with 1.2/50µS Surge and for 9Ω tower footing resistance results (Figure 5.3). This similar pattern, but with different peak values are followed for the ground resistance values of 38Ω and 146Ω (Figure-A9.3 and Figure-A9.4 on Annex-09).

However, when considering the behaviour for 8/20µS and 1.2/50µS surges, it can be seen that similar back flashover patterns have followed, but different flashover minimum peak surge currents for ground resistances of 9Ω, 38Ω and 146Ω. Also, it is concluded that there is no any protection for back flashover up to 200kA peak surge currents for any phases of the both circuits.

5.2.2.2 Results of simulations with MCIA protection (Step-2)

With 02 MCIAs installed at TOP phase of Circuit-1and Circuit-2 of Tower-M

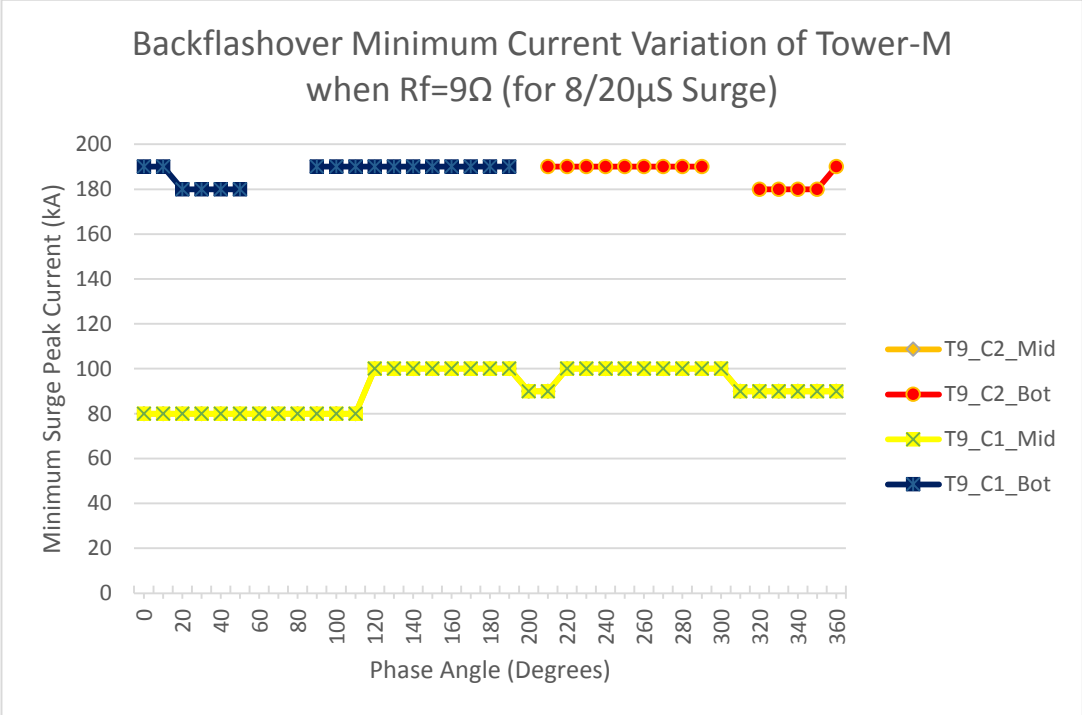

Figure 5.4 – Simulation results with two MCIA protection on TOP phases for 8/20µS Surge for the ground resistance of 9Ω

When TOP phases of the Circuit 1 & 2 are replaced by the MCIA strings, it can be clearly seen that TOP phases are protected for the back flashover effect even up to 200kA peak current surges for both 8/20µS and 1.2/50µS surges. However, MIDDLE and BOTTOM phases of both circuits are get flashover for both 8/20µS and 1.2/50µS surges with different minimum peak surge current as seen on Figure-5.4 and Figure-5.5 for all ground resistance values.

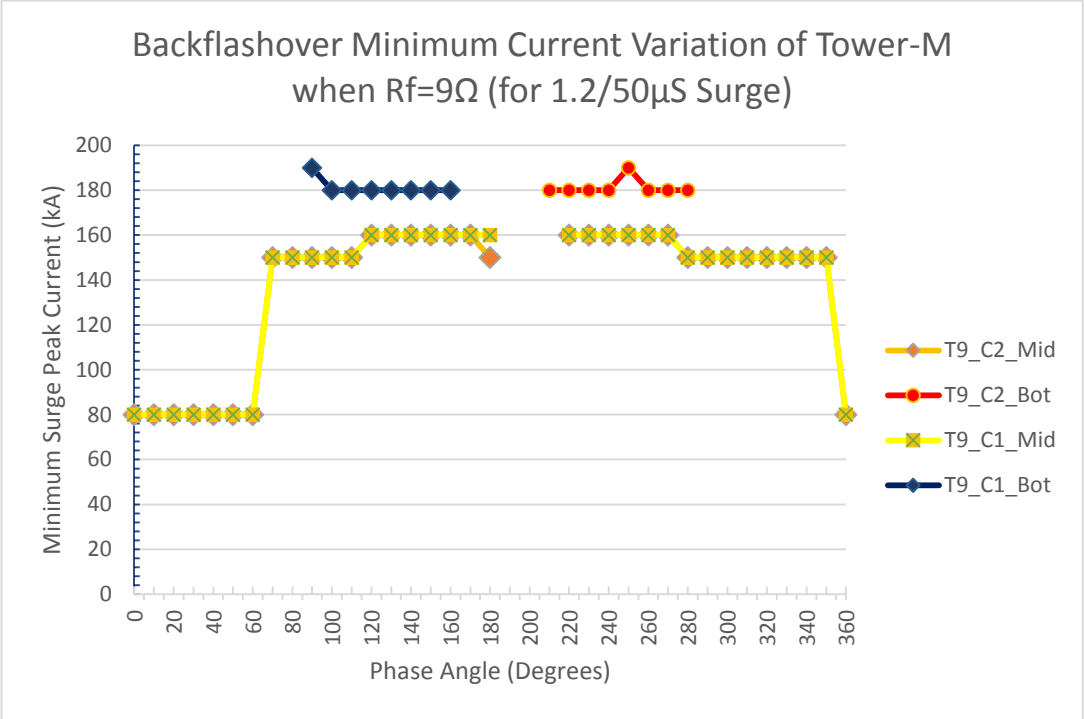

Figure 5.5 – Simulation results with two MCIA protection on TOP phases for 1.2/50µS Surge for the ground resistance of 9Ω

The minimum peak surge current values with compared to the "no MCIA protection (Step-1, Simulations 1-6)" has increased in every simulations for "with MCIA protection for top phases". This can be clearly seen from comparing Figure-5.2 with Figure-5.4 and Figure-5.3 with Figure-5.5. Likewise similar pattern can be seen from the Figure-A9.5 to Figure-A9.8 in Annex-9.

With 04 MCIA installed at TOP and MIDDLE phases of Circuit-1and Circuit-2 of Tower-M

From simulation No.13 – 18, the system was equipped with 04 Nos. of MCIA strings on TOP and MIDDLE phases of the both circuits. Figure-5.6 shows the simulation

results for 8/20µS surge when tower footing resistance of 9Ω. From this figure, it can be clearly seen that TOP and MIDDLE phases of both circuits have protection for back flashover effect up to the 200kA maximum peak surge current. However, BOTTOM phases of both circuits do not protected by the MCIA installed on TOP and MIDDLE phases of both circuits. But, it can be seen that the minimum peak surge currents that back flashover is happened has increased.

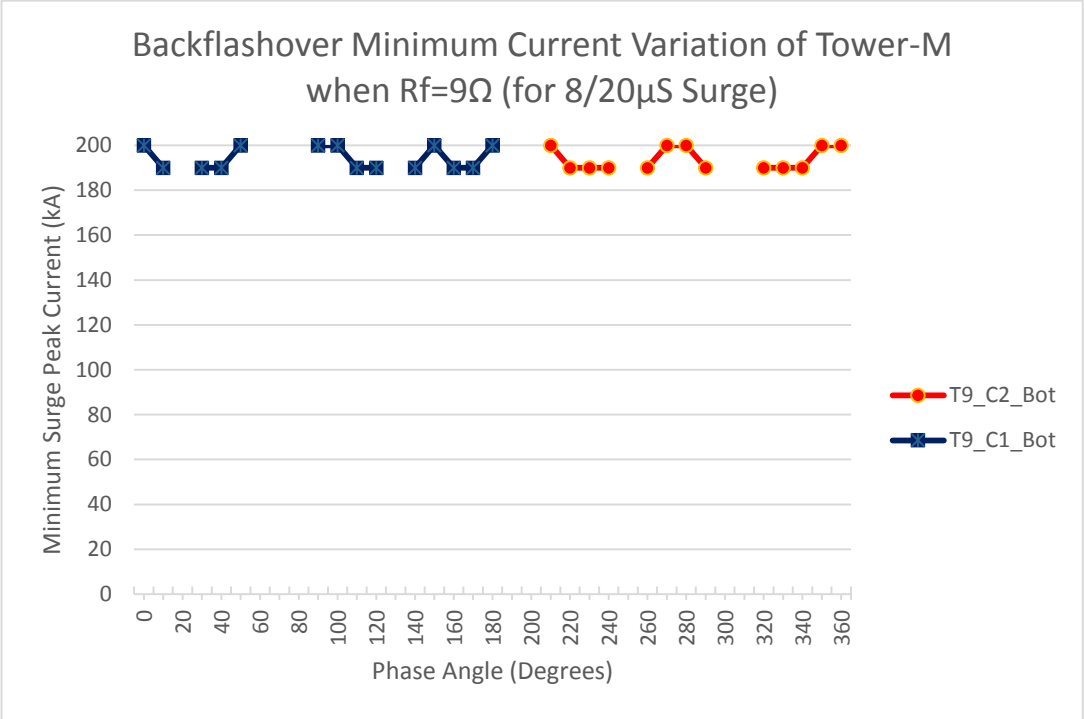

Figure 5.6 – Simulation results with Four MCIA protection on TOP and MIDDLE phases for 8/20µS Surge for the ground resistance of 9Ω

This is same for the 1.2x50µs surge (Figure-5.7) for all the grounding resistance values and Figure-A9.9 to Figure-A9.12 clearly illustrate the behaviour of 04 MCIA string protection system for the 8x20µs and 1.2x50µs surges for 38Ω and 146Ω.

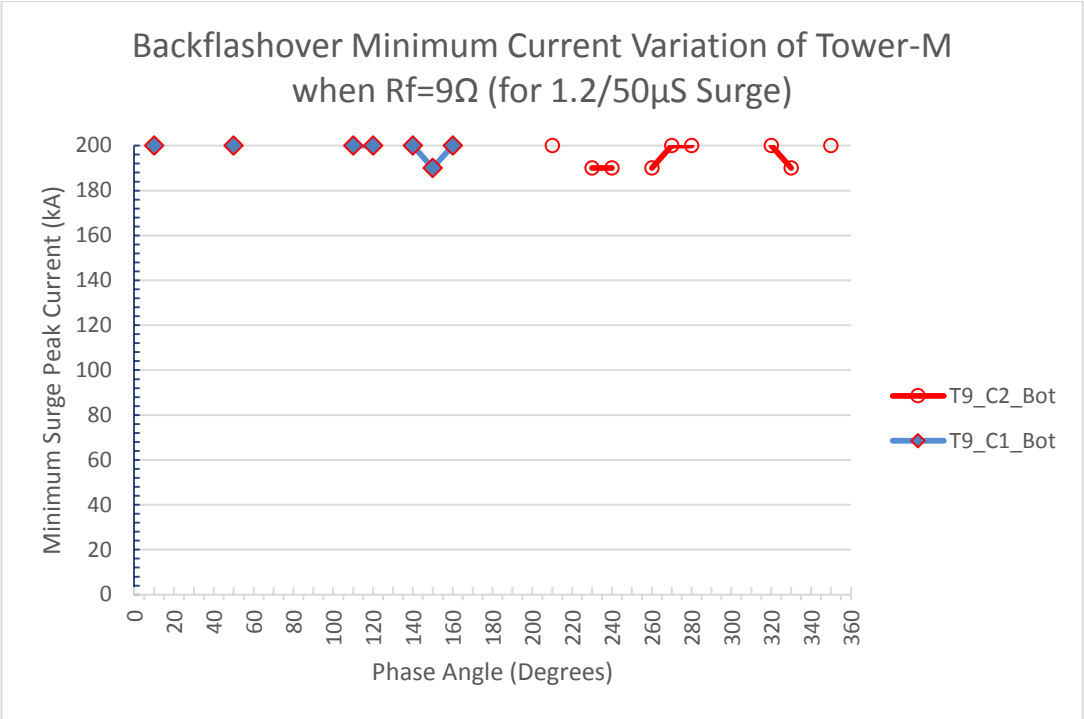

Figure 5.7 – Simulation results with Four MCIA protection on TOP and MIDDLE phases for 1.2/50µS Surge for the ground resistance of 9Ω

With 06 MCIA installed on all the phases of Circuit-1and Circuit-2 of Tower-M

- For 8x20µs surge and for 9Ω, 38Ω and 146Ω, there is no back flashover event occurred in all the six phases of the Tower-M.
- For 1.2x50µs surge and for 9Ω, 38Ω and 146Ω, there is no back flashover event occurred in all the six phases of the Tower-M.
- For 8x20µs surge and for 9Ω, 38Ω and 146Ω, there is no back flashover event occurred in all the six phases of the Tower-L.
- For 1.2x50µs surge and for 9Ω, 38Ω and 146Ω, there is no back flashover event occurred in all the six phases of the Tower-L.
- For 8x20µs surge and for 9Ω, 38Ω and 146Ω, there is no back flashover event occurred in all the six phases of the Tower-R.
- For 1.2x50µs surge and for 9Ω, 38Ω and 146Ω, there is no back flashover event occurred in all the six phases of the Tower-R.

5.2.3 Electrical and Mechanical Properties

Table 5.1 – Properties of the Conventional Insulator String and MCIA String

No.	Description	Conventional Insulator	MCIA String	Remarks
01	Spacing	146mm	146mm	
02	Diameter	255mm	413mm	
03	No of Discs	11	10	
04	Creepage Distance (Per Unit)	320mm	360mm	
05	Creepage Distance (String)	3,520mm	3,600mm	
06	Weight	5kg	6.7kg	17kg of excess load to the Cross arm and can be easily beard
07	Mechanical Strength	120kN	120kN	
08	String Length with Accessories	2,106mm (1,606+500)	2,106mm (1,606+646)	String Length can be adjusted with hardware accessories

5.3 Economic Analysis

5.3.1 Introduction

In the economic analysis, it is considered the installation/replacement cost of MCIA string with conventional insulator string and the gain acquired after installation of the MCIA. When calculating the economic gain, following criteria are considered,

- whether Kukule Regulation Pond is Spilling or not
- Whether loss of generation of Kukule is substitute from minimum thermal cost generation
- Whether the substituted power is sold to customers whose monthly usage is below 30 Units
- Whether the substituted power is sold to customers whose monthly usage is below 60 Units

In this study, the average hydro generation cost is taken as 1.68 Rs/kWh (extracted from loss and profit statement of CEB). The loss of generation of the Kukule Power

Station is considered to be substituted from the minimal cost, coal generation (Norochcholei Coal Power Plant) for a cost of 4.12 Rs/kWh and if the loss of generation is substituted from the next minimal cost thermal generation (Sapugaskanda Thermal Generation), for a cos of 17.80 Rs/kWh (from National Control Centre of CEB statistics).

CEB tariff for domestic consumers who consumes 0-30kWh per month is 2.50 Rs/kWh and 7.85 Rs/kWh for consumes above 60 kWh per month [30].

By using these data, simple payback period is calculated and described in following sections.

5.3.2 Cost Estimation for installing 06 Numbers of MCIA Strings at Tower-09

For calculation of installation cost of MCIA Strings, it is considered the cost for MCIA strings and the total installation cost of the CEB which includes labor personnel wages, overheads, equipment usage cost and transportation costs. The calculation of total installation cost is summarised below,

Cost for a MCIA String	= 2,000 USD
	≈ 290,000.00 LKR
Cost for 06 MCIA Strings	≈ 1.74 MLKR
Installation Cost (CEB)	= 200,000 LKR
Total Cost for installing 06 MCIA Strings	= 1.94MLKR

5.3.3 Loss Estimation due to tripping of line.

Kukule Power Station is connected to Mathugama Grid Substation through double circuit, Lynx lines and hence, one circuit can transfer approximately 80MW and it is equivalent to full generation capability of the Power Station. Therefore, even if there is one circuit is not available, power station can be fully utilised from a single line. Therefore, both circuits tripping incidents due to back flashover effect are considered for loss estimation due to tripping of lines.

Tripping data from the National Control Centre of the CEB is used for calculating loss due to both circuits tripping. Data was available from year 2006 to 2015, but full range of data is available only from 2010 to 2014 and used.

5.3.3.1 When considered as Kukule Regulation Pond is spilling

Even though Kukule Power Station is a run-off river type, it has a regulatory pond of 1.732MCM capacity and therefore, in this section calculations are carried out considering the regulatory pond is full and spilling. When it is spilling without generating power from the generators, the loss of water has a value and it is considered for calculations.

Specimen calculation (Year 2006)

Kukule Generation Loss = 38×10^3 kWh

Unit generation cost,

Coal Power Plant = 4.12 LKR

Sapugaskanda Power Station = 17.80 LKR

Loss of Profit = No. of Units Loss (Unit Selling Price – Unit Generation Cost of Kukule)

Loss of Profit (If generation is substituted by Coal Power Plant) = $38 \times 10^3 (4.12 - 1.68)$

= 92,720 LKR

Loss of Profit (If generation is substituted by Sapugaskanda PS) = $38 \times 10^3 (17.80 - 1.68)$

= 612,560 LKR

Accordingly, calculations ae been done for other years and Table 5.2 shows the loss of profit calculations when Kukule regulatory pond is spilling.

Table 5.2 – Loss of Profit (if Generation loss is Substitute) for Kukule Regulatory Pond is Spilling

Year	Kukule Generation Loss (MWh)	Loss of Profit (if Generation loss is Substitute) (Rs.) for Kukule Regulatory Pond is Spilling	
		Coal Power Plants	Sapugaskanda PS
2006	38	92,720.00	612,560.00
2009	76	185,440.00	122,512.00
2010	306	746,640.00	4,932,720.00
2011	64	156,160.00	1,031,680.00
2012	357	871,080.00	5,754,840.00
2013	714	1,742,160.00	11,509,680.00
2014	265	646,600.00	4,271,800.00
2015	87	212,280.00	1,402,440.00
Total	**1,907**	**4,653,080.00**	**29,638,232.00**

5.3.3.2 When considered as Kukule Regulation Pond is not spilling

When Regulatory Pond of the Kukule Power Station is not full and not spilling, then is has a capability of storing water. Therefore, during both transmission lines tripped due to back flashover period, the Regulatory Pond can store the incoming water and no waste of water. Therefore, it is considered that no water wastage and no value for the loss of water. Accordingly, loss of profit calculations are carried out as shown in Table A10.1 in Annex-10. In this calculations, it is considered as loss of generation to be sold to domestic consumers who use 30kWh per month and consumers who use above 60kWh per month.

Specimen calculation (Year 2010)

Kukule Generation Loss = 306 x 10^3 kWh

Unit generation cost,

Coal Power Plant = 4.12 LKR

Sapugaskanda Power Station = 17.80 LKR

Unit selling Price,

Consumers who use below 30 units per month = 2.50LKR/Unit

Consumers who use above 30 units per month = 7.85LKR/Unit

Loss of profit (if Kukule is not spilling) and if the loss of generation is solely used by the consumers who consumes below 30Units/month,

Loss of profit (If generation is substituted by Coal Power Plant)=306x10^3 (4.12-2.50)

= 495,720.00 LKR

Loss of profit (if Kukule is not spilling) and if the loss of generation is solely used by the consumers who consumes above 30Units/month,

Loss of profit (If generation is substituted by Coal Power Plant)=306x10^3 (4.12-7.85)

=(1,141,380.00)LKR

5.3.4 Calculation of Simple Pay Back Period

For calculation of simple payback period, year 2010-2014 period is considered as the most of data is available only for that period. Calculations are carried out considering Kukule Regulatory Pond is spilling condition and not spilling condition as shown in Table A10.2 and Table A10.3 in Annex-10.

In Table A10.3 in Annex-10, it is shown that simple payback period (when Regulatory Pond is spilling) is 2.33 years when loss of generation is substituted by the Coal Power Generation and it is 0.35 years when loss of generation is substituted by second lowest thermal generation, Sapugaskanda Power Station.

Table A10.2 in Annex-10 is shown that simple payback period (when Regulatory Pond is not spilling) is 3.5 Years when loss of generation is substituted by the Coal Power Generation and substituted generation is sold to consumers who use less than 30 kWh per month. However, Simple payback period is 0.37 Years (when

Regulatory Pond is not spilling) when loss of Generation is substituted by the second lowest thermal generation, Sapugaskanda Power Station sold to consumers who use less than 30 kWh per month.

Further, Simple payback period is 0.57 years when loss of generation is substituted by second lowest thermal generation, Sapugaskanda Power Station and substituted generation is sold to consumers who use more than 60 kWh per month.

5.3.5 Indirect benefits of installing MCIA

- Easy Installation.
- No need any modification/strengthening of cross arms or towers.
- Hot/Live line maintenances can be carried out easily and hence, no need of power interruptions for maintenances.
- 30 years of life span.

CHAPTER - 06

CONCLUSION AND RECOMMENDATIONS

6.1 Conclusion

Almost all the simulations carried out without arrester protection (Step-1) shows that the TOP phase of each circuit has a lower back flashover minimum current value compared to the rest of the phases. Therefore, it can be concluded that the TOP phases of each circuit are more likely to have back flashovers compared to the rest of the phases.

As per the results given for the Step-2 simulation Nos.07 to 12, carried out with two MCIA strings replaced in TOP phases of both circuits gives no protection for the MIDDLE phases of the both circuits beyond 70kA surges and for BOTTOM phases beyond 160kA.

According to the results of the Step-2 Simulation Nos.13 – 18, carried out with four (04) MCIA configuration, i.e MCIA replaced on TOP and MIDDLE phases of both circuits, it is observed that the protection against back flashovers is provided only for the TOP and MIDDLE phases of both circuits and for BOTTOM phases, only up to 170kA.

When all the phases of the Tower-M is replaced with MCIA strings (Step-2, Simulation Nos.19 - 24), all the six phases of the Tower-M is protected for back flashover up to 200kA surges (maximum simulation limit). Further, it is observed that all the phases of the Adjacent Left Hand tower, Tower-L, also protected (Step-2, Simulation Nos.25 - 30), for back flashover up to 200kA surges (maximum simulation limit). Furthermore, it is observed that all the phases of the Adjacent Right Hand tower, Tower-R, also protected (Step-2, Simulation Nos.31 - 36), for back flashover up to 200kA surges (maximum simulation limit).

6.2 Recommendations

According to the conclusions described in the previous section, it is recommended to replace all the conventional insulator strings (06 Nos.) with Multi Chamber Arrester (MCIA) strings of the tower of interest (in this study, Tower-09 and Tower-23)

where the most insulator damages are recorded and then, towers in the either sides of the interested tower are also protected for the back flashover effect.

Frequent inspections after installing MCIAs are recommended and later on inspections frequency can be adjusted with the observations of the performance of the MCIA strings.

It is better to inspect the Multi Chamber System (MCS) on the perimeter of the Insulator for any abnormalities and deformations. If observed, replace the respective MCIA with utility practice methods for insulator changing. Special care shall be taken not to damage the MCS of MCIA and do not repair the MCS if the MCIA.

References List

[1]. Vladimir A. Rakov and Martin A. Uman, “Lightning Physics and Effects”, Cambridge: Cambridge University Press, 2003

[2]. A. Morched, B. Gustavsen, M. Tartibi, “A Universal Line Model for Accurate Calculation of Electromagnetic Transients on Overhead Lines and Cables”, Paper PE-112-PWRD-0-11-1997

[3]. J. Rohan Lucas, “High Voltage Engineering”, Revised edition 2001, Open University of Sri Lanka, Open University Press, 2001

[4]. K.S.S. Kumara, “Lightning Performance of Sri Lankan Transmission Lines: A Case Study”, M.Sc. thesis, University of Moratuwa, Katubedda, Sri Lanka, 2009

[5]. M. Kizilcay, C. Neumann, “Back Flashover Analysis for 110kV Lines at Multi-Circuit Overhead Line Towers”, International Conference on Power Systems Transients (IPST’07) in Lyon, France on June 4-7, 2007

[6]. Chisholm, W. A.; Chow, Y. L.; Srivastara, K.D: “Travel Time of Transmission Towers”, IEEE Trans. on Power App. And Systems, Vol. PAS-104, No. 10, S.2922-2928, October 1985

[7]. CIGRE WG 33-01: “Guide to Procedures for Estimating the Lightning Performance of Transmission Lines”, Technical Brochure, October 1991.

[8]. Manitoba HVDC Research Centre, “Applications of PSCAD/EMTDC”, Application Guide 2008, Manitoba HVDC Research Centre Inc., Canada

[9]. Modeling of power transmission lines for lightning back flashover analysis. A case study: 220kV Biyagama - Kotmale transmission line, M.Sc. thesis, University of Moratuwa, Katubedda, Sri Lanka, 2010.

[10]. Nor Hidayah Nor Hassan, Ab. Halim Abu Bakar, Hazlie Mokhlis1, Hazlee Azil Illias “Analysis of Arrester Energy for 132kV Overhead Transmission Line due to Back Flashover and Shielding Failure”, IEEE International

Conference on Power and Energy (PECon), 2-5 December 2012, Kota Kinabalu Sabah, Malysia

[11]. Toshiaki Ueda, Sadanori Neo, Toshihisa Funabashi, Toyohisa Hagiwara, Hideto Watanabe, "Flashover Model for Arcing Horns and Transmission Line Arresters", International Conference on Power Systems Transients (IPST'95) in Lisbon

[12]. Toshihisa Funabashi, Toyohisa Hagiwara, Nobutaka Takeuchi, Hideto Watanabe,Tatsunori Sato, Toshiaki Ueda, Laurent Dube"Flashover Modeling of Arcing Horns Using MODELS Simuation Language", International Conference on Power Systems Transients (IPST'97) in Seatle

[13]. Juan A. Martinez-Velasco, Ferley Castro-Aranda, "Modeling of Overhead Transmission Lines for Lightning Studies" International Conference on Power Systems Transients (IPST'05) in Montreal, Canada, Paper No. IPST05 – 047

[14]. A.H.A. Bakar, D.N.A. Talib, H. Mokhlis, H.A. Illias, "Lightning back flashover double circuit tripping pattern of 132 kV lines in Malaysia"

[15]. Nur Zawani, Junainah, Imran, Mohd Faizuhar, "Modelling of 132kV Overhead Transmission Lines by Using ATP/ EMTP for Shielding Failure Pattern Recognition", Malaysian Technical Universities Conference on Engineering & Technology 2012, MUCET 2012, Part 1- Electronic and Electrical Engineering

[16]. B. Marungsri, S. Boonpoke, A. Rawangpai, A. Oonsivilai, and C. Kritayakornupong, "Study of Tower Grounding Resistance Effected Back Flashover to 500 kV Transmission Line in Thailand by using ATP/EMTP", World Academy of Science, Engineering and Technology nternational Journal of Electrical, Computer, Energetic, Electronic and Communication Engineering Vol:2, No:6, 2008

[17]. Igor Gutman, Georgij Porporkin, "Comparative performance of conventional 220 kV insulator strings and multi-chamber insulator-arresters strings under specific ice conditions of Russia", The 14th International Workshop on Atmospheric Icing of Structures, Chongqing, China, May 8 - May 13, 2011

[18]. G. V. Podporkin, E. Yu. Enkin, E. S. Kalakutsky, V. E. Pilshikov and A. D. Sivaev “Lightning Protection of Overhead Lines Rated At 3-35 kV And Above With the Help of Multi-Chamber Arresters and Insulator-Arresters”, X International Symposium on Lightning Protection 9th-13th November, 2009 – Curitiba, Brazil

[19]. Podporkin G. V, “Development of Long Flashover and Multi-Chamber Arresters and Insulator-Arresters for Lightning Protection of Overhead Distribution and Transmission Lines”, Plasma Physics and Technology 2015, 2, 3, 241-250

[20]. G. V. Podporkin, E. Yu. Enkin, E. S. Kalakutsky, V. E. Pilshikov and A. D. Sivaev, “Development of Multi-Chamber Insulator-Arresters for Lightning Protection of 220 kV Overhead Transmission Lines”, 2011 International Symposium on Lightning Protection (XI SIPDA), Fortaleza, Brazil, October 3-7, 2011

[21]. G. V. Podporkin, E. Yu. Enkin, V. E. Pilshikov, “Lightning Protection Overhead Distribution and Transmission lines by Multi Chamber Arrester and Multi Chamber Insulators Arresters of a Novel Design”, INMR World Congress, September 9-12, Vancouver, Canada

[22]. Multi-Chamber Arresters And Insulator-Arresters for lightning protection of overhead distribution and transmission lines Power Point Presentation of the Streamer Company Website (www.streamer-electric.com)

[23]. Georgij V. Podporkin, Evgeniy Yu Enkin, Evgeniy S. Kalakutsky, Vladimir E. Pilshikov, and Alexander D. Sivaev “Overhead Lines Lightning Protection by Multi-Chamber Arresters and Insulator-Arresters” IEEE TRANSACTIONS ON POWER DELIVERY, VOL. 26, NO. 1, JANUARY 2011

[24]. Gi-ichi Ikeda, “Report on Lightning Conditions in Ceylon, and Measures to Reduce Damage to Electrical Equipment”, Asian Productivity Project TES/68, 1969

[25]. Operating Manual, SiG.110.Z, Streamer International AG, (www.streamer-electric.com)

[26]. Georgij V. Podporkin, Alexander D. Sivaev, “Lightning Protection Overhead Distribution Lines by Long Flashover Arresters”, IEEE Transaction on Power Delivery, Vol 13, No.03, pp 814-823, (July 1998)

[27]. Technical Data of 115kV & 150kV strings of Smart Insulators

[28]. Matthieu ZINCK, “Multi-Chamber Arrester Field Test Experience in Asia High Lightning Density Area”, 2015 Asia-Pacific International Conference on Lightning (APL), Nagoya, Japan

[29]. EPRI, “Handbook for Improving Overhead Transmission Line Lightning Performance”, EPRI, Palo Alto, CA: 2004. 1002019

[30]. External Evaluator Report from the Hajime Sonoda (Global Group 21 Japan) done on year 2007 for Kukule Ganga Hydroelectric Power Project

[31]. Statistical Digest 2014, Ceylon Electricity Board of Sri Lanka

Appendix-01

Present Transmission System of Sri Lanka

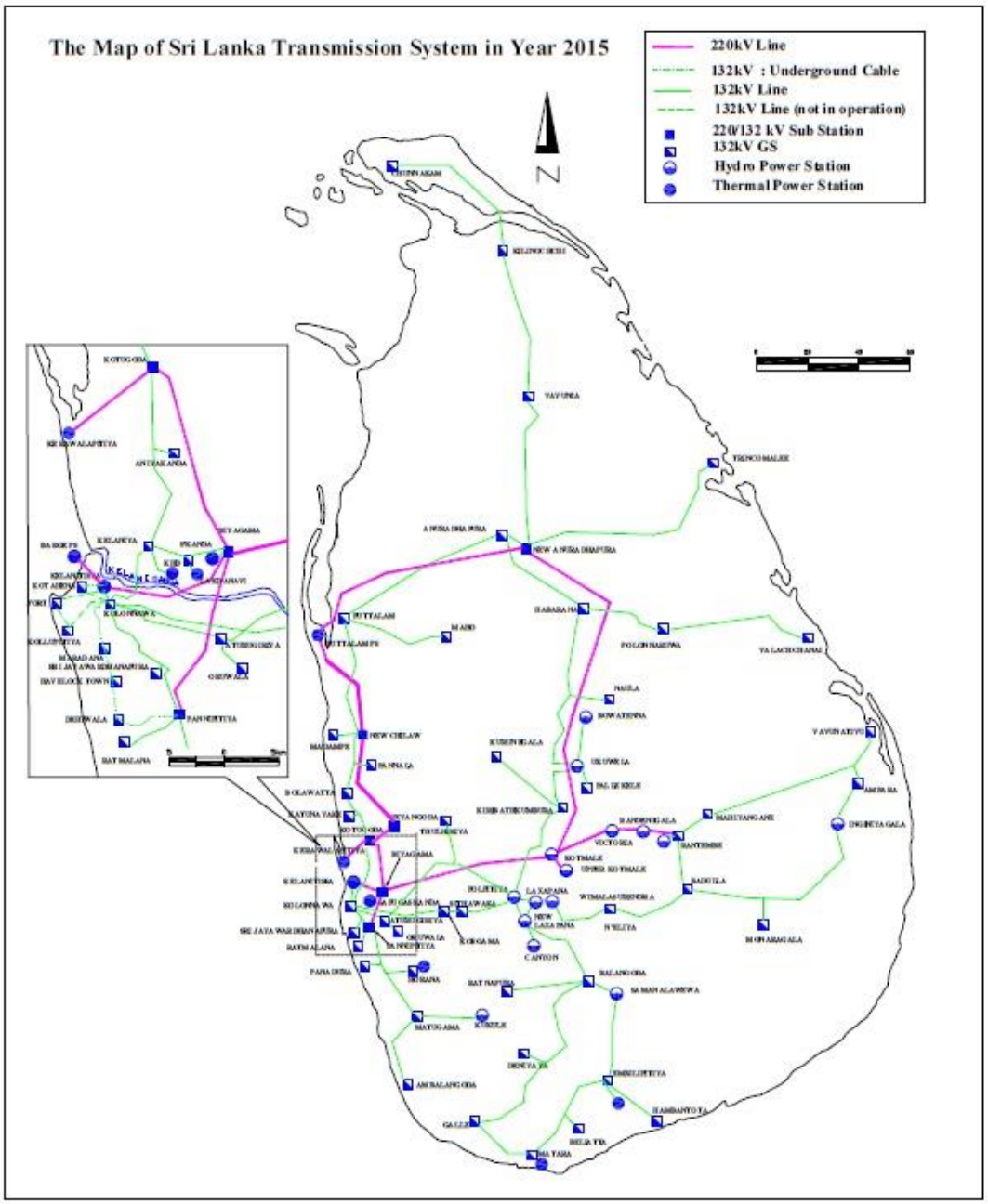

Appendix-02

Transmission System of Sri Lanka (Single Line Diagram)

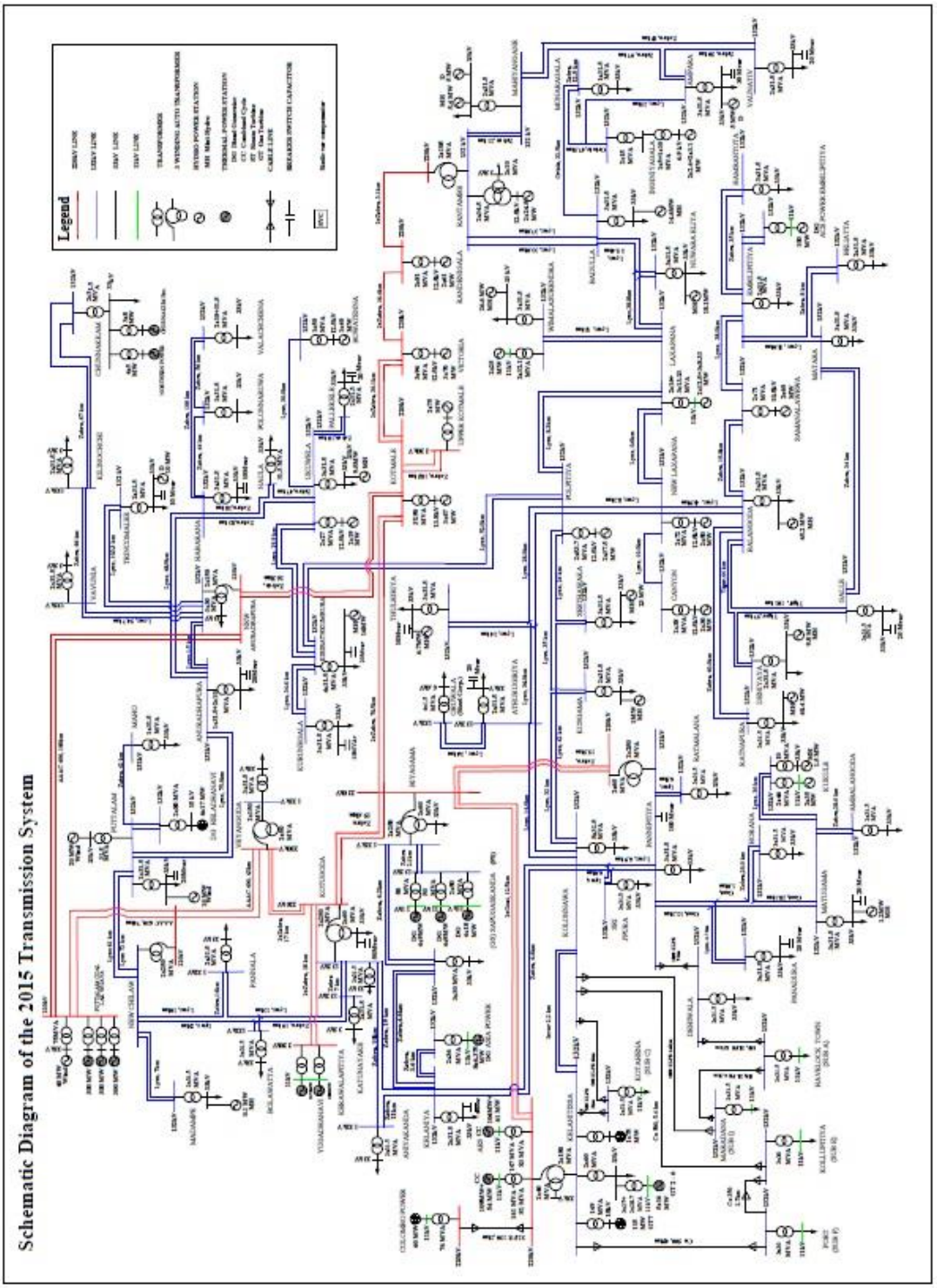

Appendix-03

Mathugama-Kukule, 132kV Transmission Line Parameters

No.	Line parameters' description	Value	Unit
1	Voltage	132	kV
2	Steady state Frequency	50	Hz
3	Line/Span length	As per the tower schedule (Appendix 5)	Km
4	Line shunt conductance	1x10-11	mΩ/m
5	No. of circuits	02	Nos.
6	Conductor Type/Name	ACSR "LYNX"	
7	Conductor size	226.2	mm^2
8	Conductor radius	0.009765	m
9	Conductor DC resistance	0.1576	Ω/km
10	Sag of all phase conductors	5.59	m
11	No. of sub conductors per phase	01	Nos.
12	No. of Earth wires	02	Nos.
13	Earth wire-1 Type/Name	GSW 7/3.25	
14	Earth wire-1 size	58.07	mm2
15	Earth wire-1 radius	0.004875	m
16	Earth wire-1 DC resistance	3.297	Ω/km
17	Earth wire-2 Type/Name	OPGW	
18	Earth wire-2 size	81.1	mm2
19	Earth wire-2 radius	0.006	m
20	Earth wire-2 DC resistance	0.519	Ω/km
21	Sag of Earth wire	4.09	m
22	Ground resistivity	1000	Ωm
23	Relative ground permeability	1.0	
24	Ideally Transposed Line	No.	

Appendix-04

Typical Transmission Tower

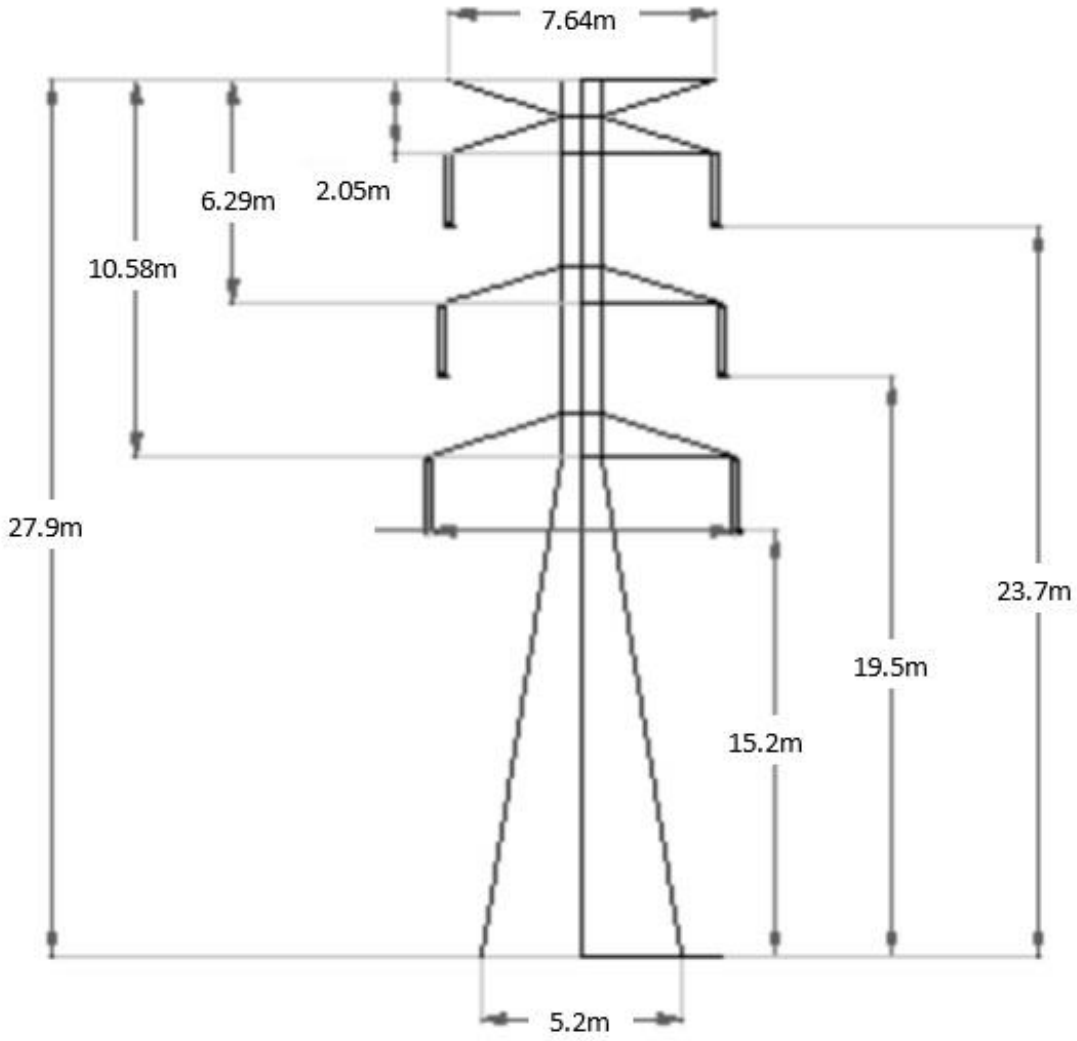

Appendix-05

Tower Schedule

Tower Number	Span (m)	Tower		Tower Number	Span (m)	Tower	
		Type	Body Ext			Type	Body Ext
Gantry	103.16			40	381.17	KMDL	0
1	164.47	KMDT	0	41	395.26	KMD1	9
2	152.45	KMD1	12	42	289.47	KMD3	9
3	449.63	KMD3	12	43	216.95	KMDL	0
4	439.39	KMD1	12	44	169.36	KMDL	0
5	283.51	KMDL	0	45	455.21	KMD1	12
6	392.42	KMDL	3	46	420.26	KMD1	0
7	513.07	KMD1	12	47	568.47	KMD1	0
8	610.77	KMD1	12	48	620.54	KMD1	0
9	506.71	KMD1	12	49	525.74	KMD1	0
10	244.24	KMD1	0	50	507.65	KMD1	12
11	259.78	KMD3	0	51	200.18	KMD1	6
12	334.60	KMD3	12	52	265.07	KMDL	6
13	194.59	KMD1	12	53	158.30	KMDL	6
14	306.09	KMDL	12	54	172.01	KMDL	0
15	233.31	KMDL	12	55	418.90	KMD1	6
16	284.89	KMD3	12	56	267.00	KMD1	6
17	241.51	KMDL	9	57	391.51	KMDL	3
18	256.72	KMDL	3	58	366.21	KMD1	6
19	306.51	KMDL	9	59	207.96	KMDL	6
20	563.00	KMD3	6	60	469.12	KMD1	6
21	543.29	KMD1	0	61	431.79	KMD1	12
22	468.59	KMD1	12	62	291.02	KMDL	0
23	496.04	KMD3	0	63	403.26	KMD1	0
24	642.45	KMD1	12	64	427.34	KMD1	12
25	322.96	KMD1	0	65	413.93	KMD1	12
26	372.77	KMDL	12	66	864.50	KMD1	3
27	278.81	KMD3	9	67	166.69	KMD1	3
28	199.77	KMDL	6	68	380.50	KMDL	0
29	428.02	KMDL	0	69	250.49	KMD3	0
30	368.73	KMD1	6	70	166.24	KMDL	0
31	376.98	KMD1	6	71	305.26	KMD1	9
32	212.93	KMDL	6	72	417.09	KMDL	12
33	278.95	KMDL	0	73	255.06	KMDL	6
34	268.50	KMDL	6	74	250.88	KMDL	6
35	230.99	KMD3	3	75	530.40	KMD1	0
36	309.44	KMDL	9	76	218.93	KMD1	0
37	354.23	KMDL	12	77	221.72	KMD1	6
38	244.67	KMD3	9	78	428.83	KMD1	3
39	348.39	KMD1	0	79	50.00	KMDT	0
				Gantry			

Appendix-06

Grounding Resistance Variation of Towers due to soil ionization effect

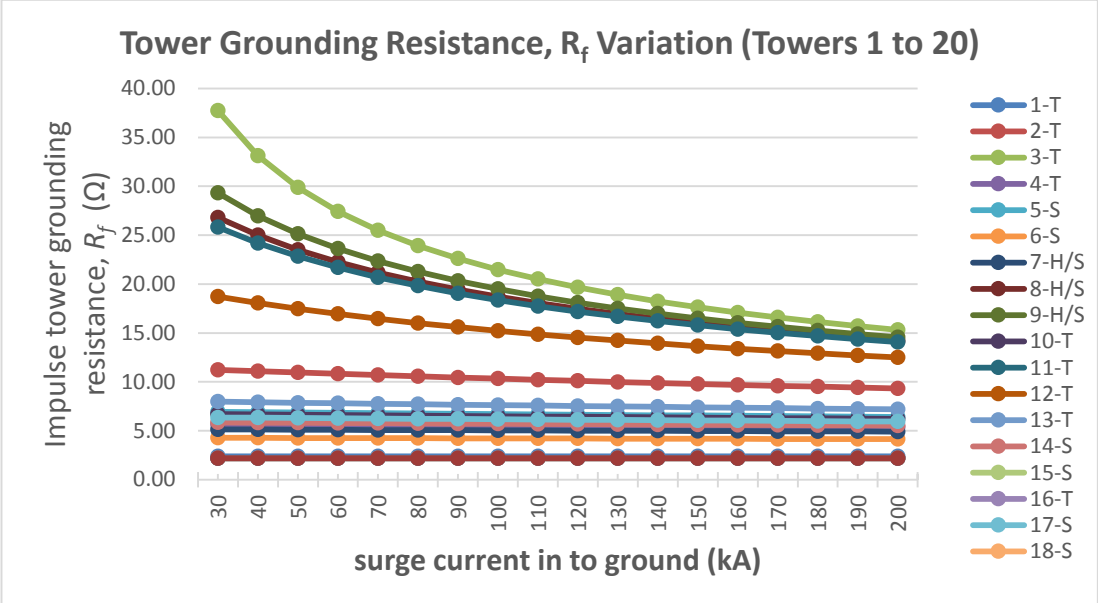

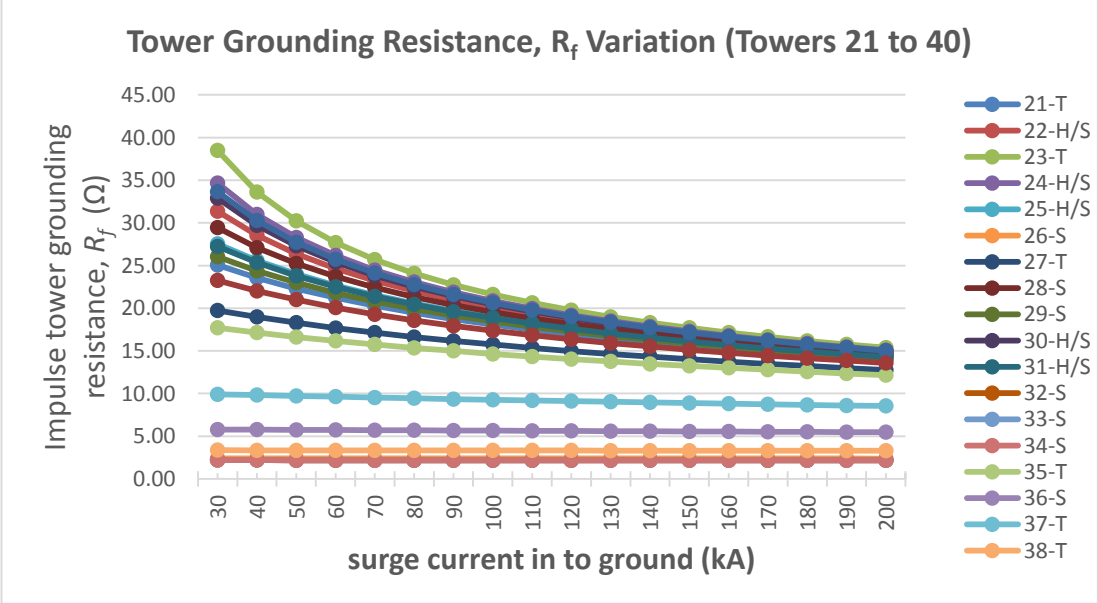

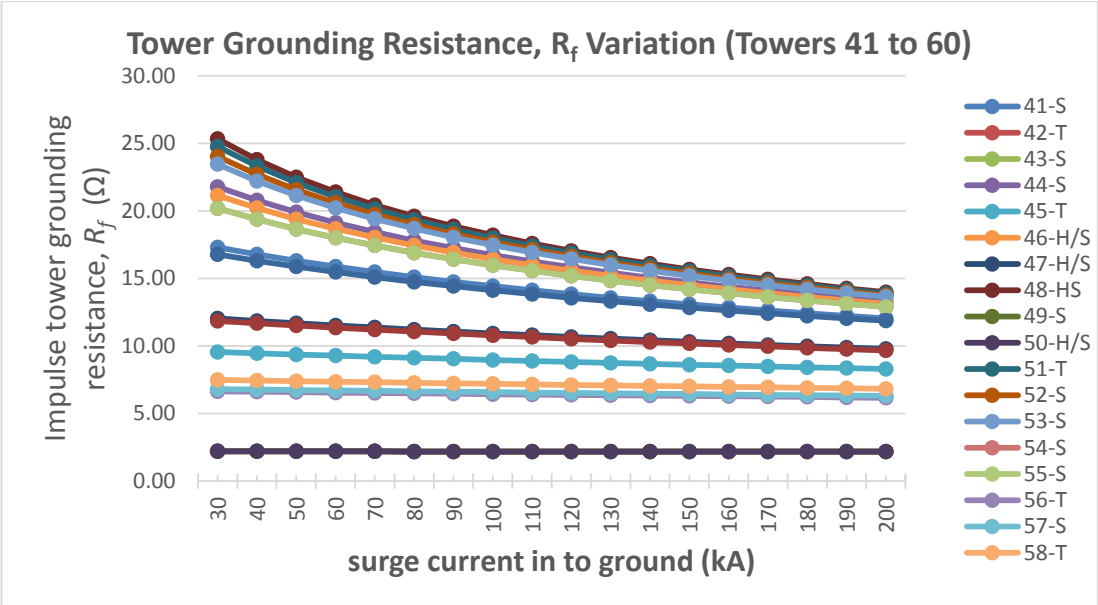
Tower Grounding Resistance, R_f Variation (Towers 41 to 60)
Impulse tower grounding resistance, R_f (Ω)
30.00
25.00
20.00
15.00
10.00
5.00
0.00
30 40 50 60 70 80 90 100 110 120 130 140 150 160 170 180 190 200
surge current in to ground (kA)
41-S
42-T
43-S
44-S
45-T
46-H/S
47-H/S
48-HS
49-S
50-H/S
51-T
52-S
53-S
54-S
55-S
56-T
57-S
58-T

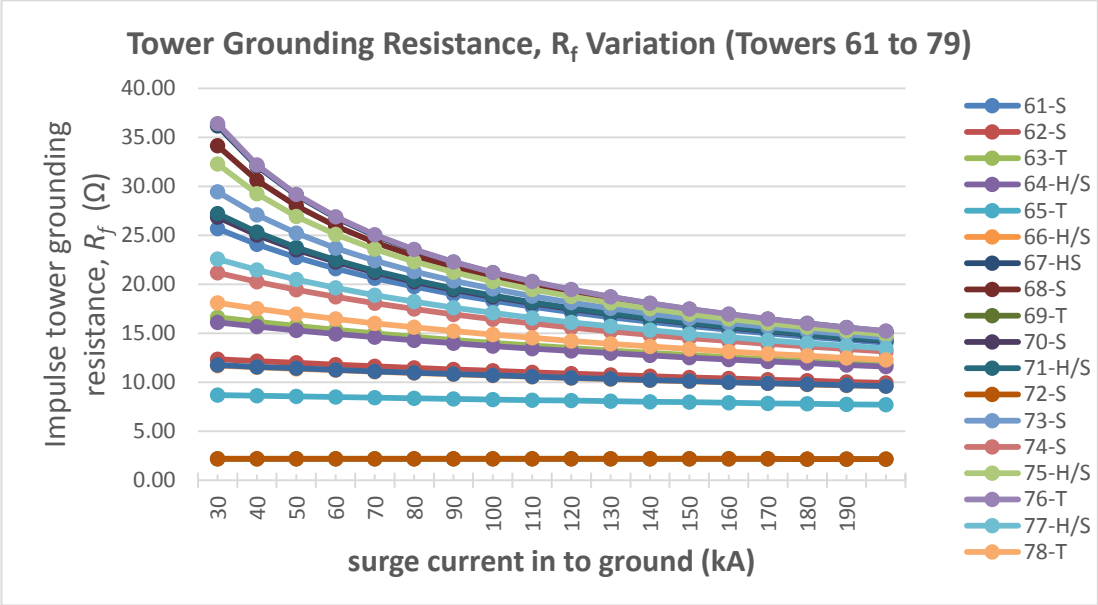
Tower Grounding Resistance, R_f Variation (Towers 61 to 79)
Impulse tower grounding resistance, R_f (Ω)
40.00
35.00
30.00
25.00
20.00
15.00
10.00
5.00
0.00
30 40 50 60 70 80 90 100 110 120 130 140 150 160 170 180 190
surge current in to ground (kA)
61-S
62-S
63-T
64-H/S
65-T
66-H/S
67-HS
68-S
69-T
70-S
71-H/S
72-S
73-S
74-S
75-H/S
76-T
77-H/S
78-T

Appendix-07

Calculations of Tower Surge Impedance [4]

1. Steps and Equations used for finding effective self-surge impedance of the conductor

Step 1: Drawing of the tower

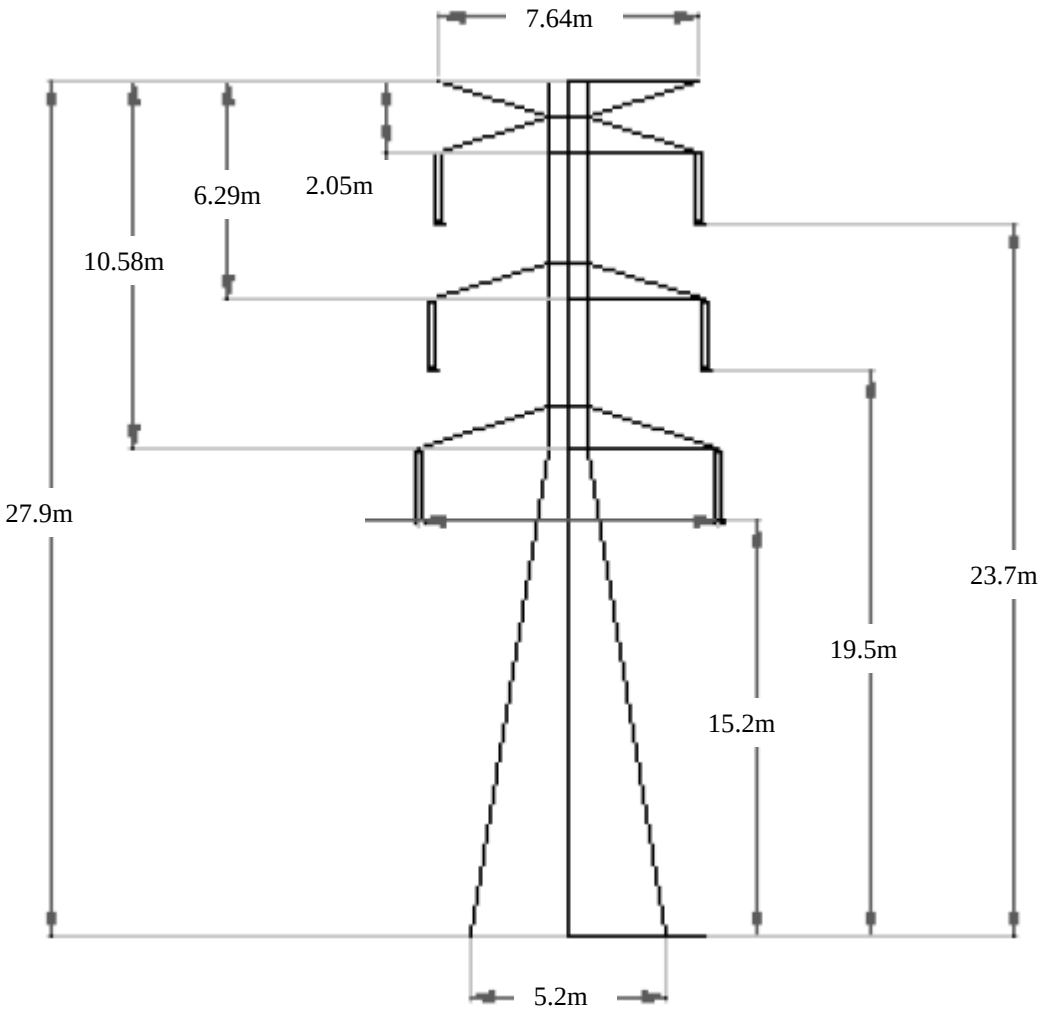

Step 2: Establishing the isokeraunic level

Isokeraunic level of the transmission line is selected for the calculations from below map.

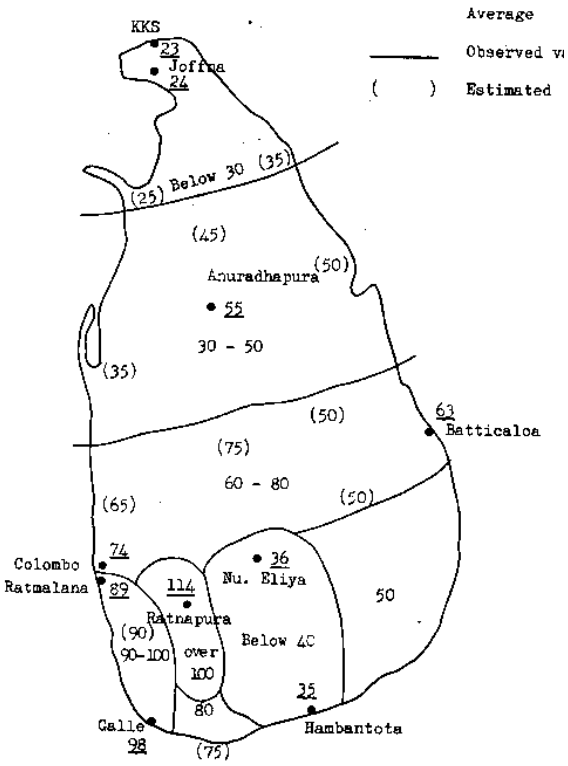

Figure A7.1 - IKL map of Sri Lanka

Mathugama-Kukule, 132kV transmission line is traversed through the Rathnapura and Colombo districts and when considering these two areas, the lowest isokauranic level is selected for the calculations.

Therefore, IKL = 89

Step 3: Computation of strokes to earth per square kilometer per year

$$N = 0.12T \qquad \text{(A7-1)}$$

where

N	Number of flashes to earth per square kilometer per year
T	Thunder days or IKL

$N = 0.12\ x\ 89 = \mathbf{10.68}$

Step 4: Computation of mean shield wire height

Since the conductor sags at the middle, a mean value is calculated

$$\hat{h} = h_s - sag \times \frac{2}{3} \quad \text{(A7-2)}$$

where

$\hat{h}$	Mean shield wire height
h_s	Height of the shield wire
sag	Sag of the shield wire

$$\hat{h} = 27.9 - 5.59 \times \frac{2}{3} = \mathbf{23.63\ m}$$

Step 5: Calculation of total number of flashes to the line

The following equation is from Whitehead,

$$N_1 = 0.012T\left(b + 4\hat{h}^{1.09}\right) \quad \text{(A7-3)}$$

where

N_1	Number of flashes to the line per 100km per year
T	Thunder days or IKL
b	Distance between parallel shield wires
$\hat{h}$	Average height of the Shield wire from Step 4

T = 89

b = 7.64 m

$\hat{h}$ = 23.63 m

$$N_1 = 0.012\ x\ 89(7.64 + 4x23.63^{1.09})$$

$$= \mathbf{142.35}\ (Flashes\ per\ year\ per\ 100km)$$

Step 6: Flashover voltage of the most exposed insulator string at 6μs

From Darveniza, Popolansky and Whitehead,

$$V = K_1 + \frac{K_2}{t^{0.75}} \quad \text{(A7-4)}$$

where

V	Flashover voltage of the most exposed insulator string at 6μs. Since the air gaps of all the insulators are the same, the same voltage applies.
h_s	Height of the shield wire,
A_g	arching horn air gap
$K_1 = 0.4 \times Ag$	Constant
$K_2 = 0.71 \times Ag$	Constant
$t = tt = 6\mu s$	Duration

$A_g = 1.5$ m

$K_1 = 0.4 \times 1{,}5 = 0.6$

$K_2 = 0.71 \times 1.5 = 1.065$

$\boldsymbol{V = 878kV}$

Step 7: Computation of mean height of the top phase conductors

$$\hat{h}_{\Phi} = h_{\Phi} - sag \times \frac{2}{3} \quad \text{(A7-5)}$$

where

$\hat{h}_{\varphi}$	Mean of phase conductor height
h_{φ}	Height of the top phase wire,
Sag	Sag of the phase wire

$h_{\varphi} = 23.74$ m

Sag = 7.09 m

$\boldsymbol{\hat{h}_{\Phi} = 19.01\ m}$

Step 8: Single conductor corona radius

$$R \ln \frac{2\hat{h}_{\Phi}}{R} = \frac{V}{E_o} \quad \text{(A7-6)}$$

where

R — Single conductor corona radius using iterative techniques

$\hat{h}_{\varphi}$ — Average height of the top phase conductor from step 7

$E_o = 1500$kV/m — Corona inception voltage gradient

V — Flashover voltage of the most exposed insulator string at 6μs from step 6

$\hat{h}_{\Phi} = 19.01$ m

$V = 878$kV

R = 0.098m

Step 9: Equivalent single conductor radius of the phase conductor

$$\boldsymbol{R_{eq} = 0.009765m}$$

Step 10: Approximate corona radius of the phase conductor

$$R_c = R_{eq} + R \quad \text{(A7-7)}$$

where

R_c — Approximate Corona radius of the phase conductor

R — Single conductor corona radius from step 8

R_{eq} — Equivalent single conductor radius of the phase conductor from step 9

$$\boldsymbol{R_c = 0.108m}$$

Step 11: Effective self surge impedance of the conductors Z_o

$$Z_{\phi} = 60\sqrt{\ln \frac{2\hat{h}_{\Phi}}{R_{eq}} \times \ln \frac{2\hat{h}_{\Phi}}{R_c}} \quad \text{(A7-8)}$$

where

Z_{φ} — Effective self surge impedance of the conductor

R_c — Approximate corona radius of the phase conductor step 10

$\hat{h}_{\varphi}$	Average height of the top phase conductor from step 7
R_{eq}	Equivalent single conductor radius of the phase conductor from step 9

$\hat{h}_{\varphi}$ = 19.01 m

$R_{eq} = 0.009765\text{m}$

$R_c = 0.108\text{m}$

$$\underline{\boldsymbol{Z_{\phi} = 417.7\ \Omega}}$$

2. Steps and Equations used for finding effective self-surge impedance of the earth wire

Step 1: Flashover voltage of the insulator string at 2μs

From Darveniza, Popolansky and Whitehead,

$$V_2 = K_1 + \frac{K_2}{t^{0.75}} \quad \text{(A7-9)}$$

where

V_2 Flashover voltage of the insulator string at 2μs

h_s Height of the shield wire

Ag Insulator string air gap

$K_1 = 0.4 \times Ag$ Constant

$K_2 = 0.71 \times Ag$ Constant

$t = tt = 2\mu s$ Rise time of wave front

$h_s = 27.90$ m

Ag = 1.5 m

$K_1 = 0.4 \times 1.5 = 0.6$

$K_2 = 0.71 \times 1.5 = 1.065$

V_2 = 1233.3 kV

Step 2: Flashover voltage of the most exposed insulator string at 6μs

From Darveniza, Popolansky and Whitehead,

$$V_6 = K_1 + \frac{K_2}{t^{0.75}} \quad \text{(A7-10)}$$

where

V_6 Flashover voltage of the insulator string at 6μs Since the air gaps of all the insulators are the same, the same voltage applies.

h_s Height of the shield wire,

A_g Insulator string air gap

$K_1 = 0.4 \times Ag$ Constant

$K_2 = 0.71 \times Ag$ Constant

$t = tt = 6\mu s$ Insulator string air gap

$K_1 = 0.6$

$K_2 = 1.065$

$h_s = 27.90$ m

V_6 = 877.8 Kv

Step 3: Estimate of tower top voltage and average for all phases (kV)

Tower Top voltage = V_2 x 1.8 = **2219.9 kV**

From Transmission Line Reference Book,

Step 4: Shield wire corona diameter at tower height

$$R \ln \frac{2h_s}{R} = \frac{V}{E_o} \quad \text{(A7-11)}$$

where

R Single conductor corona radius using iterative techniques

h_s Height of the top shield wire

E_o = 1500kV/m Corona inception voltage Gradient

V Estimated tower top voltage from step 3

Rc = 0.279m

Step 5: Self surge impedance of each shield wire at tower

$$Z_{sh} = 60\sqrt{\ln \frac{2h_s}{R_s} \times \ln \frac{2h_s}{R_c}} \quad \text{(A7-12)}$$

where

Z_{sh} Effective self surge impedance of each shield wire at tower

R_c Approximate corona radius of the shield wire, step 4

h_s Height of the top shield wire

R_s Conductor radius of the shield wire

$h_s = 27.90$ m

Rs = 0.004875 m

Rc = 0.279m

$$\underline{\boldsymbol{Z_{sh} = 422.2\Omega}}$$

Appendix - 08

Technical Data for MCIA String

streamer®
keeping the light
Streamer International AG
Masanserstrasse 17
CH- Chur Switzerland
office@streamer-electric.com

Technical Data of 115kV & 150kV strings of Smart Insulators

Rated Voltage (According to Russian Standard, kV)	115	150
Maximum continues phase-to-phase power frequency operating voltage (Usually refers as "Rated Voltage"), kV	132	172
maximum continues phase-to-ground power frequency operating voltage, kV	76.4	99.6
Quantity of insulators in a string, pcs	8	10
Minimum mechanical breaking load, kN	120	120
50% Impulse flashover voltage, kV	535	625
50% power frequency flashover voltage under dry, wet and contaminated conditions, in the rain, not less than, kV	120	150
Creepage distance, mm	2880 (360x8)	3600 (360x10)
radio interference level at 1.1 of maximum operating phase-to-ground voltage, at the most, db	55	55
Quenching time of power frequency follow current (not more, than), ms	10	10
Charge quantity, that can be passed through multi-chamber system without loss of follow-up current quenching capability, not less than, C	30	30
High Current impulse (4/10 µs), kA	100	100
Weight, kg	53.6 (6.7x8)	67.0 (6.7x10)

Appendix - 09

Simulation Results

Step-1, Simulation No. 02

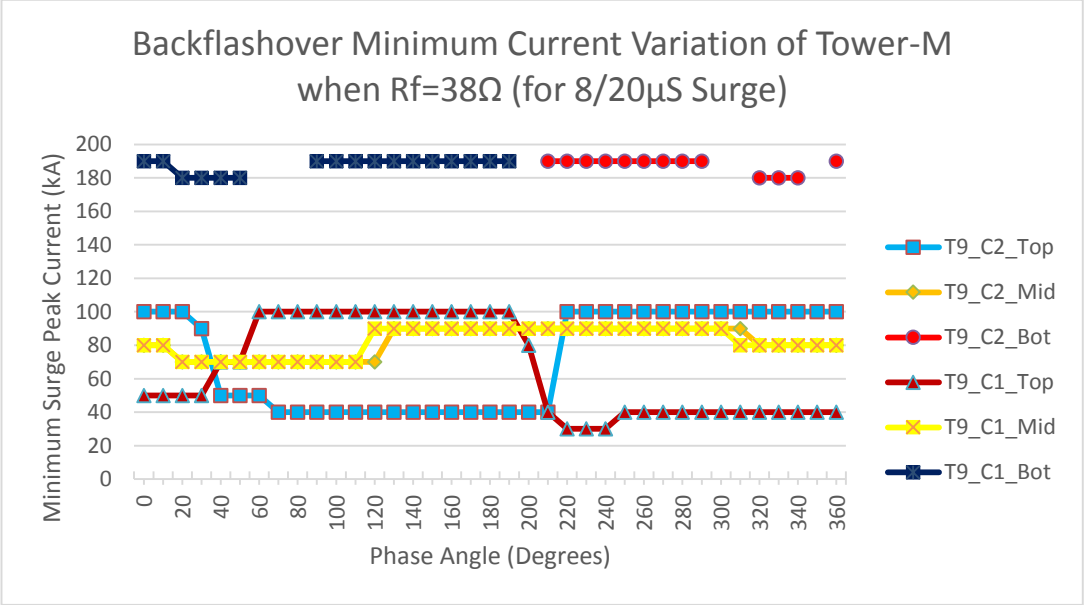

Figure A9.1 – Simulation results with no MCIA protection for 8/20μS Surge for the ground resistance of 38Ω

Step-1, Simulation No. 03

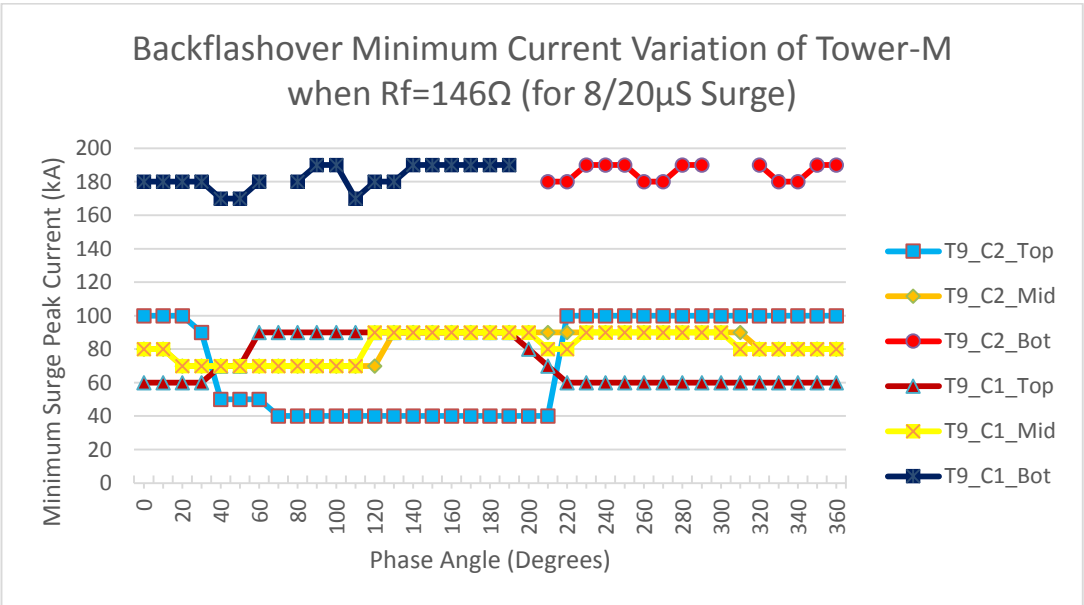

Figure A9.2 – Simulation results with no MCIA protection for 8/20μS Surge for the ground resistance of 146Ω

Step-1, Simulation No. 05

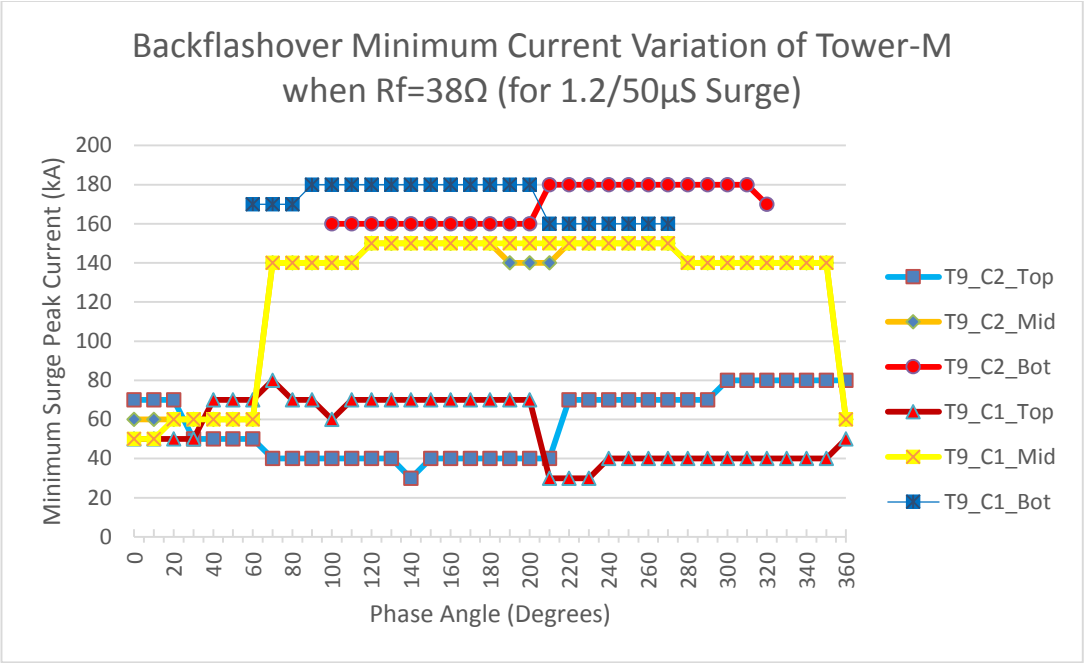

Figure A9.3 – Simulation results with no MCIA protection for 1.2/50µS Surge for the ground resistance of 38Ω

Step-1, Simulation No. 06

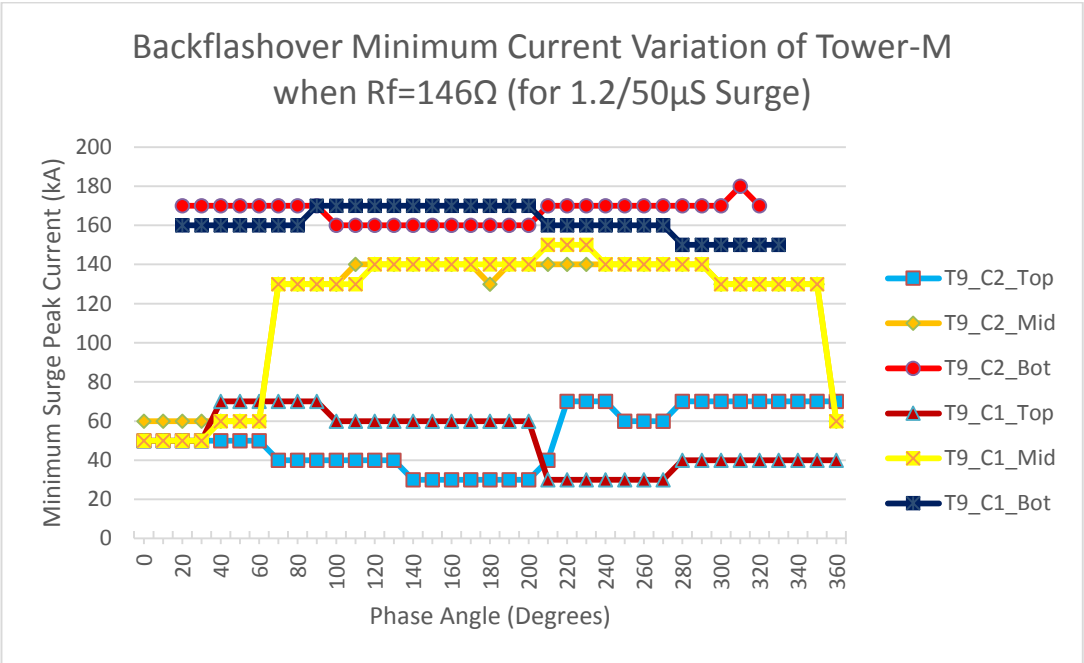

Figure A9.4 – Simulation results with no MCIA protection for 1.2/50µS Surge for the ground resistance of 146Ω

Step-2, Simulation No. 08

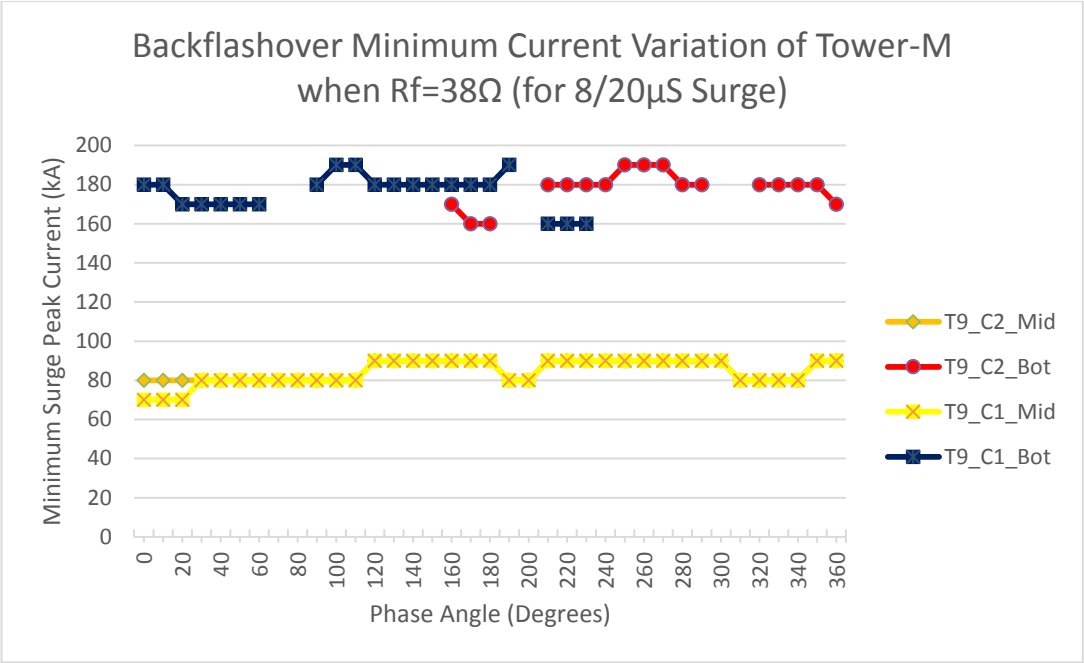

Figure A9.5– Simulation results with Two MCIA protection on TOP phases for 8/20μS Surge for the ground resistance of 38Ω

Step-2, Simulation No. 09

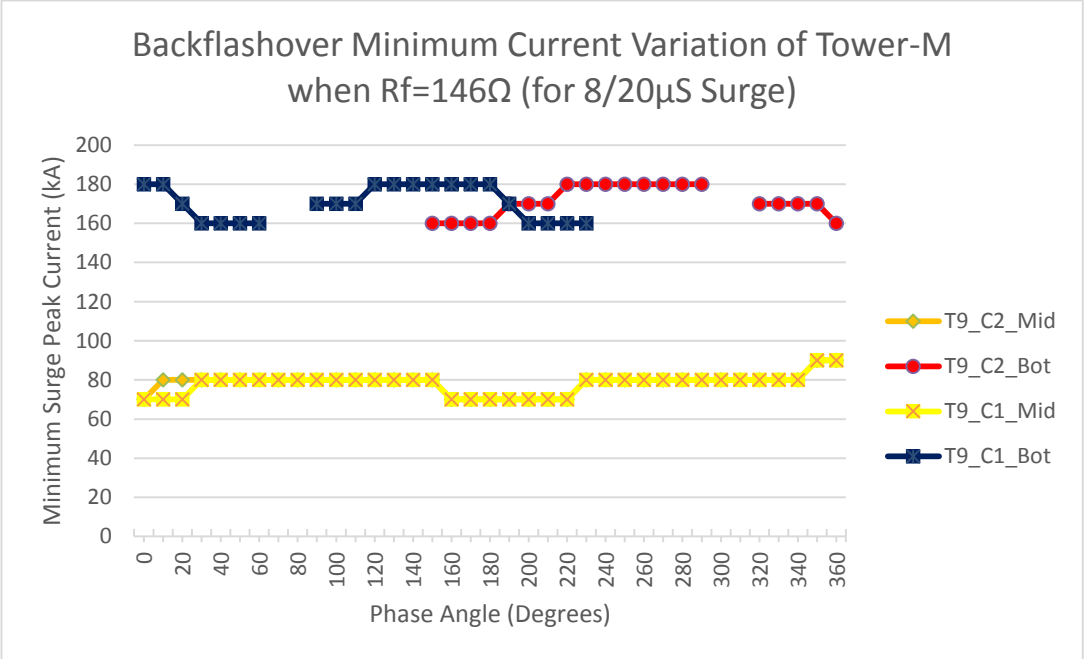

Figure A9.6– Simulation results with Two MCIA protection on TOP phases for 8/20μS Surge for the ground resistance of 146Ω

Step-2, Simulation No. 11

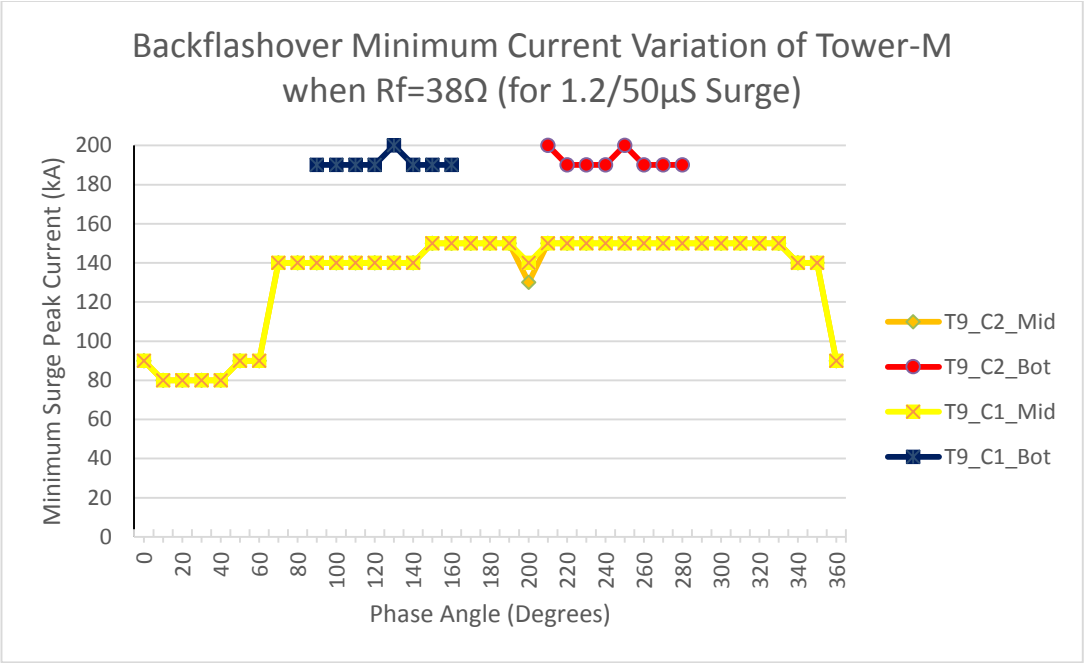

Figure A9.7– Simulation results with Two MCIA protection on TOP phases for 1.2/50µS Surge for the ground resistance of 38Ω

Step-2, Simulation No. 12

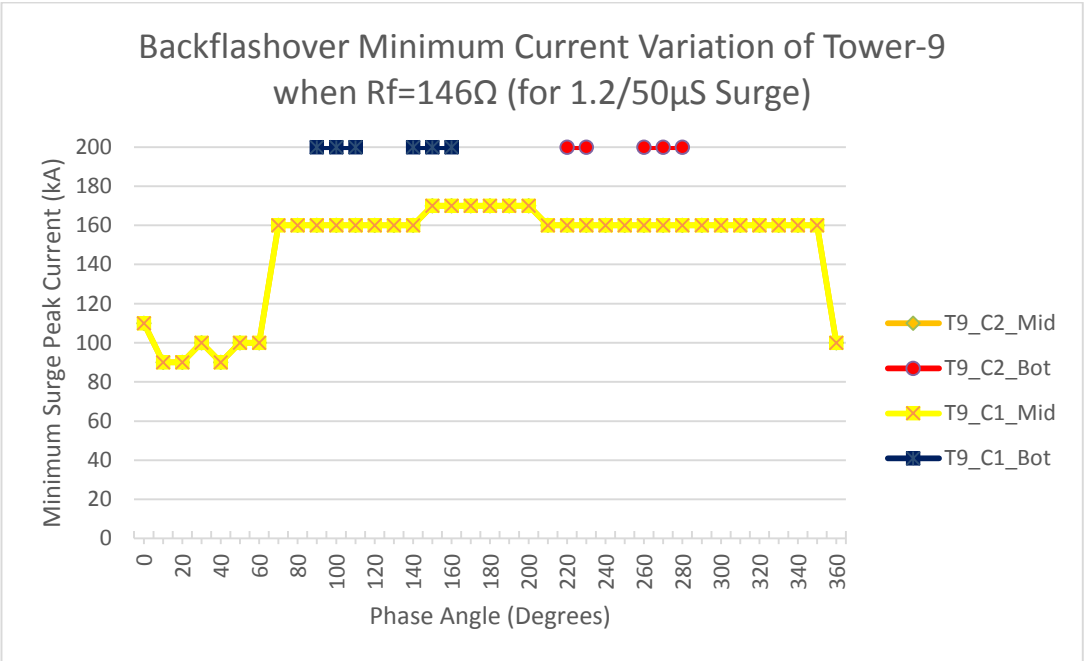

Figure A9.8– Simulation results with Two MCIA protection on TOP phases for 1.2/50µS Surge for the ground resistance of 146Ω

Step-2, Simulation No. 14

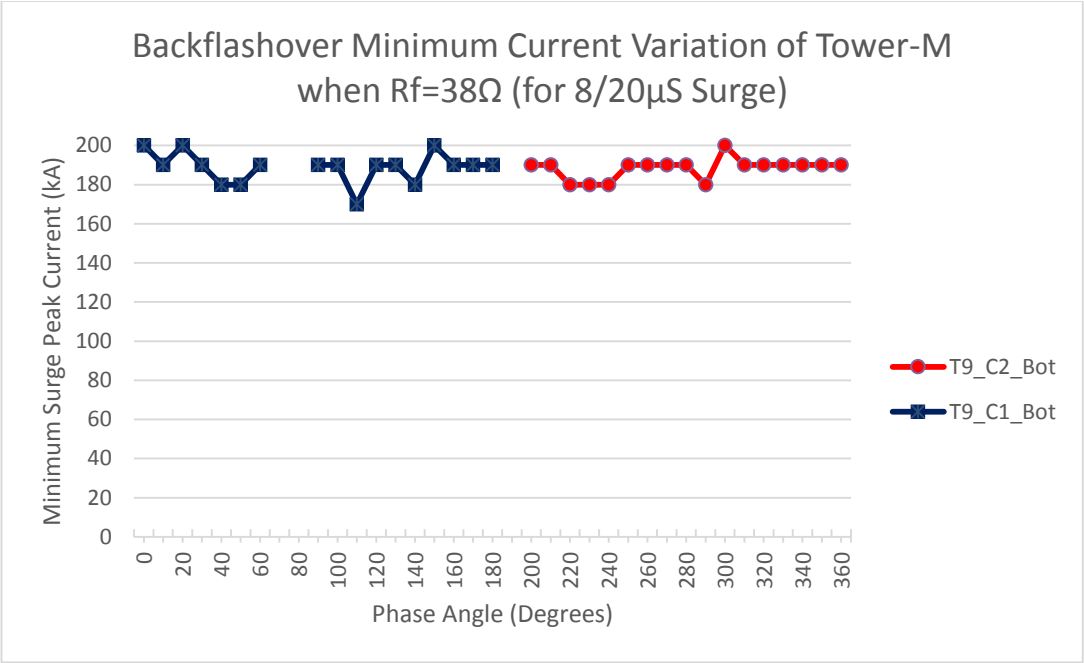

Figure-A9.9 - Simulation results with Four MCIA protection on TOP and MIDDLE phases for 8/20μS Surge for the ground resistance of 38Ω

Step-2, Simulation No. 16

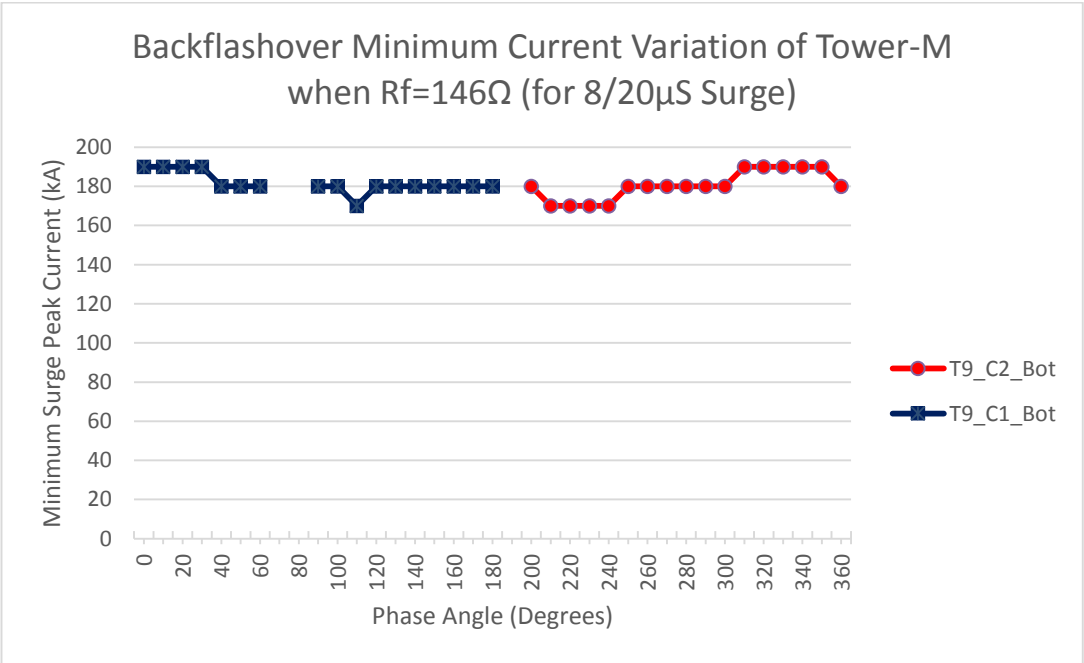

Figure-A9.10 - Simulation results with Four MCIA protection on TOP and MIDDLE phases for 8/20μS Surge for the ground resistance of 146Ω

Step-2, Simulation No. 17

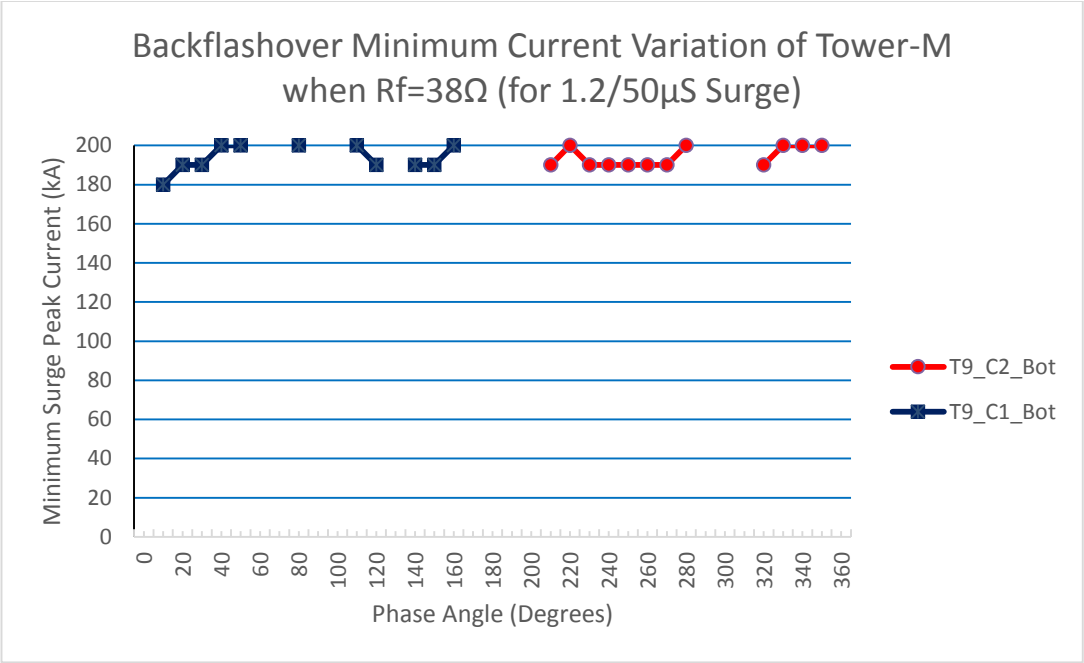

Figure-A9.11 – Simulation results with Four MCIA protection on TOP and MIDDLE phases for 1.2/50µS Surge for the ground resistance of 38Ω

Step-2, Simulation No. 18

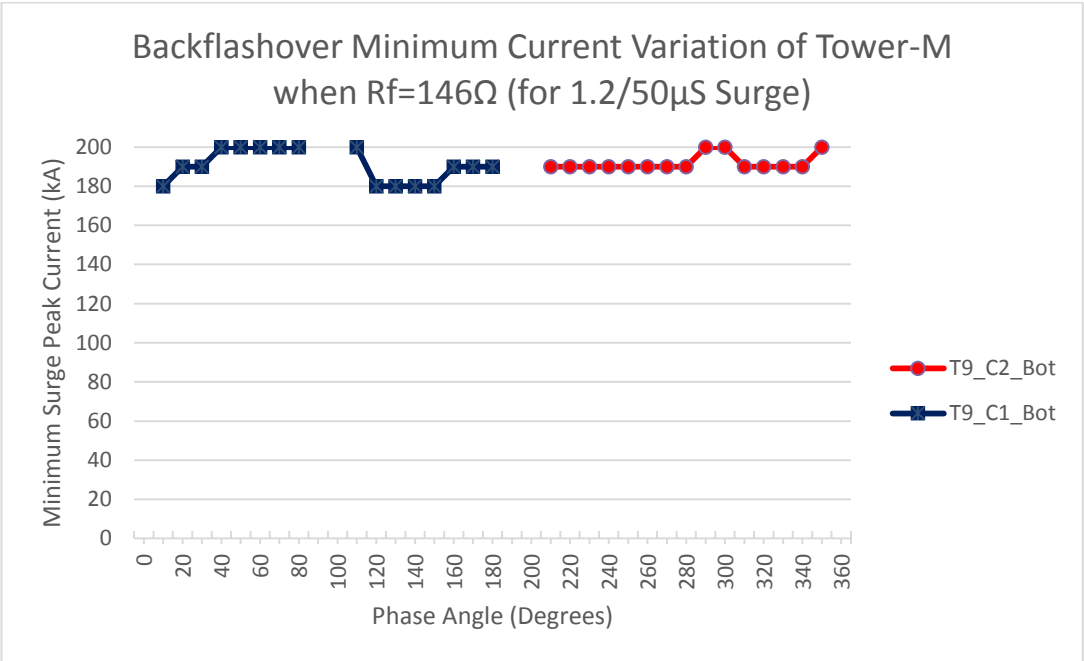

Figure-A9.12 – Simulation results with Four MCIA protection on TOP and MIDDLE phases for 1.2/50µS Surge for the ground resistance of 146Ω

Appendix - 10

Loss of Profit Calculation

Table A10.1- Loss of Profit Calculation (if Generation loss is Substitute) for Kukule Regulatory Pond is Spilling

Year	Kukule Generation Loss (MWh)	Loss of Profit (if Generation loss is Substitute) (Rs.) for Kukule Regulatory Pond is not Spilling			
		For Consumers below 30 Units monthly consumption		For Consumers above 30 Units monthly consumption	
		Coal Power Plants	Sapugaskanda PS	Coal Power Plants	Sapugaskanda PS
2006	38	61,560.00	581,400.00	(141,740.00)	378,100.00
2009	76	123,120.00	1,162,800.00	(283,480.00)	756,200.00
2010	306	495,720.00	4,681,800.00	(1,141,380.00)	3,044,700.00
2011	64	103,680.00	979,200.00	(238,720.00)	636,800.00
2012	357	578,340.00	5,462,100.00	(1,331,610.00)	3,552,150.00
2013	714	1,156,680.00	10,924,200.00	(2,663,220.00)	7,104,300.00
2014	265	429,300.00	4,054,500.00	(988,450.00)	2,636,750.00
2015	87	140,940.00	1,331,100.00	(324,510.00)	865,650.00
Total	**1,907**	**3,089,340.00**	**29,177,100.00**	**(7,113,110.00)**	**18,974,650.00**

Table A10.2- Calculation Results of Simple Payback Period when Kukule Regulatory Pond is not Spilling

Year	Kukule Generation Loss (MWh)	Loss of Profit (if Generation loss is Substitute) (Rs.) for Kukule Regulatory Pond is not Spilling			
		For Consumers below 30 Units monthly consumption		For Consumers above 30 Units monthly consumption	
		Coal Power Plants	Sapugaskanda PS	Coal Power Plants	Sapugaskanda PS
2010	306	495,720.00	4,681,800.00	(1,141,380.00)	3,044,700.00
2011	64	103,680.00	979,200.00	(238,720.00)	636,800.00
2012	357	578,340.00	5,462,100.00	(1,331,610.00)	3,552,150.00
2013	714	1,156,680.00	10,924,200.00	(2,663,220.00)	7,104,300.00
2014	265	429,300.00	4,054,500.00	(988,450.00)	2,636,750.00
Total	**1,706**	**2,763,720.00**	**26,101,800.00**	**(6,363,380.00)**	**16,974,700.00**
Simple Pay Back Period (Years)		**3.5**	**0.37**	-	**0.57**

Table A10.3 - Calculation Results of Simple Payback Period when Kukule Regulatory Pond is Spilling

Year	Kukule Generation Loss (MWh)	Loss of Profit (if Generation loss is Substitute) (Rs.) for Kukule Regulatory Pond is Spilling	
		Coal Power Plants	Sapugaskanda PS
2010	306	746,640.00	4,932,720.00
2011	64	156,160.00	1,031,680.00
2012	357	871,080.00	5,754,840.00
2013	714	1,742,160.00	11,509,680.00
2014	265	646,600.00	4,271,800.00
Total	**1,706**	**4,162,640.00**	**27,500,720.00**
Simple Pay Back Period (Years)		**2.33**	**0.35**